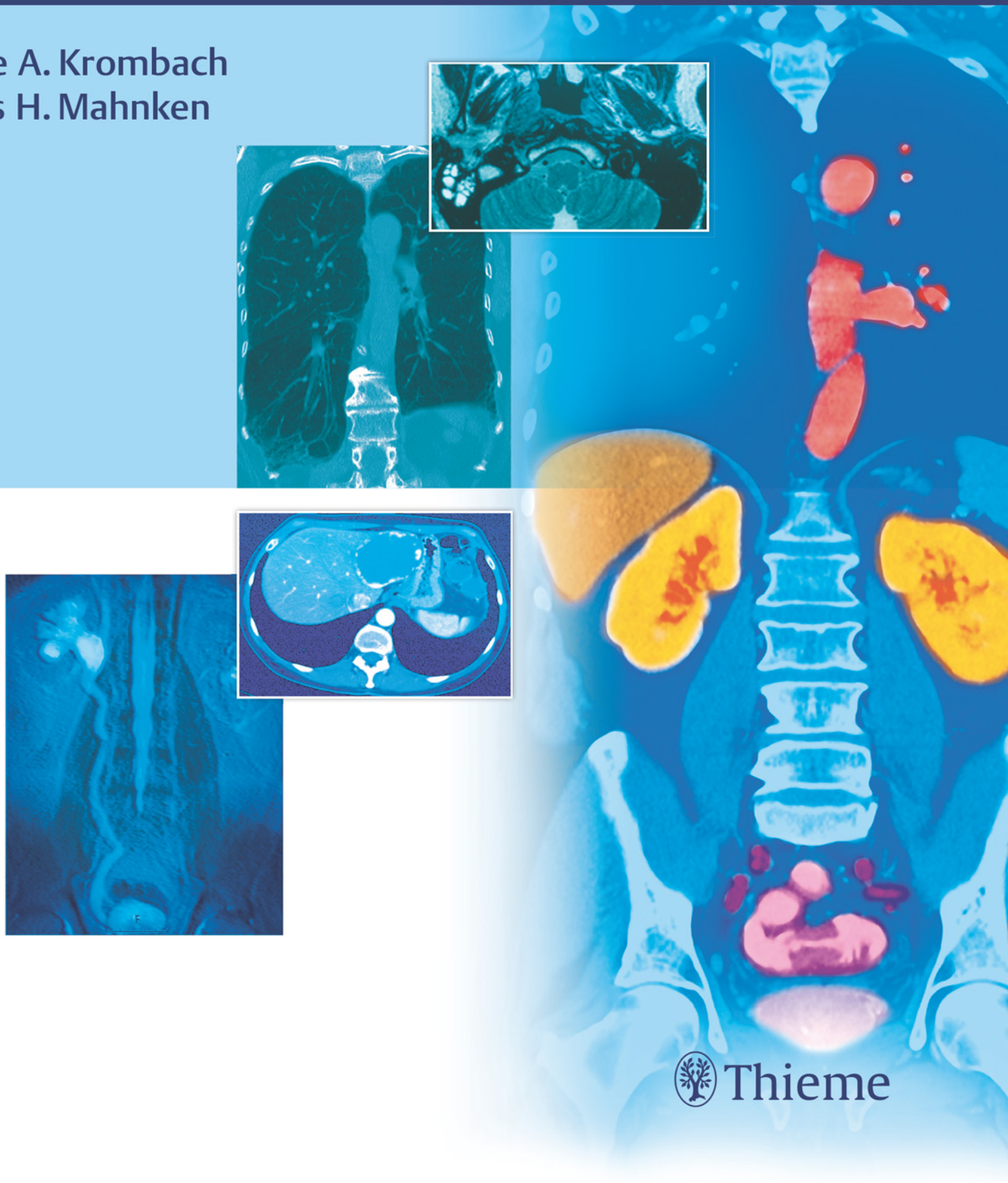


# Body Imaging: Thorax and Abdomen

Anatomical Landmarks, Image Findings, Diagnosis

Gabriele A. Krombach  
Andreas H. Mahnken









# Body Imaging: Thorax and Abdomen

Anatomical Landmarks, Image Findings, Diagnosis

**Gabriele A. Krombach, MD**

Professor and Director of the Clinic for Diagnostic and Interventional Radiology

Justus Liebig University Giessen

Giessen University Hospital

Giessen, Germany

**Andreas H. Mahnken, MD, MBA, MME**

Professor

Diagnostic and Interventional Radiology

Philipps University

Marburg University Hospital

Marburg, Germany

1509 illustrations

Thieme

Stuttgart • New York • Delhi • Rio de Janeiro

**Library of Congress Cataloging-in-Publication Data** is available from the publisher.

This book is an authorized translation of the 1st German edition published and copyrighted 2015 by Georg Thieme Verlag, Stuttgart. Title of the German edition: Radiologische Diagnostik Abdomen und Thorax. Bildinterpretation unter Berücksichtigung anatomischer Landmarken und klinischer Symptome.

Translator: Terry Telger, Fort Worth, TX, USA

Illustrator: Christine Lackner, Ittlingen, Germany. Selected anatomical images by M. Voll and K. Wesker taken from Schünke M, Schulte E, Schumacher U. Prometheus:

LernAtlas der Anatomie: Innere Organe. 2nd ed. Stuttgart, Thieme 2009; LernAtlas der Anatomie: Allgemeine Anatomie und Bewegungssystem. 3rd ed. Stuttgart, Thieme 2011; LernAtlas der Anatomie: Kopf, Hals und Neuroanatomie. 2nd ed. Stuttgart, Thieme 2009.

**Important note:** Medicine is an ever-changing science undergoing continual development. Research and clinical experience are continually expanding our knowledge, in particular our knowledge of proper treatment and drug therapy. Insofar as this book mentions any dosage or application, readers may rest assured that the authors, editors, and publishers have made every effort to ensure that such references are in accordance with the **state of knowledge at the time of production of the book.**

Nevertheless, this does not involve, imply, or express any guarantee or responsibility on the part of the publishers in respect to any dosage instructions and forms of applications stated in the book. **Every user is requested to examine carefully** the manufacturers' leaflets accompanying each drug and to check, if necessary in consultation with a physician or specialist, whether the dosage schedules mentioned therein or the contraindications stated by the manufacturers differ from the statements made in the present book. Such examination is particularly important with drugs that are either rarely used or have been newly released on the market. Every dosage schedule or every form of application used is entirely at the user's own risk and responsibility. The authors and publishers request every user to report to the publishers any discrepancies or inaccuracies noticed. If errors in this work are found after publication, errata will be posted at [www.thieme.com](http://www.thieme.com) on the product description page.

Some of the product names, patents, and registered designs referred to in this book are in fact registered trademarks or proprietary names even though specific reference to this fact is not always made in the text. Therefore, the appearance of a name without designation as proprietary is not to be construed as a representation by the publisher that it is in the public domain.

© 2018 Georg Thieme Verlag KG

Thieme Publishers Stuttgart  
Rüdigerstrasse 14, 70469 Stuttgart, Germany  
+49 [0]711 8931 421, [customerservice@thieme.de](mailto:customerservice@thieme.de)

Thieme Publishers New York  
333 Seventh Avenue, New York, NY 10001, USA  
+1-800-782-3488, [customerservice@thieme.com](mailto:customerservice@thieme.com)

Thieme Publishers Delhi  
A-12, Second Floor, Sector-2, Noida-201301  
Uttar Pradesh, India  
+91 120 45 566 00, [customerservice@thieme.in](mailto:customerservice@thieme.in)

Thieme Publishers Rio, Thieme Publicações Ltda.  
Edifício Rodolpho de Paoli, 25º andar  
Av. Nilo Peçanha, 50 – Sala 2508  
Rio de Janeiro 20020-906 Brasil  
+55 21 3172 2297 / +55 21 3172 1896

Cover design: Thieme Publishing Group  
Typesetting by DiTech Process Solutions Pvt. Ltd., India

Printed in Germany by CPI Books GmbH

5 4 3 2 1

ISBN 978-3-13-205411-0

Also available as an e-book:  
eISBN 978-3-13-205421-9



This book, including all parts thereof, is legally protected by copyright. Any use, exploitation, or commercialization outside the narrow limits set by copyright legislation without the publisher's consent is illegal and liable to prosecution. This applies in particular to photostat reproduction, copying, mimeographing, preparation of microfilms, and electronic data processing and storage.

To our teachers



# Contents

<b>Foreword</b> .....	xiii
<b>Preface</b> .....	xiv
<b>Acknowledgments</b> .....	xv
<b>Contributors</b> .....	xvi
<b>Abbreviations</b> .....	xvii

## Part 1: Chest

<b>1. Mediastinum</b> .....	2	
<i>Gabriele A. Krombach</i>		
<b>1.1 Anatomy</b> .....	2	Extragonadal Germ Cell Tumors .....
		Liposarcoma .....
		Sarcomas .....
		Cystic Masses .....
		Lymphangioma and Cystic Hygroma .....
<b>1.2 Evaluation of the Mediastinum on Conventional Radiographs</b> .....	4	<b>1.4.2 Middle Mediastinum</b> .....
1.2.1 Silhouette Sign .....	4	Sarcoidosis .....
1.2.2 Edge-on Effect .....	4	Lymphoma .....
<b>1.3 Diffuse Mediastinal Diseases</b> .....	6	Castleman's Disease (Angiofollicular Hyperplasia) .....
1.3.1 Acute Mediastinitis .....	6	<b>1.4.3 Posterior Mediastinum</b> .....
1.3.2 Chronic Mediastinitis and Multifocal Fibrosclerosis .....	8	Neurogenic Tumors .....
<b>1.4 Mediastinal Masses</b> .....	9	Extramedullary Hematopoiesis .....
1.4.1 Anterior Mediastinum .....	9	Bochdalek, Morgagni, and Larrey Hernias .....
Intrathoracic Goiter .....	9	<b>1.5 Trauma with Mediastinal Injury: Pneumomediastinum</b> .....
Thymic Hyperplasia .....	11	
Thymoma and Thymic Carcinoma .....	11	<b>Bibliography</b> .....
Thymic Cysts .....	12	
Neuroendocrine Tumors of the Thymus; Thymic and Mediastinal Carcinoids .....	13	
<b>2. Heart and Pericardium</b> .....	30	
<i>Gabriele A. Krombach</i>		
<b>2.1 Heart</b> .....	30	<b>2.2 Pericardium</b> .....
2.1.1 Anatomy .....	30	2.2.1 Anatomy .....
Cardiac Borders .....	30	2.2.2 Diseases .....
Cardiac Chambers .....	30	Pericarditis .....
<b>2.1.2 Diseases</b> .....	32	Constrictive Pericarditis .....
Heart Failure .....	32	Pericardial Masses .....
Coronary Heart Disease and Myocardial Infarction .....	34	Pericardial Aplasia .....
Cardiomyopathies .....	42	<b>Bibliography</b> .....
Cardiac Tumors .....	49	
Acquired Valvular Disease .....	60	
<b>3. Large Vessels</b> .....	72	
<i>Andreas H. Mahnken</i>		
<b>3.1 Aorta</b> .....	72	Aberrant Right Subclavian Artery and Kommerell Diverticulum ..
3.1.1 Anatomy .....	72	Patent Ductus Arteriosus .....
3.1.2 Development .....	73	Coarctation of the Aorta .....
3.1.3 Congenital Anomalies .....	73	Double Aortic Arch .....
Variants in the Origins of Supra-aortic Vessels .....	74	Right Aortic Arch .....
		Congenital Abdominal Aortic Stenosis .....

3.1.4	Diseases	79	3.2.4	Diseases	104
	Aortic Aneurysms	79		Nutcracker Syndrome	104
	Acute Aortic Syndrome	84		May–Thurner Syndrome	106
	Aortic Dissection	85		Superior Vena Cava Syndrome	107
	Intramural Hematoma	87		Vena Cava Thrombosis	108
	Penetrating Aortic Ulcer	89		Tumor Thrombi in the Vena Cava	108
	Aortic Rupture	90	<b>3.3</b>	<b>Pulmonary Vessels</b>	109
	Leriche Syndrome	92	3.3.1	Anatomy	109
	Coral Reef Aorta	92	3.3.2	Development	111
	Aortitis	94	3.3.3	Congenital Anomalies	111
	Vasculitis	96		Pulmonary Artery Agenesis	111
	Malignant Vascular Tumors	97		Pulmonary Artery Sling	111
	Aortic Fistulas	98		Anomalous Pulmonary Venous Return	112
	Subclavian Steal Syndrome	99	3.3.4	Diseases	112
	Thoracic Outlet and Thoracic Inlet Syndrome	101		Pulmonary Artery Aneurysm	112
<b>3.2</b>	<b>Vena Cava and Large Veins</b>	102		Pulmonary Embolism	113
3.2.1	Anatomy	102		Pulmonary Hypertension	116
3.2.2	Development	102		Arteriovenous Malformations	118
3.2.3	Congenital Anomalies	103		<b>Bibliography</b>	121
	Persistent Left Superior Vena Cava	103			
	Left-Sided and Duplicated Inferior Vena Cava	103			
	Azygos or Hemiazygos Continuation	104			
<b>4.</b>	<b>Lung and Pleura</b>	122			
	<i>Gabriele A. Krombach</i>				
<b>4.1</b>	<b>Anatomy</b>	122		Langerhans Cell Histiocytosis, Histiocytosis X	159
4.1.1	Pleura and Interlobar Fissures	122		Lymphangioleiomyomatosis and Pulmonary Involvement by	
4.1.2	Trachea and Pulmonary Segments	122		Tuberous Sclerosis	159
4.1.3	Vessels	123		Cystic Fibrosis	161
4.1.4	Pulmonary Veins	125	4.3.5	Pneumoconioses	162
4.1.5	Lung Parenchyma	127		Silicosis	162
<b>4.2</b>	<b>Tracheobronchial System</b>	128		Asbestosis	163
4.2.1	Normal Variant: Tracheal Bronchus	128		Other Pneumoconioses	164
4.2.2	Tracheal Stenosis and Tracheopathia Osteochondroplastica	129		Summary	165
4.2.3	Bronchiectasis	129	4.3.6	Extrinsic Allergic Alveolitis	165
4.2.4	Bronchiolitis	129	4.3.7	Pulmonary Trauma	165
4.2.5	Constrictive Bronchiolitis	131		Trauma Due to Smoke Inhalation, Fire, or Toxic Gases	165
4.2.6	Emphysema, Alpha <sub>1</sub> -Antitrypsin Deficiency, and Chronic Obstructive Pulmonary Disease	131		Mixed Aspiration Events	166
4.2.7	Atelectasis	133	4.3.8	Vasculitides	166
<b>4.3</b>	<b>Lung</b>	135		Wegener's Granulomatosis	166
4.3.1	Congenital Malformations	135		Churg–Strauss Syndrome	167
	Malformations of the Lung	135	4.3.9	Connective Tissue Diseases	168
4.3.2	Infections	139	4.3.10	Amyloidosis	169
	Pneumonia	139	4.3.11	Goodpasture's Syndrome, Intrapulmonary Hemorrhage	170
	Septic Emboli	141	4.3.12	Alveolar Microlithiasis	170
	Tuberculosis	142	4.3.13	Alveolar Proteinosis	171
	Aspergillosis	144	4.3.14	Pulmonary Infarction	172
	Swyer–James–MacLeod Syndrome	147	4.3.15	Respiratory Distress Syndrome	172
4.3.3	Neoplasms	147		Adult Respiratory Distress Syndrome	172
	Pulmonary Nodules	147		Infant Respiratory Distress Syndrome	174
	Lung Cancer	149	<b>4.4</b>	<b>Pleura</b>	175
	Hamartoma	150	4.4.1	Pneumothorax	175
4.3.4	Diffuse Lung Diseases	151	4.4.2	Pleural Effusion	176
	Interstitial Lung Diseases: Idiopathic Interstitial Pneumonias	151	4.4.3	Pleural Empyema	176
	Sarcoidosis	158		Pleural Mesothelioma	176
				<b>Bibliography</b>	178

**Part 2: Abdomen**

<b>5. Liver</b> .....	182		
<i>Guenther Schneider and Gabriele A. Krombach</i>			
<b>5.1 Anatomy</b> .....	182	Mesenchymal Lesions .....	193
<b>5.2 Anatomical Variants</b> .....	182	Primary Hepatocellular Lesions .....	206
<b>5.3 Imaging</b> .....	182	5.5.2 Secondary Hepatic Lesions .....	218
5.3.1 Landmarks .....	182	Hepatic Metastases .....	218
5.3.2 Imaging Techniques .....	182	Inflammatory Changes: Hepatic Abscess .....	221
Ultrasonography .....	182	Parasitic Lesions .....	221
Computed Tomography .....	183	5.5.3 Pseudolesions of the Liver Parenchyma .....	227
Magnetic Resonance Imaging .....	184	Focal Fatty Infiltration and Fatty Sparing .....	227
Unenhanced Imaging Techniques .....	185	<b>5.6 Diffuse Liver Diseases</b> .....	227
Contrast-Enhanced Imaging Techniques .....	185	5.6.1 Cirrhosis .....	227
<b>5.4 Vascular Diseases</b> .....	186	5.6.2 Iron Storage Diseases .....	230
5.4.1 Portal Vein Thrombosis .....	186	Hemochromatosis .....	230
5.4.2 Budd–Chiari Syndrome .....	190	Hemosiderosis .....	231
5.4.3 Rendu–Osler–Weber Disease .....	192	Hepatic Steatosis .....	232
<b>5.5 Focal Hepatic Lesions</b> .....	193	<b>5.7 Liver Injuries</b> .....	235
5.5.1 Primary Hepatic Lesions .....	193	<b>Bibliography</b> .....	239
<b>6. Gallbladder and Biliary Tract</b> .....	242		
<i>Horst D. Litzlbauer</i>			
<b>6.1 Anatomy</b> .....	242	<b>6.5 Acquired Diseases</b> .....	256
6.1.1 Biliary Fluid .....	242	6.5.1 Gallstones and Their Sequelae .....	256
6.1.2 Biliary Capillaries and Bile Ducts .....	242	Silent Cholelithiasis .....	258
6.1.3 Gallbladder .....	242	Symptomatic Cholecystolithiasis .....	261
6.1.4 Blood Vessels, Lymphatics, and Nerves .....	243	Gallbladder Hydrops and Empyema .....	264
<b>6.2 Physiology and Pathophysiology</b> .....	243	Chronic Cholecystitis and Porcelain Gallbladder .....	266
6.2.1 Cholestasis (Obstructive Jaundice) .....	243	Mirizzi’s Syndrome .....	268
<b>6.3 Imaging</b> .....	245	6.5.2 Inflammatory and Infectious Biliary Tract Diseases .....	270
6.3.1 Conventional Radiography .....	245	Ascending Cholangitis .....	270
6.3.2 Ultrasonography .....	245	Primary Sclerosing Cholangitis .....	272
Initial Ultrasound Examination .....	245	6.5.3 Benign Tumors and Hyperplastic Changes .....	273
Ultrasound Evaluation of Gallbladder Function .....	246	Gallbladder Polyps .....	273
6.3.3 Computed Tomography .....	246	Benign Hyperplasia of the Gallbladder Wall (Adenomyomatosis and Cholesterosis) .....	275
6.3.4 Magnetic Resonance Imaging and Magnetic Resonance Cholangiopancreatography .....	246	Intraductal Papillary Mucinous Neoplasm .....	277
6.3.5 Percutaneous Transhepatic Cholangiodrainage .....	247	6.5.4 Malignant Tumors .....	277
<b>6.4 Normal Variants, Developmental Anomalies, and Congenital Disorders</b> .....	248	Gallbladder Carcinoma .....	277
6.4.1 Anatomical Variants .....	249	Biliary Cystadenocarcinoma .....	280
Variants of the Gallbladder .....	249	Cholangiocarcinoma .....	281
Variants of the Bile Ducts and Biliary Vessels .....	249	6.5.5 Injuries and Posttherapeutic Changes .....	283
6.4.2 Biliary Atresia .....	250	Injuries of the Gallbladder and Biliary Tree .....	283
6.4.3 Choledochal Cysts .....	253	Changes after Cholecystectomy .....	287
6.4.4 Caroli’s Disease and Caroli’s Syndrome .....	254	Changes after Endoscopic Retrograde Cholangiopancreatography and Percutaneous Transhepatic Cholangiodrainage .....	289
<b>7. Pancreas</b> .....	295	Chemotherapy-induced Cholangitis and Cholecystitis .....	291
<i>Lars Grenacher and Franziska Fritz</i>			
<b>7.1 Anatomy</b> .....	295	<b>Bibliography</b> .....	293
7.1.1 Position .....	295		
Histology .....	295		

7.1.2	Blood Supply	295	7.3.3	Cystic Lesions	308
7.1.3	Development	295		Unilocular Cysts: Pseudocysts	308
7.1.4	Imaging Landmarks	295		Microcystic Lesions: Serous Cystadenoma	309
7.1.5	Normal Variants and Congenital Anomalies	297		Macrocystic Lesions	311
	Pancreas divisum	297		Cysts with Solid Components: Solid Pseudopapillary Tumor	313
	Annular Pancreas	297		Differential Diagnosis of Cystic Tumors	313
<b>7.2</b>	<b>Nonneoplastic Diseases</b>	297		Summary	313
7.2.1	Acute Pancreatitis	297	<b>7.4</b>	<b>Generalized Pancreatic Changes</b>	313
7.2.2	Chronic Pancreatitis	300	7.4.1	Pancreatic Lipoma	313
	Subtype: Autoimmune Pancreatitis	303	7.4.2	Cystic Fibrosis	314
<b>7.3</b>	<b>Neoplastic Diseases</b>	303	7.4.3	Primary Hemochromatosis	317
7.3.1	Ductal Adenocarcinoma	303		<b>Bibliography</b>	319
7.3.2	Neuroendocrine Tumors	306			
<b>8.</b>	<b>Gastrointestinal Tract</b>	322			
	<i>Thomas C. Lauenstein and Lale Umutlu</i>				
<b>8.1</b>	<b>Anatomy</b>	322	8.4.7	Gastric Carcinoma	337
8.1.1	Position and Divisions	322	<b>8.5</b>	<b>Diseases of the Jejunum and Ileum</b>	338
8.1.2	Imaging Landmarks	323	8.5.1	Meckel's Diverticulum	338
<b>8.2</b>	<b>Imaging</b>	325	8.5.2	Intestinal Obstruction	338
8.2.1	Radiography	325	8.5.3	Intussusception	339
8.2.2	Computed tomography and Magnetic Resonance Imaging	326	8.5.4	Mesenteric Ischemia	340
8.2.3	Contrast Media	326	8.5.5	Hemorrhage	342
<b>8.3</b>	<b>Diseases of the Esophagus</b>	326	8.5.6	Crohn's Disease	342
8.3.1	Achalasia	326	8.5.7	Adenocarcinoma	345
8.3.2	Esophageal Diverticula	327	8.5.8	Carcinoid Tumors	346
8.3.3	Esophageal Varices	328	<b>8.6</b>	<b>Diseases of the Colon and Rectum</b>	347
8.3.4	Esophageal Atresia and Tracheoesophageal Fistula	329	8.6.1	Volvulus	347
8.3.5	Hiatal Hernia	330	8.6.2	Appendicitis	348
8.3.6	Esophageal Carcinoma	330	8.6.3	Epiplioic Appendagitis	349
<b>8.4</b>	<b>Diseases of the Gastroduodenum</b>	331	8.6.4	Pseudomembranous Colitis	349
8.4.1	Hypertrophic Pyloric Stenosis	332	8.6.5	Ulcerative Colitis	349
8.4.2	Diverticula	333	8.6.6	Imaging signs	350
8.4.3	Peptic Ulcer Disease	333	8.6.7	Clinical features	350
8.4.4	Zollinger–Ellison Syndrome	335	8.6.8	Diverticulosis and Diverticulitis	351
8.4.5	Gastrointestinal Stromal Tumors	336	8.6.9	Colorectal Carcinoma	351
8.4.6	Lymphoma	336	8.6.10	Ogilvie's Syndrome	353
				<b>Bibliography</b>	354
<b>9.</b>	<b>Spleen and Lymphatic System</b>	355			
	<i>Christoph Thomas</i>				
<b>9.1</b>	<b>Introduction</b>	355		Splenic Infarction	359
<b>9.2</b>	<b>Spleen</b>	355		Splenic Cysts	360
9.2.1	Anatomy	355		Splenic Abscess	361
9.2.2	Imaging	355		Neoplastic Diseases	362
	Radiography	355		Splenic Metastases	362
	Ultrasound	356		Splenic Rupture	364
	Computed Tomography	356		Splenic Artery Aneurysm	364
	Magnetic Resonance Imaging	357	<b>9.3</b>	<b>Lymph Nodes</b>	365
9.2.3	Anomalies and Normal Variants	357	9.3.1	Anatomy	365
	Accessory Spleen	357	9.3.2	Imaging	365
	Asplenia and Polysplenia	357		Ultrasound	366
9.2.4	Diseases	358		Chest Radiography	366
	Differential Diagnosis of Splenomegaly	358		Computed Tomography	366
				Magnetic Resonance Imaging	366

9.3.3	Positron Emission Tomography–Computed Tomography	366	Sarcoidosis	370
	Diseases	366	Multiple Myeloma	370
	Differential Diagnosis of Lymph Node Enlargement	366	<b>Bibliography</b>	373
	Malignant Lymphoma	367		
	Castleman's Disease	370		
<b>10.</b>	<b>Adrenal Glands</b>	374		
	<i>Andreas Saleh</i>			
<b>10.1</b>	<b>Anatomy</b>	374	Hypercortisolism	381
<b>10.2</b>	<b>Imaging</b>	374	Hyperaldosteronism	381
10.2.1	Ultrasound	374	Pheochromocytoma	382
	Adults	374	Virilization	384
	Children	374	Adrenocortical Insufficiency	385
10.2.2	Computed Tomography	376	<b>10.3.3 Tumors</b>	385
10.2.3	Positron Emission Tomography–Computed Tomography	377	Adrenal Cysts	385
10.2.4	Magnetic Resonance Imaging	377	Adrenal Myelolipoma	385
10.2.5	Adrenal Vein Sampling	379	Adrenal Adenomas	387
<b>10.3</b>	<b>Diseases</b>	379	Adrenal Metastases	387
10.3.1	Incidentalomas	379	Neuroblastoma	388
10.3.2	Functional Disorders	381	Adrenal Hematoma	388
			Adrenocortical Carcinoma	390
			<b>Bibliography</b>	391
<b>11.</b>	<b>Kidney and Urinary Tract</b>	393		
	<i>Ulrike Attenberger, Johanna Nissen, and Metin Sertdemir</i>			
<b>11.1</b>	<b>Kidney</b>	393	11.1.4 Renal Transplantation	420
11.1.1	Imaging	393	Preoperative Evaluation	420
	Ultrasound	393	Postoperative Period	420
	Radiography	393	<b>11.2 Urinary Tract</b>	420
	Voiding Cystourethrography	393	11.2.1 Retroperitoneal Masses	420
	Computed Tomography	393	11.2.2 Congenital Variants	421
	Magnetic Resonance Imaging	394	11.2.3 Bladder Masses	422
11.1.2	Anatomy and Congenital Variants	394	11.2.4 Urothelial Carcinoma of the Upper Urinary Tract	425
	Anatomy	394	11.2.5 Ureteral Stones	427
	Congenital Variants	395	11.2.6 Urachal Cysts	429
11.1.3	Diseases	396	<b>Bibliography</b>	429
	Masses	396		
	Inflammatory Changes	413		
	Vascular Changes	417		
<b>12.</b>	<b>Female Pelvis</b>	430		
	<i>Céline D. Alt</i>			
<b>12.1</b>	<b>Anatomy</b>	430	12.3.1 Bicornuate Uterus, Uterus Didelphys, and (Sub) Septate Uterus	435
12.1.1	External and Internal Genitalia	430	12.3.2 Hymenal Atresia	435
12.1.2	Suspensory Apparatus	432	12.3.3 Uterovaginal Agenesis	436
12.1.3	Pelvic Floor	432	<b>12.4 Diseases</b>	436
12.1.4	Blood Supply	432	12.4.1 Inflammatory Changes	436
12.1.5	Lymphatic Drainage	432	Tuberculosis of the Genital Tract	437
<b>12.2</b>	<b>Imaging</b>	432	Vaginal Fistulas	438
12.2.1	Transabdominal Ultrasound	433	<b>12.4.2 Benign Lesions and Pseudotumors</b>	438
12.2.2	Magnetic Resonance Imaging	433	Cysts of the Uterus, Vulva, and Vagina	438
12.2.3	Computed Tomography	434	Ovarian and Tubal Torsion	440
12.2.4	Differential Diagnosis	434	Polyps	440
<b>12.3</b>	<b>Congenital Anomalies</b>	435	Leiomyomas	441
			Endometriosis	442

12.4.3	Malignant Lesions	447			
	Endometrial Carcinoma	447			
	Cervical Carcinoma	449			
	Vaginal Carcinoma	451			
	Vulvar Carcinoma	453			
	Recurrent Tumors	455			
				Sarcomas of the Pelvic Organs	455
				Pelvic Lymphoma	457
				Ovarian Tumors	458
				Fallopian Tube Carcinoma	461
				<b>Bibliography</b>	464
<b>13.</b>	<b>Male Pelvis</b>				467
	<i>Tobias Franiel</i>				
<b>13.1</b>	<b>Testis and Epididymis</b>	467	<b>13.2</b>	<b>Penis</b>	477
13.1.1	Imaging	467	13.2.1	Imaging	477
13.1.2	Anatomy	467	13.2.2	Anatomy	477
13.1.3	Congenital Disorders: Cryptorchidism (Undescended Testis)	469	13.2.3	Vascular Disorders	478
13.1.4	Vascular Diseases	469		Priapism	478
	Varicocele	469		Cavernosal Thrombosis	479
	Testicular Torsion	470	13.2.4	Inflammatory Disorders: Peyronie's Disease	479
13.1.5	Inflammatory Diseases: Epididymitis and Epididymo-orchitis	471	13.2.5	Traumatic Disorders: Penile Fracture	479
13.1.6	Traumatic Disorders: Testicular Trauma	471	13.2.6	Penile Carcinoma	482
13.1.7	Benign Intrasrotal Masses	471	<b>13.3</b>	<b>Prostate and Seminal Vesicles</b>	483
	Hydrocele	471	13.3.1	Imaging	483
	Spermatocele	472	13.3.2	Anatomy	483
	Testicular Microlithiasis	473	13.3.3	Prostatitis	484
13.1.8	Malignant Neoplasms	474	13.3.4	Benign Prostatic Hyperplasia	486
	Testicular Tumors	474	13.3.5	Prostate Cancer	487
	Epididymal Tumors	477		<b>Bibliography</b>	489
<b>Index</b>					491

# Foreword

Anyone who has seen the lively public interest in the printed media sold at conferences and book fairs might easily conclude that the “electronic media revolution” does not exist.

On the other hand, it is clear that growing numbers of younger people are no longer reading printed media, especially newspapers and periodicals. Fortunately, this trend has not yet reached the world of science and professional education, which still values the classic printed text and still thirsts for technical information drawn from the print medium. This climate has helped to motivate the authors of this book.

Diagnostic imaging of the chest and abdomen accounts for much of the routine daily work in radiology. Anyone who has written a book knows how much work and effort are needed to convey facts and knowledge in a didactically appealing way. That challenge has been met here with outstanding success. A book of this kind can expect a wide readership, especially in the setting of

specialist training and also as a reference work for practicing radiologists and interested physicians in other disciplines.

The editors of this book are from the radiology department at Aachen University Hospital, Germany, which I directed for many years, and I am pleased that they have worked together from their academic offices in Giessen and Marburg to complete this challenging project.

I hope, therefore, that *Body Imaging: Thorax and Abdomen* will be well received, will gain a wide readership, and will resonate strongly with the medical community.

*Professor Rolf W. Guenther, MD  
Department of Radiology  
Charité Hospital  
Berlin, Germany*

# Preface

Radiology plays a central role in the diagnostic algorithm for most patients. Selecting a modality that is best for a particular case represents the first challenge on the path to a correct diagnosis. Guidelines or evidence-based recommendations have already been established for most indications and inquiries, helping physicians to make the correct decision for any given case. Once the appropriate modalities have been selected and the images have been obtained, the results must be interpreted within the context of the clinical presentation. This process requires an awareness of possible causative disorders, a directed look at specific body regions, and a systematic image analysis that includes the critical evaluation of all available findings. For an experienced radiologist, anatomical landmarks provide an indispensable aid for image analysis. Radiologists have honed their skills over many years and apply them on an intuitive basis. But this option is not available to beginners, who must painstakingly learn and learn to recognize anatomical landmarks and the typical signs of pathologic changes.

The authors contributing to this book are all experts in their respective fields. Their goal was to introduce less experienced readers to diagnostic imaging of the chest and abdomen, placing special emphasis upon clinical signs and symptoms and relevant anatomical landmarks.

The modalities of plain radiography, ultrasonography, CT, and MRI are all covered in this textbook. The scope of the book reflects the application of these modalities in routine clinical use. Every author has made a special effort to take note of current guidelines and recommendations. The images have been selected for their value as teaching aids and are supplemented by diagrams and drawings.

The text in each section is arranged by subheads—Brief Definition, Clinical Features, Imaging Signs, Differential Diagnosis, and Key Points (and occasionally others)—so that readers can quickly and easily locate specific areas of interest relating to radiological interpretation. Important teaching points have been condensed and highlighted in color boxes.

In presenting the triad of clinical symptoms, anatomical landmarks, and radiological findings, this book seeks to familiarize current and future generations of radiologists and allied specialties with this systematic approach to image interpretation.

We hope that our readers will derive the greatest possible benefit from this approach and will gain a lasting understanding of radiological interpretation in the chest and abdomen.

*Gabriele A. Krombach, MD  
Andreas H. Mahnken, MD, MBA, MME*

# Acknowledgments

We thank all our authors for their contributions, which they managed so capably while meeting the demands of their clinical practice. We also thank all of our colleagues at radiology centers and departments, whose excellent work has brought forth the illustrations used in this book.

We express special thanks to the team at Georg Thieme Verlag, especially Dr. Siegfried Steindl, who was instrumental in conceiving the idea for this book; Ms. Susanne Huis, MA, who made the concept a reality with unparalleled warmth and

dependability; and Dr. Christian Urbanowicz and Mr. Florian Toniutti—all of whom pooled their talents to create a highly professional and efficient team.

We also thank our referring colleagues for the close, ongoing dialogue that is essential for the substantive practice of radiology.

*Gabriele A. Krombach, MD*  
*Andreas H. Mahnken, MD, MBA, MME*

# Contributors

## Editors

**Gabriele A. Krombach, MD**  
**Professor**  
Department of Diagnostic and Interventional Radiology  
Justus Liebig University Giessen  
Giessen University Hospital  
Giessen, Germany

**Andreas H. Mahnken, MD, MBA, MME**  
**Professor**  
Diagnostic and Interventional Radiology  
Philipps University  
Marburg University Hospital  
Marburg, Germany

## Contributing Authors

**Céline D. Alt, MD**  
Department of Diagnostic and Interventional Radiology  
Düsseldorf University Hospital  
Düsseldorf, Germany

**Ulrike I. Attenberger, MD**  
**Professor**  
Department of Clinical Radiology and Nuclear Medicine  
Mannheim University Hospital  
Specialty: Oncologic and Preventive Medicine  
Mannheim, Germany

**Tobias Franiel, MD**  
**Associate Professor**  
Department of Diagnostic and Interventional Radiology  
Jena University Hospital  
Jena, Germany

**Franziska L. Fritz, MD**  
Department of Diagnostic and Interventional Radiology  
Heidelberg University Hospital  
Heidelberg, Germany

**Lars Grenacher, MD**  
**Professor**  
Department of Diagnostic and Interventional Radiology  
Heidelberg University Hospital  
Heidelberg, Germany

**Thomas C. Lauenstein, MD**  
**Professor**  
Department of Diagnostic and Interventional Radiology and  
Neuroradiology  
Essen University Hospital  
Essen, Germany

**Horst D. Litzlbauer, MD**  
Center for Radiology  
Giessen University Hospital  
Giessen, Germany

**Johanna Nissen, MD**  
Department of Clinical Radiology and Nuclear Medicine  
Mannheim University Medical Center  
Mannheim, Germany

**Andreas Saleh, MD**  
**Professor**  
Department of Diagnostic and Interventional Radiology and  
Pediatric Radiology  
Schwabing Hospital  
Munich, Germany

**Guenther Schneider, MD**  
**Professor**  
Department of Diagnostic and Interventional Radiology  
Saarland University Hospital  
Homburg, Germany

**Metin Sertdemir, MD**  
Diagnostic Group Practice  
Karlsruhe, Germany

**Christoph Thomas, MD**  
**Associate Professor**  
Department of Diagnostic and Interventional Radiology  
Düsseldorf University Hospital  
Düsseldorf, Germany

**Lale Umutlu, MD**  
**Associate Professor**  
Department of Diagnostic and Interventional Radiology and  
Neuroradiology  
Essen University Hospital  
Essen, Germany

# Abbreviations

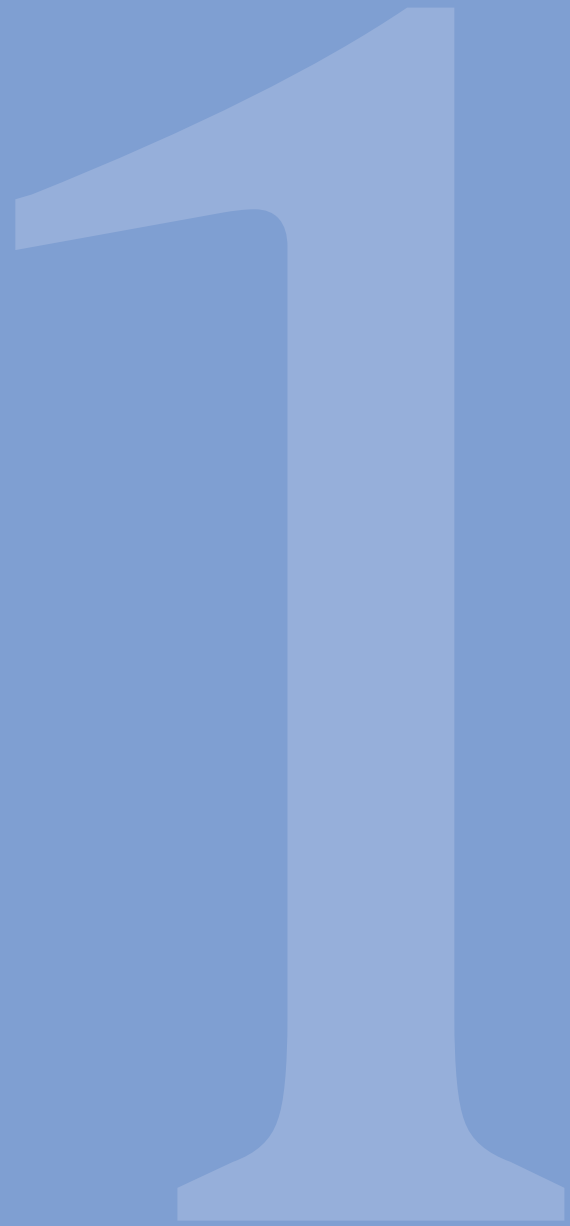
AAST	American Association for the Surgery of Trauma	HU	Hounsfield unit
ACE	angiotensin-converting enzyme	IASLC	International Association for the Study of Lung Cancer
ACTH	adrenocorticotrophic hormone	ICU	intensive care unit
ADC	apparent diffusion coefficient	IgA	immunoglobulin A
ADPKD	autosomal dominant polycystic kidney disease	IGCCCG	International Germ Cell Cancer Collaborative Group
AECC	American–European Consensus Conference	IIP	idiopathic interstitial pneumonia
AFP	alpha-fetoprotein	ILO	International Labor Organization
AHA	American Heart Association	INSS	International Neuroblastoma Staging System
AIP	acute interstitial pneumonia	IPAS	intrapancreatic accessory spleen
AJCC	American Joint Committee on Cancer	IPF	idiopathic pulmonary fibrosis
ANCA	antineutrophil cytoplasmic antibody	IPMN	intraductal papillary mucinous neoplasm
ANP	atrial natriuretic peptide	IRDS	infant respiratory distress syndrome
AP	anteroposterior	IV	intravenous
APACHE	acute physiology and chronic health evaluation	LAVA	liver acquisition with volume acceleration
ARDS	acute respiratory distress syndrome	LIP	lymphoid interstitial pneumonia
ARPKD	autosomal recessive polycystic kidney disease	LLD	left lateral decubitus
ATP	adenosine triphosphate	μm	micrometer
ATS	American Thoracic Society	MALT	mucosa-associated lymphoid tissue
AWMF	(German) Association of Scientific Medical Societies	MEN	multiple endocrine neoplasia
BALT	bronchus-associated lymphoid tissue	MIBG	metaiodobenzylguanidine
BPH	benign prostatic hyperplasia	MP RAGE	magnetization-prepared rapid-acquisition gradient echo
BW	body weight	MRA	magnetic resonance angiography
cANCA	cytoplasmic antineutrophil cytoplasmic antibodies	MRCP	magnetic resonance cholangiopancreatography
CNS	central nervous system	mRECIST	modified response evaluation criteria in solid tumors
COP	cryptogenic organizing pneumonia	MRI	magnetic resonance imaging
COPD	chronic obstructive pulmonary disease	MRS	magnetic resonance spectroscopy
CPAP	continuous positive airway pressure	ms	millisecond
CREST	calcinosis, Raynaud phenomenon, esophageal dysmotility, sclerodactyly, and telangiectasia	M <sub>z</sub>	longitudinal magnetization
CRP	C-reactive protein	NASH	nonalcoholic steatohepatitis
CSF	cerebrospinal fluid	NSAIDs	nonsteroidal anti-inflammatory drugs
CT	computed tomography	NSIP	nonspecific interstitial pneumonia
CTA	CT angiography	NSTEMI	non–ST segment elevation myocardial infarction
DIP	desquamative interstitial pneumonia	PA	<i>posteroanterior; pulmonary artery</i>
DSA	digital subtraction angiography	PACS	picture archiving and communication system
DWI	diffusion-weighted imaging	pANCA	perinuclear antineutrophil cytoplasmic antibodies
ECG	electrocardiogram, electrocardiography	PaO <sub>2</sub>	arterial oxygen partial pressure
EPI	echo planar imaging	PCR	polymerase chain reaction
ER	emergency room	PEEP	positive end-expiratory pressure
ERCP	endoscopic retrograde cholangiopancreatography	PET	positron emission tomography
ERS	European Respiratory Society	PPFE	pleuroparenchymal fibroelastosis
ESR	erythrocyte sedimentation rate	PSA	prostate-specific antigen
ESUR	European Society of Urogenital Radiology	PTC	percutaneous transhepatic cholangiography
FDG	fluorodeoxyglucose	PTCD	percutaneous transhepatic cholangiodrainage
FIGO	International Federation of Gynecology and Obstetrics	PUD	peptic ulcer disease
FiO <sub>2</sub>	fraction of oxygen concentration in the inspired air	RB-ILD	respiratory bronchiolitis associated interstitial lung disease
GBM	glomerular basement membrane	RECIST	response evaluation criteria in solid tumors
Gd-DTPA	gadolinium diethylenetriamine pentaacetic acid	ROI	region of interest
GIST	gastrointestinal stromal tumor	SALT	skin-associated lymphoid tissue
gRE	global relative enhancement	SE	spin echo
GRE	gradient echo (sequence)	SI	signal intensity
HASTE	half-Fourier acquisition single-shot turbo spin-echo	SIOPEL	International Childhood Liver Tumor Strategy Group
HCG	human chorionic gonadotropin	SE	spin echo
HHT	hereditary hemorrhagic telangiectasia	SIOP	International Society of Pediatric Oncology
HIDA	hepatobiliary iminodiacetic acid	SIRT	selective internal radiation therapy
HIV	human immunodeficiency virus	SOFA	sequential organ failure assessment
HNPCC	hereditary nonpolyposis colorectal cancer	SPECT	single-photon emission computed tomography
HRCT	high-resolution computed tomography		

SPIO	supraparamagnetic iron oxide	TSE	turbo spin echo
STEMI	ST segment elevation myocardial infarction	TWIST	time-resolved angiography with interleaved stochastic trajectories
STIR	short tau inversion recovery	UICC	Union for International Cancer Control ( <i>Union Internationale contre le Cancer</i> )
T1W	T1-weighted	UIP	usual interstitial pneumonia
T2W	T2-weighted	VIBE	volume-interpolated breath-hold examination
TACE	transarterial chemoembolization	VIN	vulvar intraepithelial neoplasia
TASC	Transatlantic Inter-Society Consensus	WHO	world health organization
TAVI	transcatheter aortic valve implantation	XDR	extremely drug-resistant
Tc	technetium		
TIPS	transjugular intrahepatic portosystemic shunt		
TrueFISP	true fast imaging with steady precession		

# Part 1

## Chest

1	Mediastinum	2
2	Heart and Pericardium	30
3	Large Vessels	72
4	Lung and Pleura	122



# 1 Mediastinum

Gabriele A. Krombach

## 1.1 Anatomy

► **Location and divisions.** The mediastinum extends from the thoracic inlet to the diaphragm and is bounded laterally by mediastinal pleura. The mediastinum constitutes a single, coherent space that has no natural (fascial) barriers to the spread of tumors or inflammation. Nevertheless, it is useful conceptually to divide the mediastinum into parts because various diseases tend to occur at specific sites within the mediastinum, and the location of a pathologic process can be helpful in narrowing the diagnosis. The mediastinum is divided into anterior, middle, and posterior parts (► Fig. 1.1). The cervical fasciae communicate freely with the mediastinum, allowing inflammatory processes to spread contiguously from the neck into the mediastinum.

The mediastinum is further subdivided into the superior mediastinum and inferior mediastinum. The superior mediastinum extends downward from the thoracic inlet to the pericardium.

► **Radiographic landmarks.** ► Fig. 1.2 shows the mediastinal landmarks that appear on a standard chest radiograph.

### Note

- The *anterior mediastinum* contains the thymus, lymph nodes, and fat. Its upper portion extends from the chest wall to the ascending aorta and superior vena cava, its lower portion from the retrosternal surface to the pericardium.
- The largest of the three compartments, the *middle mediastinum*, contains the heart, trachea, and large vessels arising from the aortic arch.
- The *posterior mediastinum* contains the esophagus, descending aorta, azygos and hemiazygos veins, and thoracic duct.



### Caution

The pericardial reflection extends far in a cranial direction anteriorly and encloses almost the entire ascending aorta as far as the horizontal segment of the aortic arch.

► **CT landmarks (► Fig. 1.3)**

- The sternum and ascending aorta provide landmarks for the *thymic bed*, which is located between those structures.

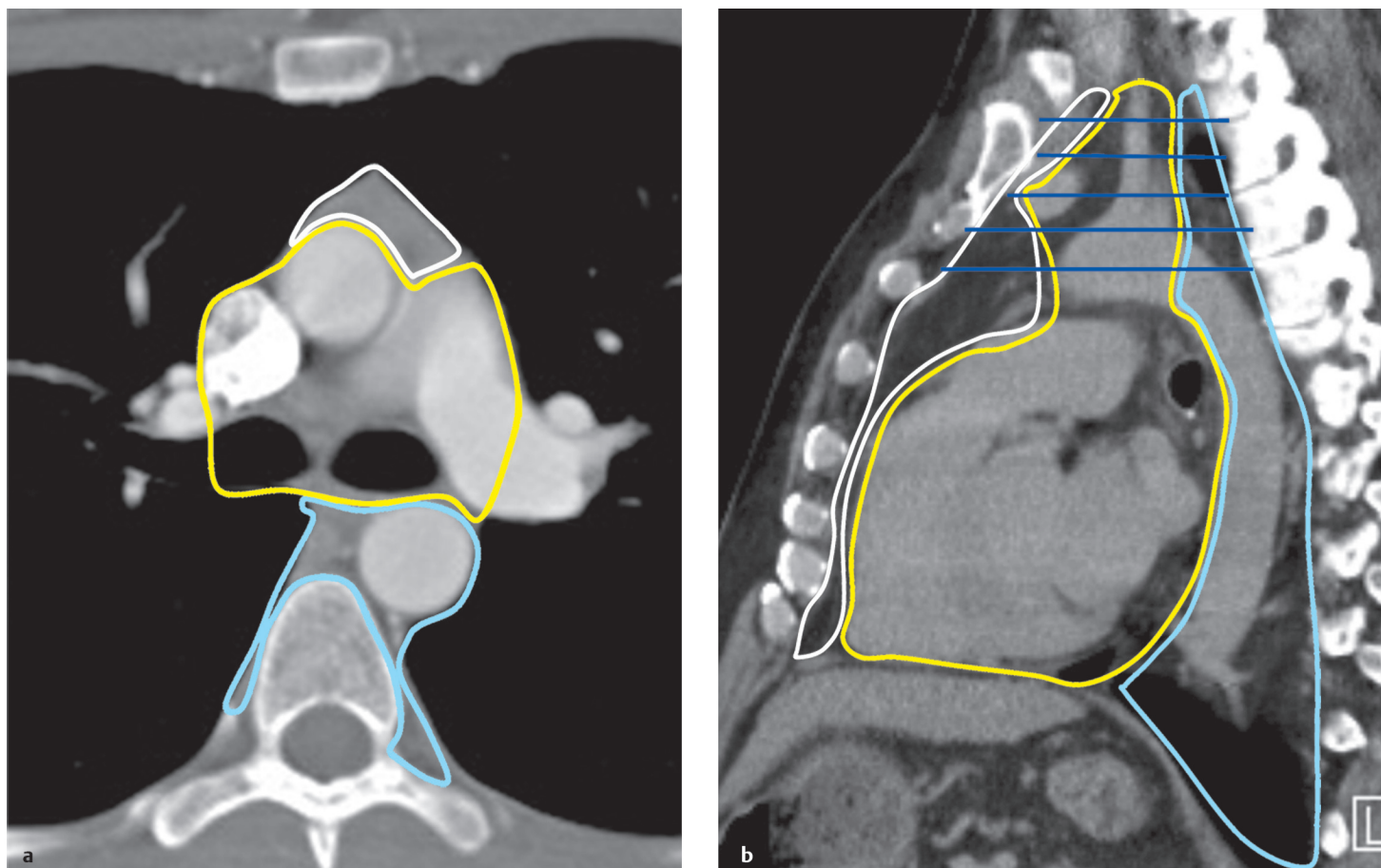


**Fig. 1.1 Divisions of the mediastinum.** (a) The divisions outlined in an axial CT scan. (b) The divisions outlined in a sagittal reformatted CT image. White indicates the anterior mediastinum (thymus, lymph nodes, and fatty tissue); yellow indicates the middle mediastinum (heart, aortic arch, pulmonary artery trunks, vena cava, trachea); light blue indicates the posterior mediastinum (descending aorta, esophagus, azygos and hemiazygos veins, thoracic duct); horizontal darker blue lines indicate the superior mediastinum (space above the pericardial reflection).

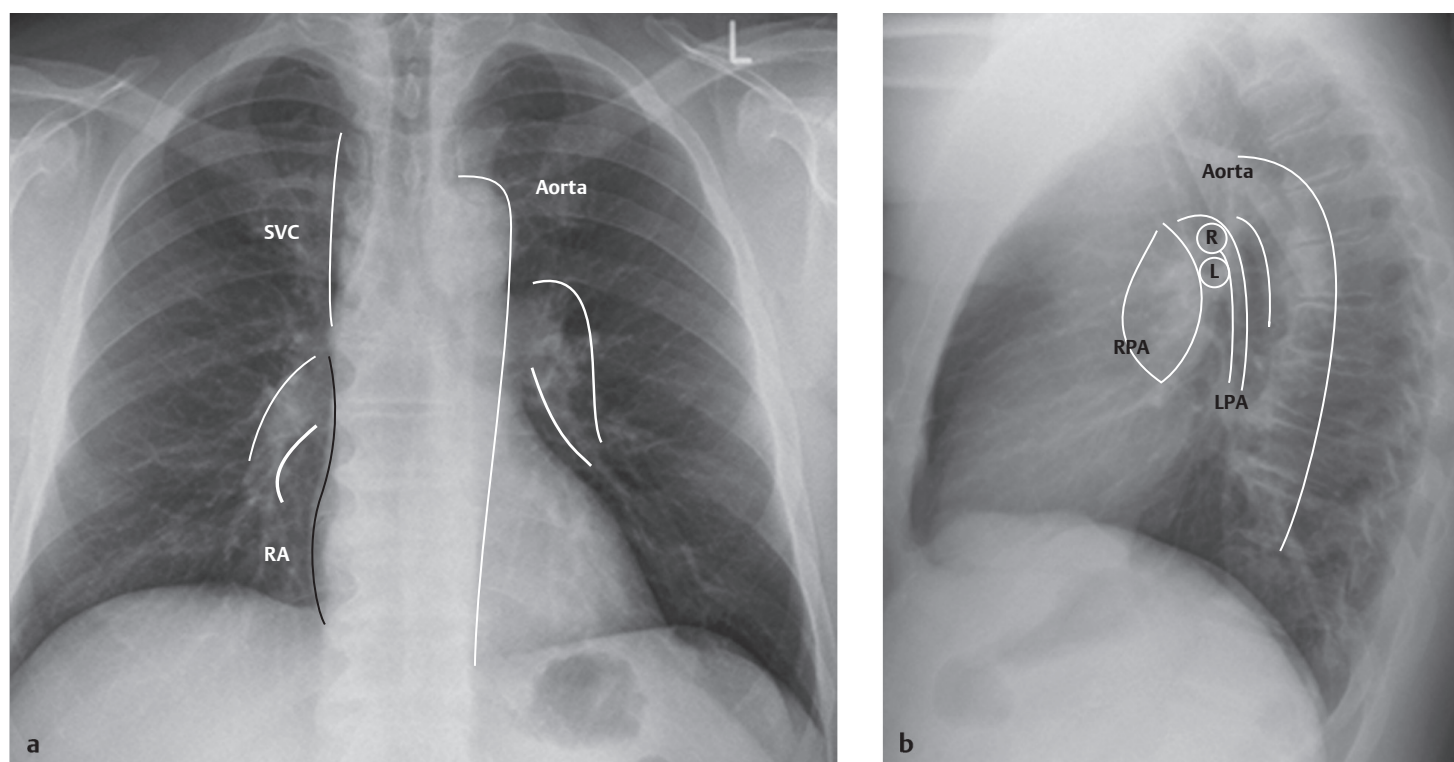


**Fig. 1.2 Landmarks for mediastinal structures on chest radiographs.** (a) PA view: the right mediastinal borders are formed by the superior vena cava (SVC), the pulmonary arteries in the hilum, and the right atrium (RA). The aortic contour is prominent on the left side. The left atrial appendage and left ventricle form the cardiac borders. The paravertebral line (black) is an edge-on projection of the pleura and immediate paravertebral soft tissues. (b) Lateral view: the left pulmonary artery (LPA) forms a cane-shaped figure that arches over the left main bronchus (L). The right pulmonary artery (RPA) runs for some distance across the mediastinum and appears end-on in the lateral view, creating an elliptical figure. The right main bronchus (R) runs just above it. The left main bronchus is projected below the right main bronchus. The aortopulmonary window is the gap between the left pulmonary artery and the aorta visible in the lateral projection.

- The most important landmarks in the superior mediastinum are the *supra-aortic branch vessels*. From right to left they are the brachiocephalic trunk, which branches into the right subclavian artery and common carotid artery; the left carotid artery; and the left subclavian artery (see ► Fig. 1.3a). The next vessel to the right is the superior vena cava. The trachea is located behind those vessels and is just anterior to the esophagus.
  - The *thoracic duct* ascends to the right of the aorta and opens into the junction of the left subclavian vein and left jugular vein. It collects lymphatic fluid from the lower extremities and abdominal organs in the upper left half of the body except for the left lower lobe of the lung. Its maximum diameter in the mediastinum is approximately 5 mm. The remaining areas on the right side are drained by the smaller right lymphatic duct.
  - The *vagus nerve* descends with the major vessels in the neck, entering the chest through the thoracic inlet. Below the level of the aortic arch it accompanies the esophagus in its descent through the mediastinum.
  - The right *recurrent laryngeal nerve* leaves the vagus nerve at the level of the subclavian artery, winds around that vessel, and ascends to the neck in the groove between the trachea and esophagus. The left recurrent laryngeal nerve is longer; it leaves the vagus nerve at the level of the aortic arch, passes behind the ductus arteriosus and around the aorta, and runs cephalad between the trachea and esophagus (► Fig. 1.4). Compression or infiltration of the nerve by a tumor leads to hoarseness.
  - The *phrenic nerve* arises from the C3–C5 nerve roots, leaves the brachial plexus, and accompanies the subclavian artery and vein through the thoracic inlet. It descends in the middle mediastinum along the pericardium to the diaphragm. Infiltration of the phrenic nerve by a mass leads to unilateral elevation of the diaphragm (► Fig. 1.5).
- **Selection of modalities.** The most common mediastinal diseases are masses. These present clinically with nonspecific complaints caused by the compression of surrounding structures. Typical presenting complaints are dyspnea, foreign-body sensation, and dysphagia. Chest radiographs in two planes are the imaging study of first choice in these cases; they can further narrow the diagnosis and may indicate a need for sectional imaging by CT or MRI. When mediastinal imaging is required in patients with a known disease entity or in cases where the history and symptoms are suspicious for a particular disease, CT is the modality of choice for defining the location and extent of the changes and for tumor staging. MRI should be added in selected cases where CT alone cannot detect or exclude conditions such as tumor infiltration of the pericardium or invasion of the spinal canal through the neural foramina. Ultrasound imaging has a minor role and may have limited applications in the anterior superior mediastinum. Transesophageal ultrasonography is needed to access the posterior mediastinum with ultrasound.

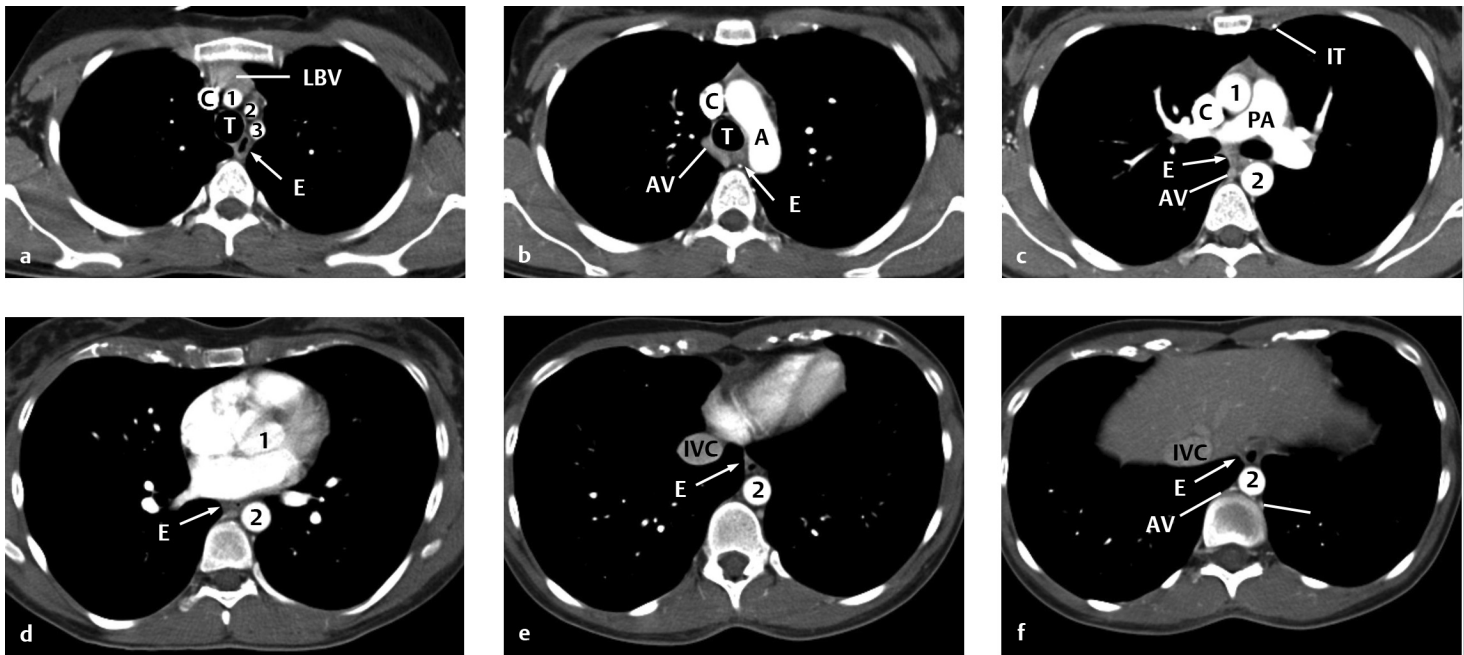


**Fig. 1.3 Landmarks for mediastinal structures on axial CT.** (a) Superior mediastinum, supra-aortic branches. Just posterior to the sternum is the left brachiocephalic vein (LBV). Just to the left of it are the vessels arising from the aortic arch, the brachiocephalic trunk (1), left common carotid artery (2), and left subclavian artery (3), which run anterior to the trachea (T). Just posterior to the trachea is the esophagus (E), whose small lumen can be traced through all the slices down to its passage through the diaphragm at the esophageal hiatus. The superior vena cava (C) can be traced through all slices from the union of both brachiocephalic veins to the right atrium. It occupies a right anterolateral position relative to the trachea and borders the brachiocephalic trunk on the right side. (b) At the level of the aortic arch (A), the azygos vein (AV) curves around the right main bronchus and opens into the superior vena cava (C). Additional landmarks for identifying the vessel are the spinal column and trachea (T). The azygos vein follows a right prevertebral path. (c) Below the aortic arch are the main trunk of the pulmonary artery and its division into the right and left pulmonary arteries, which forms a typical Y-shaped structure (PA). The left and right internal thoracic artery and vein, which arise from the subclavian artery and drain into the subclavian vein, respectively, follow a parasternal path on the inner chest wall. 1, ascending aorta; 2, descending aorta; C, superior vena cava; E, esophagus; IT, internal thoracic artery; AV, azygos vein. (d) The ascending aorta (1) arises from the middle of the heart. The descending aorta (2) occupies a left anterolateral position relative to the spinal column. E, esophagus. (e) The inferior vena cava (IVC) is identified at this level. 2, descending aorta; E, esophagus. (f) The hemiazygos vein ascends in a left prevertebral path to approximately the level of the T7 vertebral body, where it empties into the azygos vein (AV). 2, descending aorta; E, esophagus; IVC, inferior vena cava.

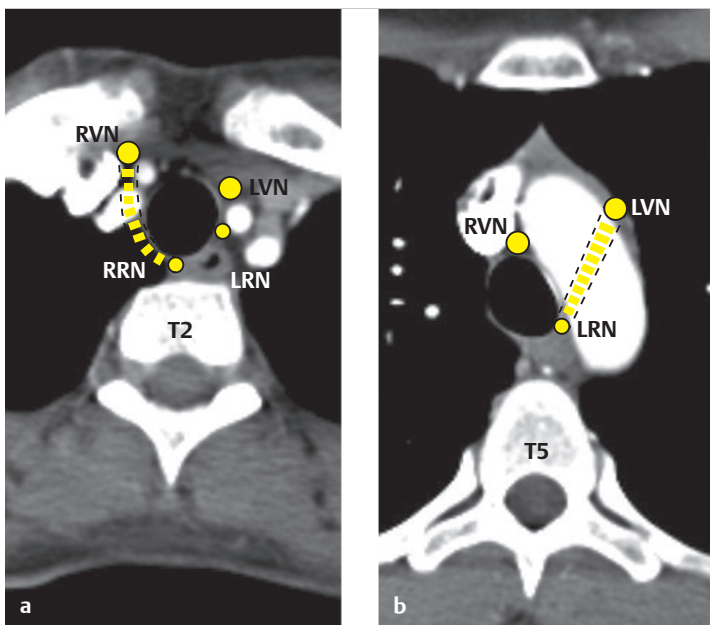


**Fig. 1.4 The course of the vagus nerve and the recurrent laryngeal nerve.** Axial scans demonstrate the course of the right vagus nerve (RVN) and left vagus nerve (LVN) and the right and left recurrent laryngeal nerve (RRN, LRN). The vagus nerve emerges from the skull base through the jugular foramen and runs behind the carotid artery in the carotid sheath. (a) The right recurrent laryngeal nerve leaves the vagus nerve at the level of the subclavian artery origin, loops around the vessel, and ascends to the larynx between the trachea and esophagus. (b) The left recurrent laryngeal nerve leaves the vagus nerve at the level of the aortic arch and runs below the aortic arch between the trachea and esophagus, where it ascends toward the head.

## 1.2 Evaluation of the Mediastinum on Conventional Radiographs

### 1.2.1 Silhouette Sign

When seen on conventional radiographs, soft tissues such as muscles, organs, and fluid are indistinguishable from one another in terms of their radiographic density. The radiographic phenomenon termed the silhouette sign may be helpful in determining the location of a mass.

- When organs of equal density border directly on one another, they form a composite silhouette of uniform density when viewed on a projection radiograph. This image resembles a paper cutout (the original “silhouette”) with one continuous outline and no internal gradations of shading or color (► Fig. 1.6).
- When two structures of equal density are located at different depths in the chest and are separated by a third structure of lower density, the two structures will appear sharply outlined relative to each other (► Fig. 1.7). They do not exhibit the silhouette sign.

### 1.2.2 Edge-on Effect

In conventional radiography, the edge-on effect describes the visualization of a very thin structure, such as the pleura, when

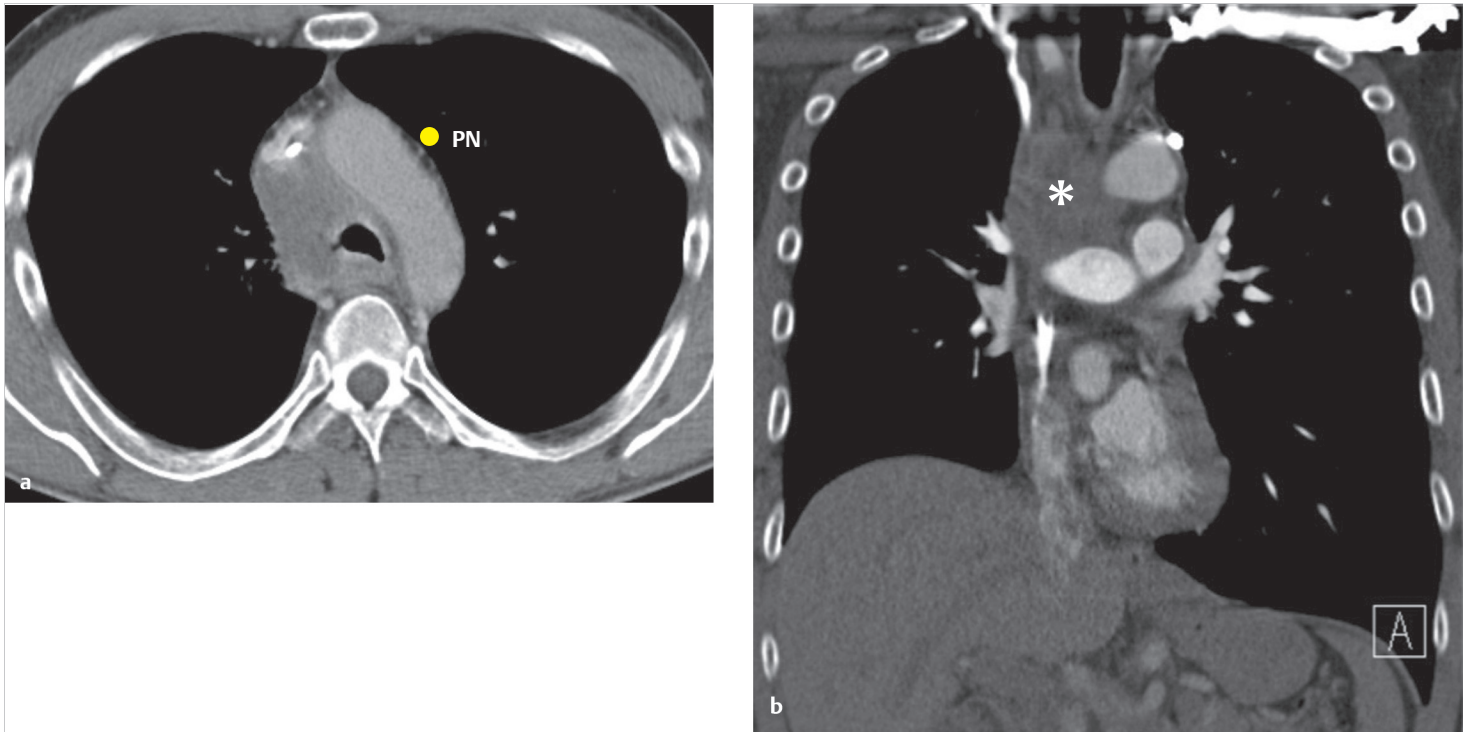


Fig. 1.5 Infiltration of the right phrenic nerve by a mediastinal metastasis (asterisk in [b]) has led to elevation of the diaphragm on the affected side. The location of the phrenic nerve (PN) is indicated in image (a). (a) Axial CT after IV injection of contrast medium. (b) Coronal reformatted image.

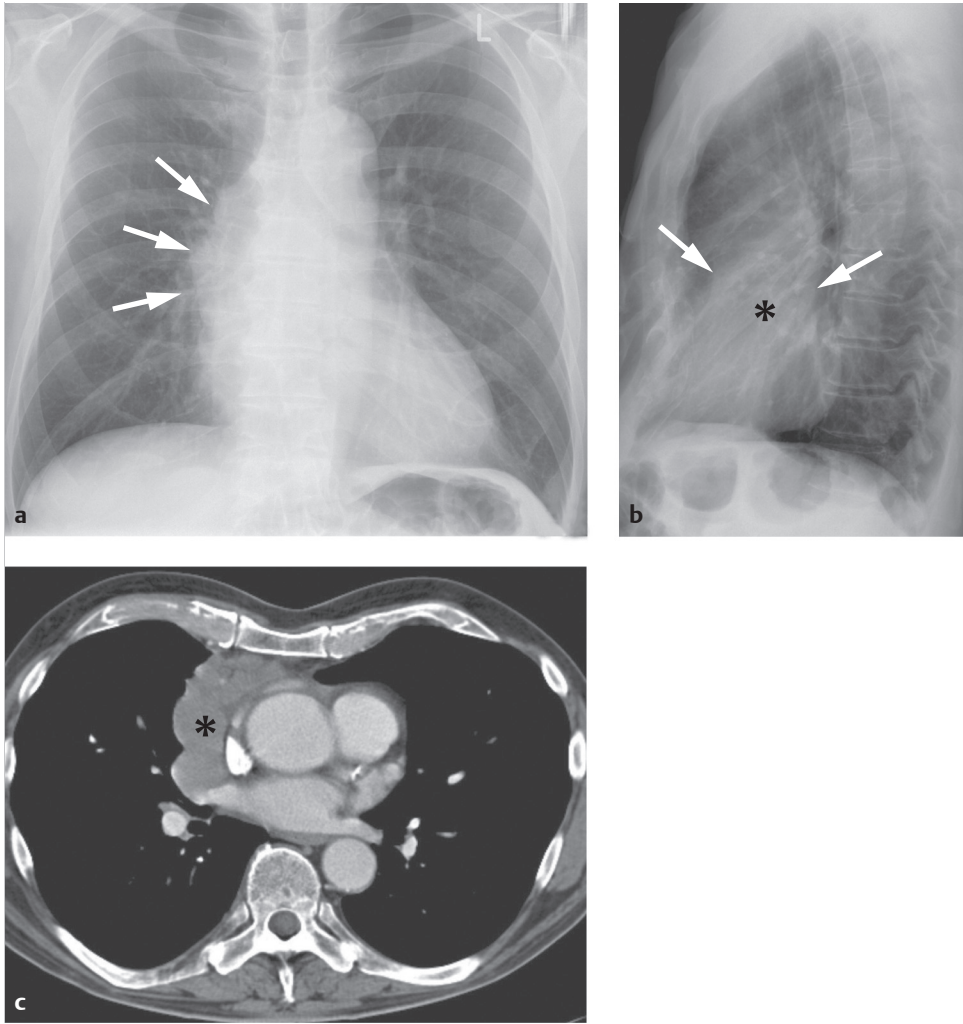
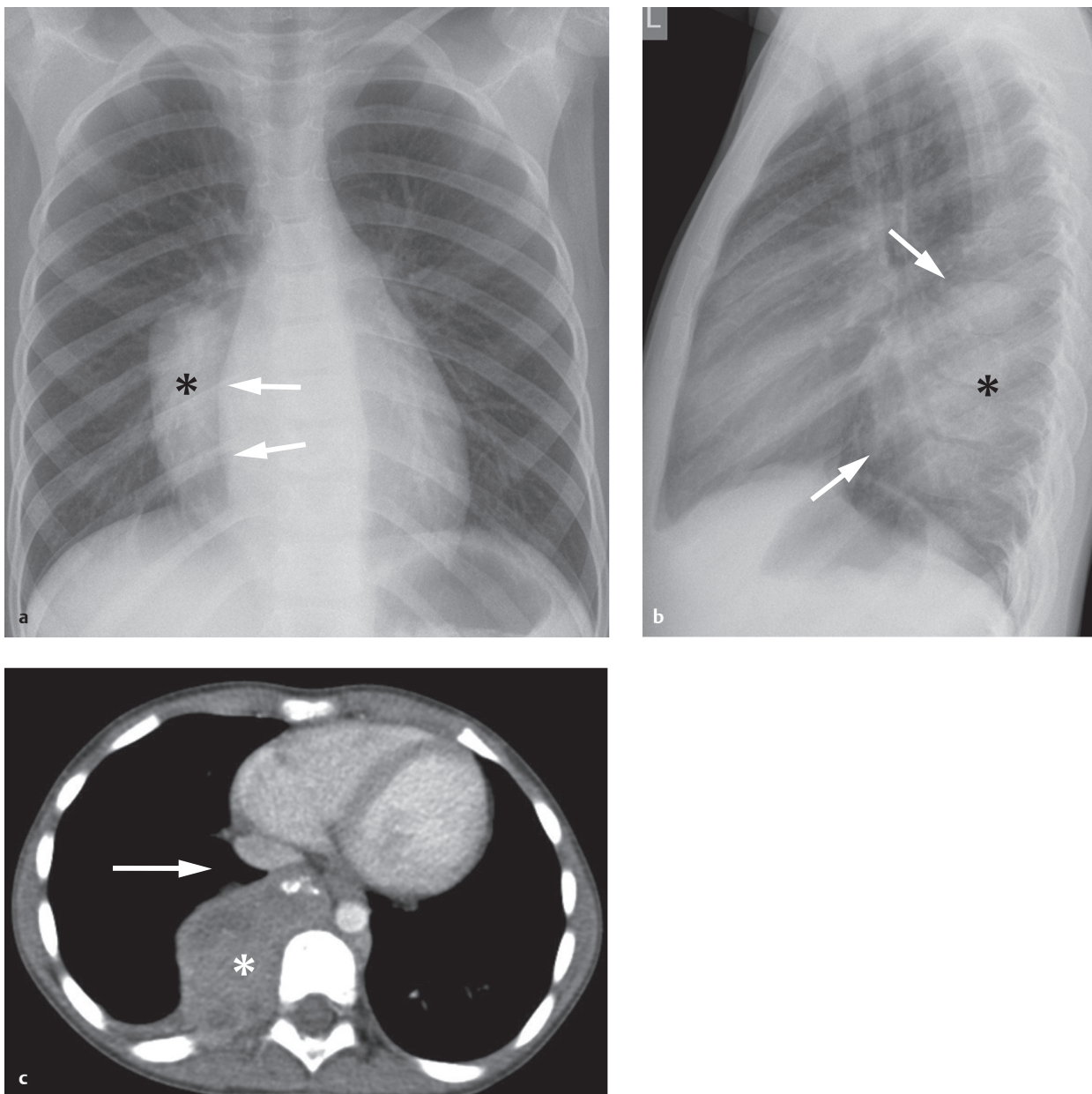


Fig. 1.6 Positive silhouette sign of a thymoma. (a) AP chest radiograph: the right mediastinal border is widened by a mass (arrows) abutting the heart and hilum. The mass and heart appear to have the same density in this frontal projection, so the boundary between them is indistinct (negative silhouette sign). (b) The lateral view confirms the anterior location of the tumor (asterisk; arrows indicate the tumor margins). (c) Axial CT demonstrates the enhancing mass (asterisk) in the anterior and middle mediastinum.



**Fig. 1.7 Negative silhouette sign of neuroblastoma.** (a) In the PA chest radiograph, a sharp line separates the cardiac border (arrows) from the mass (asterisk). This sign proves that a structure of different density—in this case aerated lung—is located between the cardiac border and mass and that both are in different planes. This radiographic sign is called a “negative silhouette sign”. (b) Lateral view: the tumor (asterisk; arrows indicate the tumor margins) is posterior to the heart and is not in direct contact with it. (c) Axial CT confirms the location of the mass (asterisk) in the posterior mediastinum. The arrow indicates lung tissue that is interposed between the heart and mass and is responsible for the positive silhouette sign.

several centimeters of that structure occupy a plane that is oriented “edge-on” relative to the detector. Another common example of this effect is the visualization of the pulmonary interlobar fissures in a lateral chest radiograph.

When the mediastinum is viewed in a PA chest radiograph, multiple lines can be seen due to the edge-on effect as well as the density difference between the soft tissues and lung. Lines visible in the anterior and middle mediastinum include the right paraesophageal line, the anterior pleural interface line, and the paracaval line (► Fig. 1.8). Lines visible in the posterior mediastinum include the paravertebral and para-aortic lines. The close proximity of masses or inflammatory processes may disrupt these lines (e.g., obliteration of the right paravertebral line [see ► Fig. 1.7]).

#### Note

It is important to realize that lines produced by an edge-on projection are visible in healthy subjects only if the structures in question are aligned in the plane of the detector. It is very rare for all the lines to be visualized in a healthy individual.

## 1.3 Diffuse Mediastinal Diseases

### 1.3.1 Acute Mediastinitis

► **Brief definition.** Acute mediastinitis is a bacterial infection of the mediastinal fat and connective tissue that may be a mixed

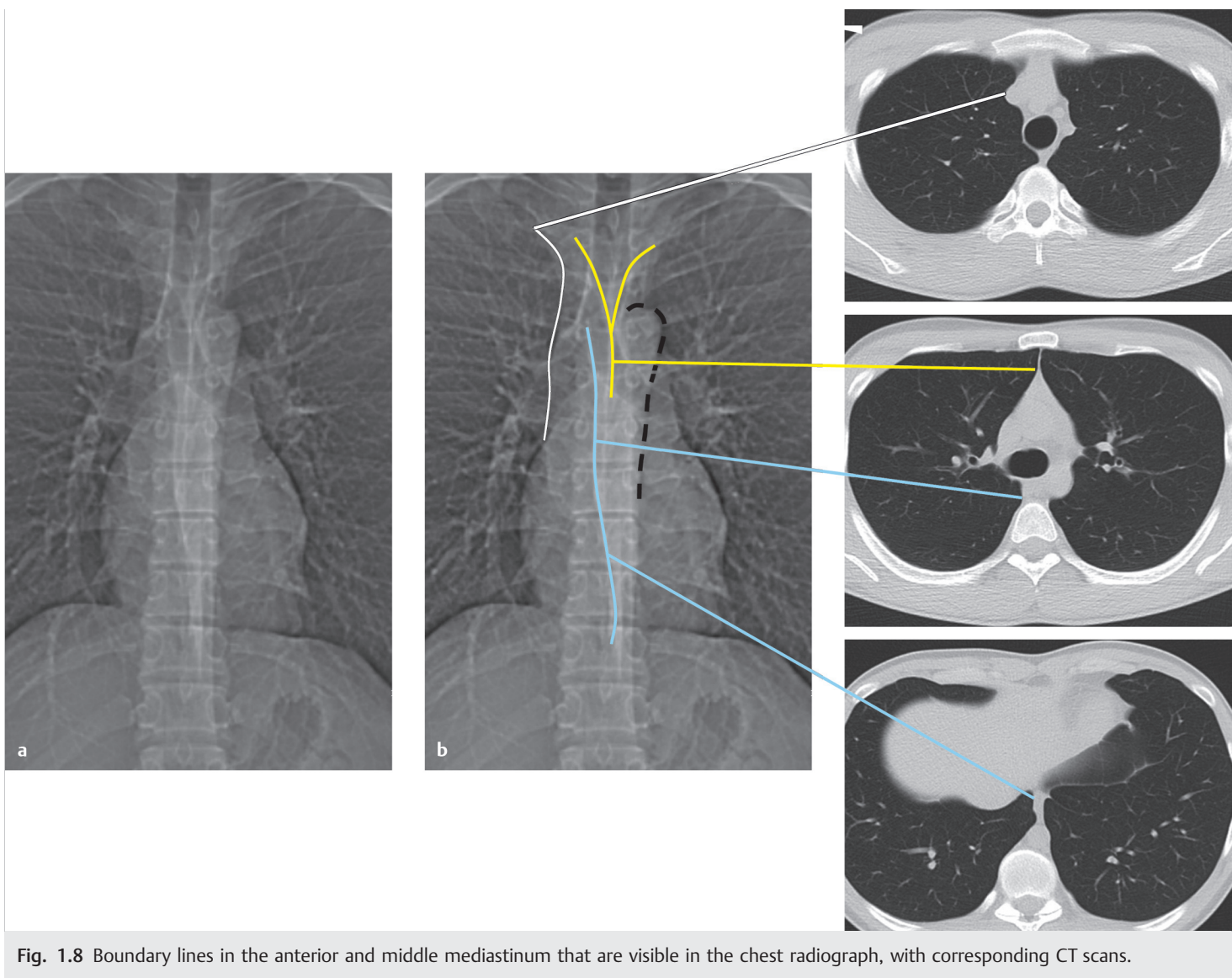


Fig. 1.8 Boundary lines in the anterior and middle mediastinum that are visible in the chest radiograph, with corresponding CT scans.

infection (type I) or may be caused by group A beta-hemolytic streptococci (type II). It may develop as a postoperative complication, after trauma including esophageal perforation, or in the form of descending necrotizing mediastinitis secondary to a deep soft tissue infection in the neck.<sup>1</sup> The majority of cases result from an esophageal perforation. The negative intrathoracic pressure generated by each inspiration promotes the contiguous spread of infectious organisms from the cervical soft tissues to the mediastinal connective tissue. This leads to a high tissue concentration of bacterial toxins, resulting in tissue necrosis. Predisposing factors are diabetes mellitus, obesity, and alcohol and nicotine abuse. If untreated, the necrotizing mediastinitis will lead to generalized sepsis and death. In recent decades the mortality rate of this disease has declined from 49% in the early 1900s to the current level of 11 to 15% as a result of prompt imaging evaluation combined with aggressive surgical and interventional therapy (excision of the necrotic tissue and drain insertion).<sup>2</sup>

#### ► Imaging signs

- The chest radiograph shows widening of the mediastinum as a nonspecific sign. CT after IV administration of contrast medium is the modality of choice for confirming the diagnosis and planning treatment.

- Mediastinitis may present as a diffuse, suppurative inflammation of the mediastinal fat and connective tissue, or may lead to the formation of necrotic tracks and abscesses in the mediastinum. In diffuse mediastinitis, the mediastinal fat initially shows streaky infiltration followed later by homogeneous, diffusely increased density with positive attenuation values (► Fig. 1.9). Reactive lymphadenopathy is often present.
- If the mediastinitis results from an esophageal perforation, imaging may reveal small air inclusions or larger collections including mediastinal emphysema.
- Fluid collections are found in mediastinitis with abscess formation. Like abscesses elsewhere in the body, a mediastinal abscess may display an enhancing rim formed by inflammatory cells. This rim is not always initially defined in early acute cases, however, so the absence of enhancement in the tissue surrounding a fluid collection does not exclude mediastinitis.
- In very pronounced cases, mediastinitis may spread into the lung through the hila. This creates a streaky pattern of perihilar density.
- Mediastinal abscess may be complicated by perforation of the abscess into the esophagus or trachea.

► **Clinical features.** Acute mediastinitis presents as a highly acute, severe illness of sudden onset with rapid debilitation,

fever, chills, elevated ESR, left shift, and elevated C-reactive protein. The history may suggest the correct diagnosis, for example:

- Previous esophageal perforation (either iatrogenic or due to vomiting as in Boerhaave syndrome).
- Previous endoscopy.
- Esophageal carcinoma (perforation).
- Sinusitis.
- Tonsillitis.
- Dental root infection.
- Retropharyngeal abscess.

► **Differential diagnosis.** Postoperative air inclusions, postoperative hematomas, and chronic mediastinitis with increased

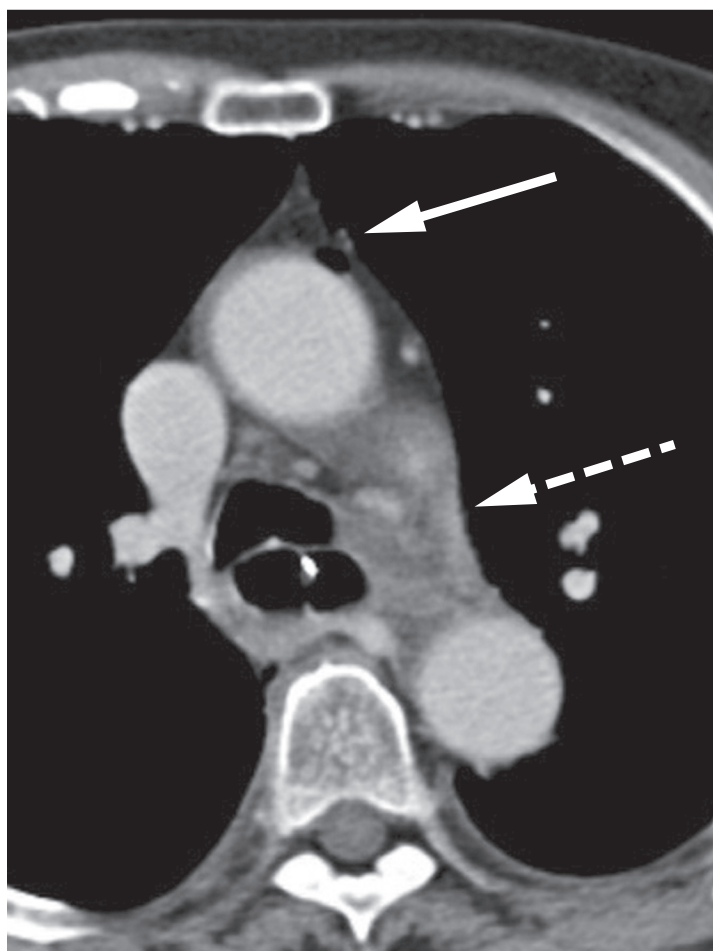


Fig. 1.9 Mediastinitis. The mediastinal fat (dashed arrow) shows increased density and contains air inclusions (solid arrow).

mediastinal density and pruning of vessels should be considered in the differential diagnosis.

► **Pitfalls.** Mediastinitis is difficult to diagnose in the early postoperative period. Mediastinal air inclusions may persist for up to 3 weeks after surgery. Postoperative hematomas may lead to increased density of mediastinal fat and persist for up to 2 months after surgery. They are difficult to distinguish from mediastinitis by their imaging appearance, as the changes are similar. The clinical presentation is the decisive factor.

► **Key points.** Acute mediastinitis has a high mortality rate without treatment. Cardinal CT features are increased density of the mediastinal fat, fluid collections, and air inclusions. In patients who have just undergone surgery, these features require differentiation from postoperative changes that may display the same imaging characteristics. Laboratory values and clinical symptoms aid differentiation.

### 1.3.2 Chronic Mediastinitis and Multifocal Fibrosclerosis

► **Brief definition**

- *Chronic mediastinitis* is a fibrosing inflammation that may have a variety of causes such as infection (e.g., *Actinomyces israelii* or *Aspergillus* species), prior radiotherapy, or autoimmune processes.
- *Multifocal fibrosclerosis* is a disorder characterized by the occurrence of fibrous lesions at various sites. The fibrosis may be retroperitoneal (Ormond's disease), intraorbital, or may occur in the form of a Riedel goiter.<sup>3</sup> To date, fewer than 50 cases of multifocal fibrosclerosis with mediastinal involvement have been described in the literature. The disease is characterized histologically by the presence of lymphocytes and plasma cells. Leukocytes are absent, so the disease is interpreted as an autoimmune inflammation. The extracellular collagen proliferation and fibrosis are attributed to cell mediators from eosinophilic granulocytes.<sup>4</sup> No causative organism has been isolated in any case of multifocal fibrosclerosis described to date. The current treatment of choice is anti-inflammatory steroid therapy.

► **Imaging signs.** Increased density is noted in the mediastinal fat (► Fig. 1.10). CT and MRI frequently show narrowing of the mediastinal vessels.

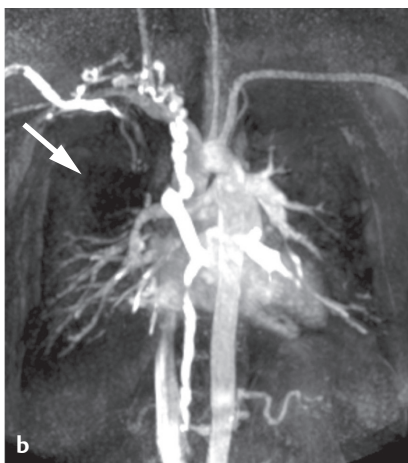
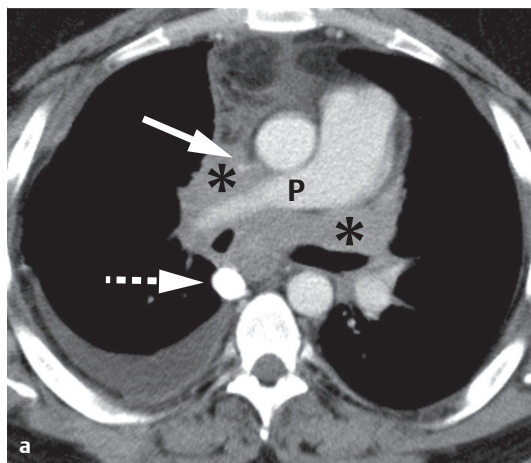


Fig. 1.10 Mediastinal fibrosis. (a) CT shows increased density in the mediastinum with connective tissue proliferation (asterisks). The superior vena cava is occluded (arrow), giving rise to collateral flow through the azygos vein (dashed arrow) and hemiazygos vein into the inferior vena cava. The right pulmonary artery (P) is narrowed. The mediastinal fat and perivascular areas provide useful landmarks for image interpretation. (b) MR angiography shows the decreased perfusion of the right upper lobe (arrow) due to stenosis of the anterior trunk (upper lobar artery).

► **Clinical features.** Symptom onset is insidious, occurring gradually over a period of time. Inflammatory markers are only slightly elevated. The most common signs and symptoms relate to compression of the superior vena cava with “superior vena cava syndrome” (swelling of the neck and face, bluish discoloration of the face, distended veins in the face and neck, headache, vision problems). Other common findings are narrowing of the trachea (stridor) and stenosis of the pulmonary arteries with decreased lung perfusion and dyspnea. The stenosing processes are responsible for the mortality in chronic mediastinitis, and the stenoses should be treated surgically or by interventional radiology in accordance with the symptoms.

► **Differential diagnosis.** Unlike acute mediastinitis, chronic mediastinitis is not associated with the presence of fluid collections.

► **Key points.** Chronic mediastinitis is a rare disorder. Dominant clinical findings relate to the stenosis of blood vessels or the trachea. Inflammatory markers are not elevated. On imaging, increased density is noted on CT and fibrotic tissue is found on MRI. Fluid collections do not occur.

## 1.4 Mediastinal Masses

Mediastinal masses caused by malignant tumors may manifest clinically through B symptoms or symptoms relating to the compression or invasion of neighboring structures:

- Narrowing of the *trachea* leads to dyspnea, while obstruction of the *superior vena cava* by the mass leads to superior vena cava syndrome. Sudden onset of clinical complaints requiring emergency diagnosis may result from a fast-growing tumor or from decompensated stenosis due to a slower-growing tumor. When vascular narrowing occurs gradually, circulation can be maintained by the development of collaterals, and superior vena cava syndrome does not occur.
- If the recurrent laryngeal nerve is damaged by compression or infiltrated by a mass, the result is unilateral vocal cord paralysis with hoarseness. Persistent hoarseness may be the only symptom of a small tumor impinging on the recurrent laryngeal nerve.

### Note

In patients with longstanding hoarseness and no associated cold symptoms, exclusion of a tumor involving the recurrent laryngeal nerve is necessary.

► **Selection of modalities.** The initial imaging study is often a plain chest radiograph, which can demonstrate the location and extent of a mediastinal tumor. The radiographic signs described earlier are helpful in determining the location of a mass. Sectional imaging can then accurately define the extent of the lesion while also revealing the compression or possible infiltration of adjacent organs. CT is most commonly used for this purpose, as it can display structures in high resolution while scanning the entire chest for any metastases that may already be present. MRI, on the other hand, is more time-consuming and usually does not add new information. It should be reserved for specific questions that could not be answered by CT.

Important considerations:

- The *location* of mediastinal tumors will often suggest the correct diagnosis.
- Morphological imaging criteria such as the *distribution of enhancement* within a mass and the *morphological appearance* of the tissue (homogeneity, necrosis, calcifications, fat content, relationship to neighboring structures with possible displacement, invasion, or cystic components) can further narrow the diagnosis. Cystic masses can be differentiated from solid tumors.

The correlation of imaging findings with the clinical presentation, including patient age and gender, is sufficient for making a differential diagnosis and may even allow characterization of the lesion in many cases. The presumptive diagnosis is then confirmed histologically by CT-guided percutaneous biopsy or excision.

### Note

In the reporting of mediastinal masses, it is important to describe the exact size, location, and relationship of the mass to neighboring structures.

### 1.4.1 Anterior Mediastinum

The most common masses in the anterior mediastinum are goiters with intrathoracic extension, thymoma and thymic carcinoma, extragonadal germ cell tumors (usually the benign variant of teratoma but occasionally malignant teratomas, seminomas, embryonic cell carcinomas, and other germ cell tumors).

#### Intrathoracic Goiter

► **Brief definition.** Iodine deficiency leads to enlargement of the thyroid gland in patients with a euthyroid or hypothyroid metabolic state. Approximately 15 to 30% of all adults, depending on eating habits, have an enlarged thyroid gland. If more than 50% of the enlarged gland extends into the chest, the patient is said to have an intrathoracic (or retrosternal) goiter. Intrathoracic goiter is a common incidental finding on chest radiographs, CT, and MRI in iodine-deficient geographic regions.

► **Imaging signs.** When viewed on chest radiographs, an intrathoracic goiter appears as a sharply circumscribed density in the superior mediastinum that displaces the trachea laterally at the level of the thoracic inlet in the PA view (► Fig. 1.11) and displaces it anteriorly in the lateral view. This feature is useful in distinguishing goiters from other diseases in the superior mediastinum, since other tumors as well as mediastinal widening due to other causes will rarely cause tracheal displacement. If tracheomalacia (pressure injury to the cartilage leading to tracheal instability during respiration) is suspected on clinical grounds, a standard tracheal radiograph should be obtained during a Valsalva maneuver (bearing down against a closed glottis to raise the intrathoracic pressure) and a Müller maneuver (inspiring against a closed glottis with the nostrils held shut to increase the negative intrathoracic pressure). If the luminal width changes by more than 50% during these maneuvers, tracheomalacia is present (► Fig. 1.12). A sectional imaging diagnosis of intrathoracic goiter relies on two main criteria:

- The mediastinal mass is in continuity with the thyroid gland.
- The tissue has the same density (CT) or signal intensity (MRI) as the thyroid gland.

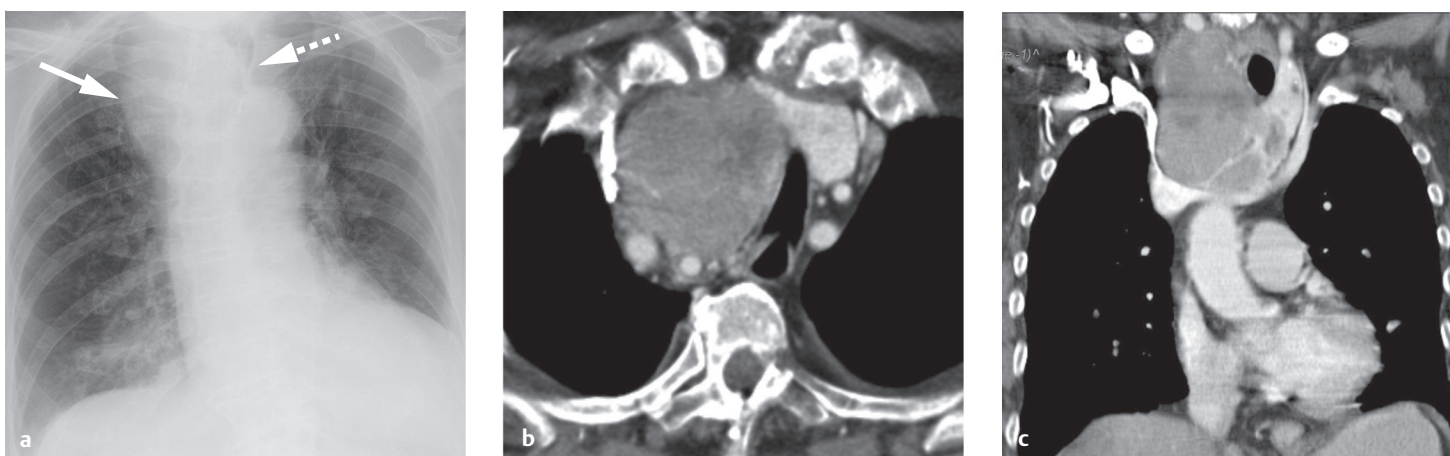


**Fig. 1.11 Multinodular goiter.** (a) Chest radiograph demonstrates mediastinal widening (arrow). The trachea is markedly displaced to the left (dashed arrow). (b) Axial CT: the thyroid parenchyma appears inhomogeneous after IV injection of contrast medium. (c) Coronal reformatted image shows continuity of the goiter from the cervical to intrathoracic level.

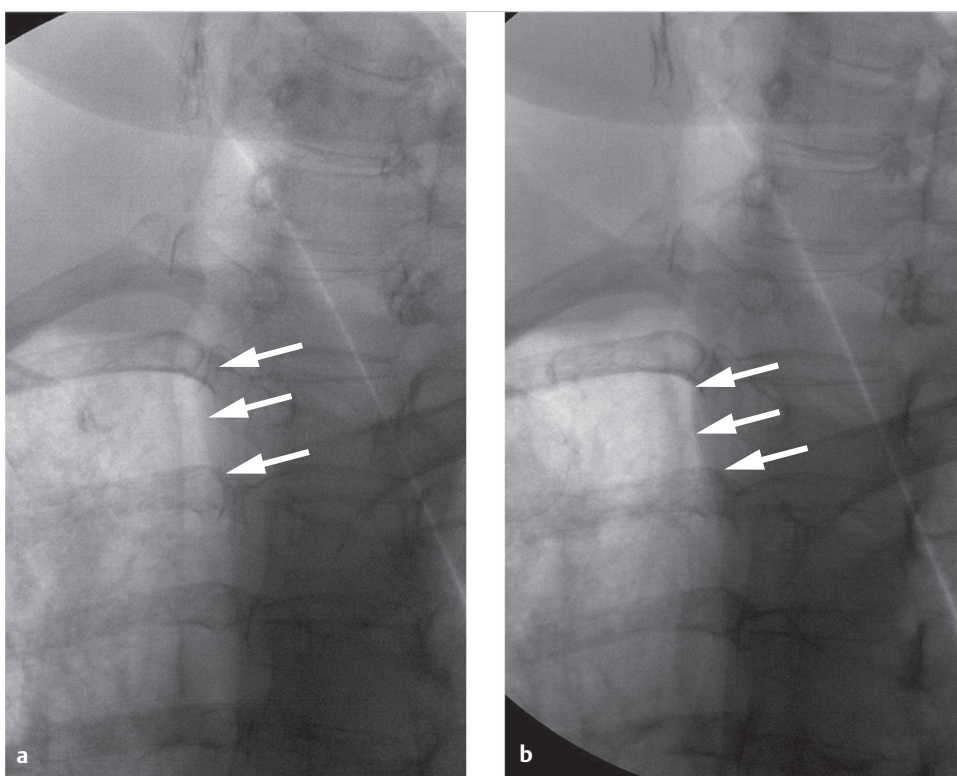


**Fig. 1.12 Tracheomalacia due to extrinsic compression by a goiter.** In tracheal spot views, the luminal width of the trachea changes by more than 50% (arrows) in response to Valsalva maneuver (a) and a Müller maneuver (b).

Both the thyroid gland and ectopic thyroid tissue are markedly hyperdense to muscle on plain CT scans due to their high iodine content. Their unenhanced attenuation values are in the range of 65 to 120 HU. Thyroid tissue shows intense contrast enhancement owing to its rich blood supply. Large goiters generally contain calcifications. Most extend into the anterior mediastinum, and some may even extend as far as the middle or posterior mediastinum. Because most goiters are multinodular and contain colloid cysts, intrathoracic goiters often have a heterogeneous CT appearance and include areas that enhance less than the surrounding thyroid tissue.

► **Clinical features.** Patients usually present clinically with visible enlargement of the thyroid gland, typically located at a supraclavicular level in the midline. The goiter may become symptomatic

due to tracheal displacement, and large goiters may cause tracheomalacia with cough, dyspnea, and inspiratory stridor.

► **Differential diagnosis**

- Enlargement of the thyroid gland may be a result of *thyroiditis* or *thyroid carcinoma*. CT scans of thyroid carcinoma may show only indirect signs such as extraglandular growth or the invasion of adjacent structures. Small carcinomas in the thyroid gland are indistinguishable from regressive nodules or thyroid adenomas by ultrasound or CT. Thyroid carcinoma may also contain calcifications, so the presence of calcifications is not a useful criterion for benign/malignant differentiation. Iodine 123 ( $^{123}\text{I}$ ) (or iodine 131 [ $^{131}\text{I}$ ]) thyroid scintigraphy can detect nodules that do not concentrate iodine. Suspicious nodules are then evaluated by ultrasound-guided fine needle aspiration biopsy to exclude thyroid carcinoma.

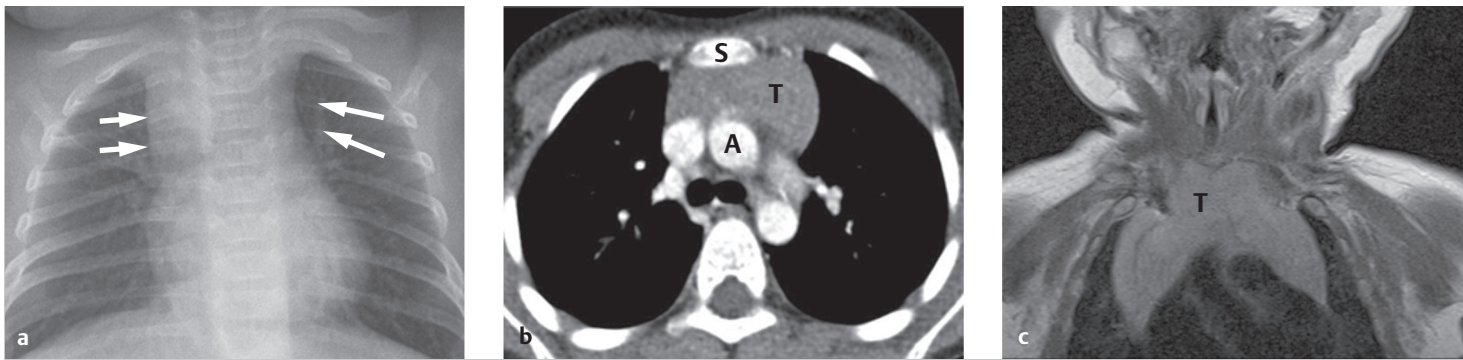


**Fig. 1.13 Normal thymus in three patients.** (a) Chest radiograph of an 8-week-old infant. The superior mediastinum is markedly widened by the thymus (arrows). (b) CT scan in a 6-year-old girl. The thymus (T) shows homogeneous contrast enhancement. The sternum (S) and aorta (A) serve as landmarks, as the thymus is located between them. (c) Coronal T2 W MR image in a 6-week-old infant. The thymus (T) extends well beyond the heart.

- **Ectopic thyroid tissue** in the mediastinum is rare. It has smooth margins and its enhancement characteristics are identical to those of thyroid tissue. With an ectopic thyroid gland in the mediastinum, the compartment normally occupied by the thyroid gland will be empty.

- ▶ **Key points.** Intrathoracic goiter is a common incidental radiological finding in iodine-deficient geographic regions. In imaging, the intrathoracic tissue is continuous with the thyroid gland and has the same attenuation values on CT and same signal intensity on MRI.

## Thymic Hyperplasia

- ▶ **Brief definition.** The thymus originates from the third pharyngeal pouch, and during embryogenesis it ascends from the level of the pharynx into the anterior mediastinum in front of the aortic arch. Thymic cysts may form anywhere along this path. The imaging appearance of the thymus varies with age. In newborns, the thymus may be larger than the heart (▶ Fig. 1.13). It begins to atrophy at puberty, continues to regress with aging, and by age 40 years is visible on CT scans in only about 5 to 17% of the population. Reactive thymic hyperplasia, known also as rebound hyperplasia, may occur as a result of chemotherapy, chemoradiotherapy, or severe illness and characterizes recovery of the immune system. During this period the thymus may grow up to 50% larger than its original size. On average, reactive thymic hyperplasia occurs 6 months after the cessation of chemotherapy in children and 9 months after in adults, but intervals from 2 months to 5 years have been reported in the literature.<sup>5</sup> Rebound hyperplasia may occur in just 2 to 3 weeks in children who discontinue steroid therapy, taking somewhat longer in adults. Thymic hyperplasia also occurs in response to thyrotoxicosis, lupus erythematosus, Behçet's syndrome, Addison's disease, and Hashimoto's thyroiditis.

- ▶ **Imaging signs.** Viewed in axial images, the thymus in adults usually presents a triangular shape with the apex pointing toward the sternum. Severe diseases, chemotherapy, and steroid therapy elicits rapid atrophy of the thymus, which later recovers to a state of reactive hyperplasia. The hyperplastic thymus may abut blood vessels but never displaces them, whereas actual tumors of the thymus will cause vascular displacement. Another criterion for the diagnosis of reactive hyperplasia is the arrow-head shape that is typical of the thymus.

- ▶ **Clinical features.** Thymic hyperplasia has no clinical manifestations.

- ▶ **Differential diagnosis.** An important differential diagnosis is a thymoma, which usually has an oval shape unlike that of a normal or hyperplastic thymus. Recurrent lymphoma also requires differentiation from reactive hyperplasia, especially if there has been previous thymic involvement by lymphoma. It may be difficult in any given case to distinguish a recurrence from reactive thymic hyperplasia after the cessation of chemotherapy.

- ▶ **Key points.** The thymus slowly atrophies after puberty. This atrophy may occur rapidly after severe illness or chemotherapy, followed by rebound enlargement of the gland after recovery from the disease or the withdrawal of chemotherapy. This reactive hyperplasia requires differentiation from recurrent lymphoma, especially if there was primary involvement of the thymus.

## Thymoma and Thymic Carcinoma

- ▶ **Brief definition.** Thymoma is a tumor originating from the epithelial cells of the thymus that are responsible for the maturation of T lymphocytes. Often the thymus is also found to contain collections of abnormal T cells that have been influenced by the excessive proliferation of altered epithelial cells. These cells form autoantibodies that may cause myasthenia gravis by blocking acetylcholine receptors at the motor end plates of striated muscle. Approximately 15% of patients with myasthenia gravis have a thymoma. By the same token, the thymus is not always enlarged in patients with a clinical diagnosis of myasthenia gravis. Histology in these patients shows a lymphoid reaction with an increased number of T lymphocytes in the thymus, which does not correlate with imaging abnormalities. Thymoma is most commonly diagnosed in the fourth to sixth decades and accounts for approximately 20% of all masses in the anterior mediastinum. As a general rule, thymomas have a smooth round or oval shape and enhance markedly after administration of contrast medium. Thymomas are typically located in the anterior superior mediastinum (▶ Fig. 1.14, see also ▶ Fig. 1.6), but 10% are found in the posterior mediastinum. Thymomas may contain cysts or calcifications. Numerous classifications were used for thymoma until 1999, when the WHO proposed a uniform classification that is often used today in its 2004 modification. This histological classification is based on the presence and number of cellular atypias. Types A,

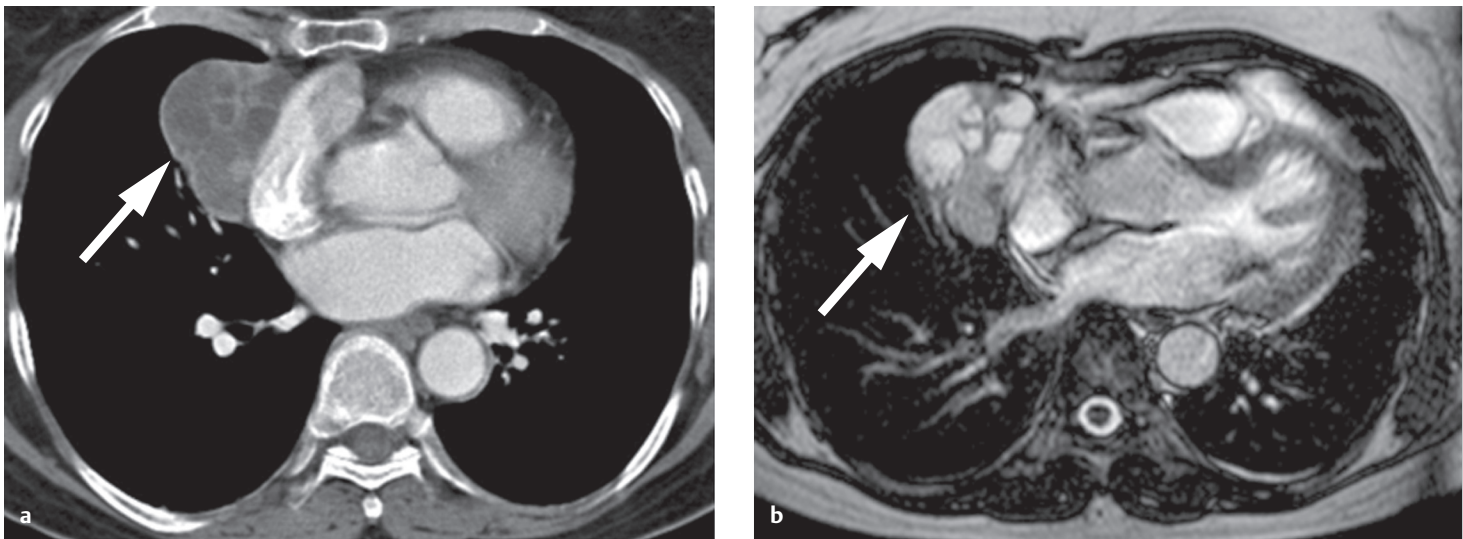


Fig. 1.14 Thymoma. (a) On axial CT the tumor (arrow) displays cystic and solid components. Its solid portions enhance faintly after administration of contrast medium. (b) T2W/T1W TrueFISP MRI sequence demonstrates the multiple cysts (arrow). (TrueFISP, true fast imaging with steady precession.)

AB, and B1 are low-risk thymomas, types B2 and B3 are high-risk thymomas; and type C is thymic carcinoma.<sup>6</sup> All thymomas, even type A, may be locally invasive and may give rise to distant metastases, leading many authors to question the validity of the WHO classification. The incidence of thymoma and thymic carcinoma in the United States and Europe is 1 per 1 million population.

► **Imaging signs.** Thymomas have soft tissue attenuation on CT and enhance markedly with administration of intravenous contrast medium. They may contain cysts. Thymic carcinoma frequently invades blood vessels, with associated intravascular extension into the heart (► Fig. 1.15). If the tumor does not transgress the boundaries of the thymus, only histology can distinguish between thymoma and thymic carcinoma and provide an accurate classification. Recent studies suggest that thymic carcinoma has a higher standardized flurodeoxyglucose (FDG) uptake value on PET/CT than low- and high-risk thymomas.<sup>7</sup> On MRI, thymomas are hyperintense in T2 W images, are isointense to muscle on unenhanced T1 W images, and enhance intensely after administration of contrast medium. If thymoma is suspected, the entire chest and upper abdomen should be evaluated by CT, as 15% of patients will be found to have drop metastases along the pleura, and intra-abdominal metastasis may occur through the physiologic apertures in the diaphragm.

► **Clinical features.** One-third of all thymomas lead to myasthenia gravis, with presenting symptoms of muscle weakness, fatigue, and ptosis. Another one-third of thymomas present with signs and symptoms attributable to local tumor growth. These include chest pain, superior vena cava syndrome, and a visible and palpable cervical mass with tumors that have grown up through the thoracic inlet. Another one-third of thymomas are detected incidentally by imaging done for a different indication. Given the difficulty of distinguishing benign thymoma from thymic carcinoma, all lesions should be resected.

► **Differential diagnosis.** Enlargement of the thymus in adults may also result from its involvement by Hodgkin's disease, non-Hodgkin's lymphoma, or acute lymphocytic leukemia. It is

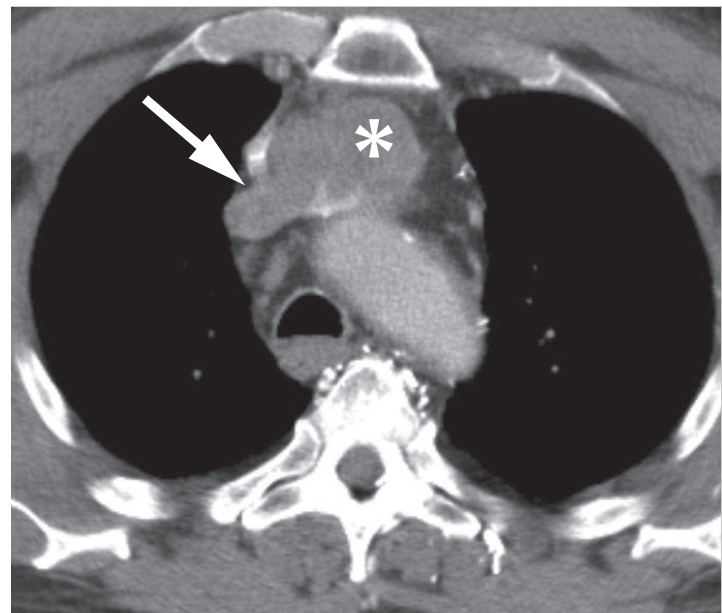


Fig. 1.15 Thymic carcinoma (asterisk). The tumor has invaded the left brachiocephalic vein (arrow).

important to be aware of the presence or otherwise of these diseases in making a differential diagnosis.

► **Key points.** Thymoma and thymic carcinoma are distinguishable by imaging only if the invasion of surrounding structures can be demonstrated.

## Thymic Cysts

► **Brief definition.** Cysts of the thymus may be congenital or acquired. The thymus originates from the third pharyngeal pouch, and cysts may develop along the path by which it descends from the level of the pharynx to the anterior mediastinum at the level of the aortic arch. The peak incidence is from 3 to 15 years of age.

► **Imaging signs.** Thymic cysts display CT features that are characteristic of cysts: an enhancing wall with contents that are

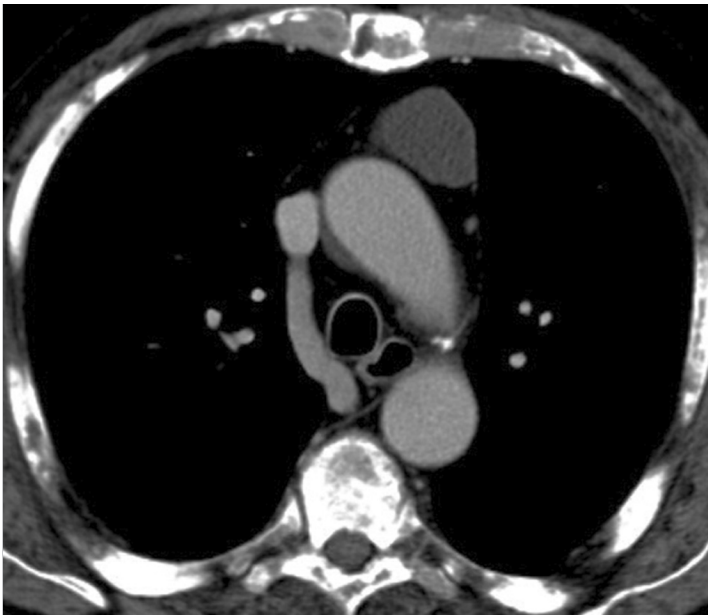


Fig. 1.16 Thymic cyst. CT scan demonstrates the thin-walled cyst anterior to the aortic arch.

isodense to water, or hyperdense if intracystic hemorrhage has occurred (► Fig. 1.16). MRI shows the high T2W signal intensity and low T1W signal intensity that are typical of cysts. Thymic cysts may form outside or inside the thymus.

► **Clinical features.** Thymic cysts are usually an asymptomatic incidental finding on chest radiographs or sectional images.

► **Differential diagnosis.** Cysts located within the thymus require differentiation from seminomas, which may also develop large cysts. Equivocal cases should be resolved by percutaneous biopsy. Thymic cysts may also be associated with carcinomas of variable size.

► **Key points.** Thymic cysts may develop within the thymus or outside the thymus along its path of descent during embryogenesis. They have typical attenuation values on CT (0 HU) and typical cystic signal intensity on MRI (high T2W signal, low T1W signal, with a reversal of signal intensities in cysts with a high protein content). Most thymic cysts are incidental imaging findings.

## Neuroendocrine Tumors of the Thymus; Thymic and Mediastinal Carcinoids

► **Brief definition.** Carcinoids are tumors of neuroendocrine origin that arise from primitive stem cells. Carcinoids are usually slow-growing and may metastasize. They are most common in middle age, and men are affected more frequently than women.

► **Imaging signs.** Carcinoids of the thymus are often indistinguishable from thymoma or thymic carcinoma by their imaging appearance. They may occur in the mediastinum and other sites and may not be localized to a particular organ (► Fig. 1.17), appearing on CT as an enhancing mass of soft tissue density. Carcinoids have high T2W signal intensity on MRI. They are isointense to muscle on T1W images and show marked contrast enhancement.

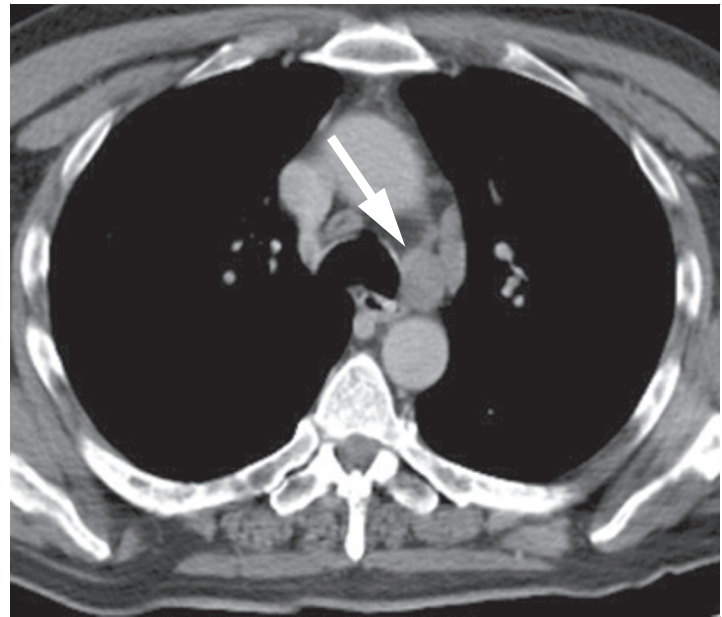


Fig. 1.17 Carcinoid (arrow) and adjacent lymph node metastases.

► **Clinical features.** Symptoms result from hormones produced in the tumor. Approximately one-third of carcinoids form adrenocorticotropic hormone leading to Cushing's syndrome. Hypertension, diarrhea, and paroxysmal flushing due to capillary vasodilation may also occur.

► **Differential diagnosis.** The differential diagnosis should include thymoma, thymic carcinoma, and sarcoma.

► **Pitfalls.** Carcinoids cannot be diagnosed from imaging findings alone. Diagnosis requires the correlation of imaging findings with clinical symptoms relating to hormone production or with histology.

► **Key points.** Carcinoids may occur within the thymus or separately in the mediastinum. They do not have typical imaging features that permit a definite diagnosis. This requires clinical and laboratory correlation.

## Extragonadal Germ Cell Tumors

"Extragonadal germ cell tumors" is a collective term for all tumors that originate from embryonic germ cells and are histologically indistinguishable from tumors of the gonads. They include teratomas (benign and malignant forms), seminomas, dermoid cysts, embryonic cell carcinomas, and chorionic carcinomas. Extragonadal germ cell tumors occur predominantly in the mediastinum and comprise 15% of all mediastinal tumors. Approximately 80% are benign teratomas. Seminomas follow teratomas in absolute numbers and account for most malignant forms (ca. 40% of malignant germ cell tumors in the mediastinum).

## Teratomas; Dermoid and Epidermoid Cysts

► **Brief definition**

- **Teratomas** may contain tissue elements derived from all three germ layers (mesoderm, endoderm, and ectoderm). Ectodermal cells may give rise to cutaneous appendages such as hair and

sebaceous glands as well as teeth. Muscle, cartilage, and bone may develop from mesodermal cells, while epithelium and pancreatic glands may arise from endodermal cells. Mature teratomas are benign, with a peak age of incidence in young adulthood (20 to 40 years).

- **Dermoid cysts** are composed of ectodermal and mesodermal elements and are not distinguishable from cystic teratomas by their imaging morphology. In 5% of cases, squamous cell carcinoma develops in dermoid cysts.
- **Epidermoid cysts** are composed entirely of ectodermal elements. They contain squamous epithelium and may gradually enlarge through desquamation.

The great majority of teratomas, dermoid cysts, and epidermoid cysts occur in the anterior superior mediastinum. Only about 8% of all cases occur in the posterior mediastinum.

► **Imaging signs.** Imaging of teratomas often reveals cystic components (88% of teratomas) and fatty components (76% of teratomas) that contrast with areas of soft tissue density found in almost every teratoma. Calcified areas are found in 53% of teratomas (► Fig. 1.18). Teratomas or dermoid cysts that form teeth or bone are easily diagnosed by CT. Teratomas and dermoid cysts present a heterogeneous tissue structure on both CT and MRI. Diffusion imaging of dermoid and epidermoid cysts shows severe diffusion abnormalities: imaging at high  $b$  values ( $b=1000$ ) shows an intense signal with a marked decrease in the apparent diffusion coefficient. Fat–fluid levels in cystic areas have repeatedly been described as pathognomonic in individual case reports but are very rarely found. Epidermoid cysts are purely cystic in almost all cases. All three tumor entities are smoothly marginated. Malignant teratoma has indistinct margins and an inhomogeneous matrix; it is also composed of elements of all three germ layers and may therefore contain fatty tissue and calcifications. Their other imaging features coincide with those of teratomas.

► **Clinical features.** Teratomas and dermoid and epidermoid cysts are generally asymptomatic. Large teratomas or dermoid cysts may compress adjacent structures, resulting in symptoms that may include chest pain. Intralesional hemorrhage in a

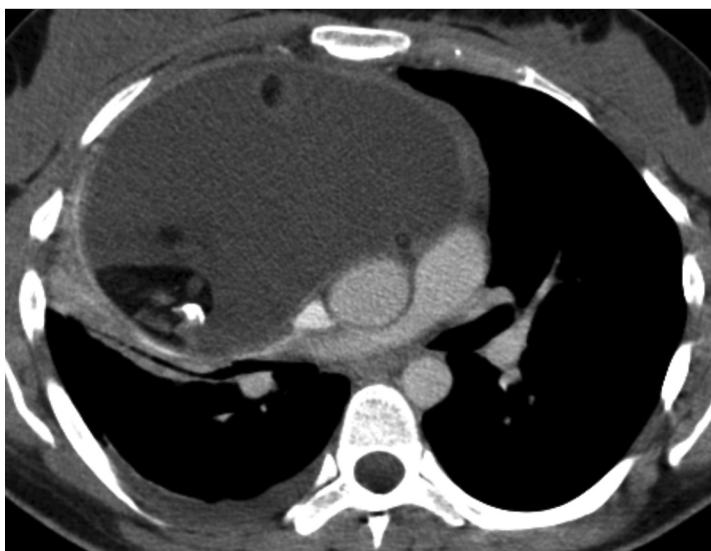


Fig. 1.18 Teratoma. CT scan shows the well-circumscribed mass with mixed attenuation values

teratoma or dermoid cyst may cause sudden enlargement of the mass, leading to sudden compression of mediastinal structures with associated symptoms. The treatment of a mature teratoma or mature dermoid or epidermoid cyst is complete resection of the mass. If this is accomplished, the tumor will not recur.

► **Differential diagnosis.** Differential diagnosis of teratomas requires mainly differentiation from sarcomas. With malignant teratomas, differential diagnosis cannot always rely on imaging findings. Lymphomas are another possibility but are more homogeneous. Dermoid and epidermoid cysts can be classified more accurately by diffusion-weighted MRI.

► **Key points.** Teratomas have components derived from all three germ layers and a heterogeneous imaging appearance. Dermoids are composed of ectodermal and mesodermal elements, while epidermoids are purely ectodermal. Dermoids and epidermoids can be differentiated from other cysts by diffusion-weighted MRI.

## Primary Seminomas

► **Brief definition.** Primary extragonadal seminomas are rare malignant masses. The most common site of occurrence is the anterior mediastinum, followed by the pineal gland and retroperitoneum. Approximately 10% of all malignant mediastinal tumors are primary seminomas. Over 90% of all primary seminomas in the mediastinum occur in males, with a peak age of incidence at 20 to 40 years. It is now believed that primary extragonadal seminomas arise from pluripotent primitive germ cells that become trapped in the mediastinum as they migrate across the midline into the gonads during early embryogenesis. These heterotopic cells may differentiate into both ectodermal and endodermal tissues; they are believed to be responsible for the development of chorionic carcinoma, embryonic cell carcinoma, and other germ cell tumors in the mediastinum.

► **Imaging signs.** Primary seminomas of the mediastinum are usually quite large by the time they are diagnosed. They have smooth, lobulated margins. Seminomas may contain stippled calcifications and cysts along with other areas showing slight, homogeneous enhancement. They have homogeneous signal intensity on MRI, appearing hyperintense in T2W images and showing intense contrast enhancement.

► **Clinical features.** The symptoms of primary mediastinal seminoma are nonspecific and result from the compression of structures in the superior mediastinum. Compression of a recurrent laryngeal nerve may cause cough and hoarseness. Other possible symptoms are dyspnea, dysphagia, and chest pain; obstruction of the superior vena cava is rare. Approximately one-third of patients are asymptomatic. Tumor markers such as alpha-fetoprotein (AFP) and human chorionic gonadotropin ( $\beta$ -HCG) (see ► Table 1.1) are not elevated. Primary seminomas of the mediastinum are treated by excision, followed if necessary by adjuvant radiation. Recent reports describe the addition of cisplatin chemotherapy and indicate very high survival rates with this combination.

► **Differential diagnosis.** Seminomas resemble lymphomas in their imaging appearance. Unlike lymphomas, however, seminomas compress surrounding structures, most notably vessels, and

**Table 1.1** Markers for various extragonadal germ cell tumors

Tumor entity	Typical tumor markers
Seminoma	None
Embryonic cell carcinoma	AFP
Chorionic carcinoma	$\beta$ -HCG
Malignant teratoma	AFP, $\beta$ -HCG
Yolk sac tumor	AFP

Abbreviations: AFP, alpha-fetoprotein; HCG, human chorionic gonadotropin.

may also show vascular invasion. Differentiation is mainly required from sarcomas and thymomas, which may also contain cysts and calcifications.

### Note

Primary seminomas are not distinguishable from other mediastinal tumors by their imaging appearance; their diagnosis requires biopsy.

► **Pitfalls.** Following the histological diagnosis of a mediastinal seminoma or other mediastinal germ cell tumor, a primary gonadal tumor should be definitively excluded before a mediastinal extragonadal germ cell tumor is diagnosed.

► **Key points.** Extragonadal seminomas of the mediastinum arise from pluripotent primitive germ cells that become trapped in the mediastinum as they migrate across the midline to the gonads during early embryogenesis. The peak age of incidence is 20 to 40 years with a male predilection. The tumors show prominent enhancement at imaging and may contain cysts and calcifications. Given the lack of pathognomonic imaging features, the diagnosis of extragonadal seminoma should be confirmed histologically.

## Chorionic Epithelioma, Embryonic Cell Carcinoma, and Mixed Germ Cell Tumors

► **Brief definition.** Malignant germ cell tumors that are histologically distinct from primary mediastinal seminoma are associated with a poorer prognosis. Like seminomas, these tumors arise from pluripotent primitive germ cells that become trapped in the mediastinum. These cells may differentiate in various ways:

- *Embryonic cell carcinoma* is composed of various poorly differentiated cell types.
- *Chorionic carcinoma* contains syncytiotrophoblasts and cytotrophoblasts. Hematogenous metastasis is common. This property is analogous to the ability of the placenta to invade blood vessels.
- As noted earlier, *malignant teratoma* is composed of cells derived from all three germ layers.

Germ cell tumors may be considered “caricatures” of embryogenesis. The various tumor types differentiate from pluripotent germ cells along different lines and reflect the varying cellular components of embryogenesis.<sup>8</sup> These tumors, unlike seminomas, form tumor markers (► Table 1.1) that are useful in monitoring treatment response and detecting recurrence. Like other tumors, they occur predominantly in the anterior mediastinum.



**Fig. 1.19** Germ cell tumor in the anterior mediastinum. On CT the mass shows low attenuation and inhomogeneous enhancement. It has compressed the superior vena cava and right pulmonary artery.

► **Imaging signs.** Extragonadal germ cell tumors of the mediastinum have a heterogeneous appearance on CT and MRI with areas of varying density or signal intensity. They show a non-homogeneous pattern of enhancement (► Fig. 1.19). Because of their rapid growth, malignant germ cell tumors other than seminoma are prone to intratumoral hemorrhage and often exhibit necrotic areas. They may also contain cysts. The various tumor types may not be clearly distinguishable from one another by their imaging features and require a histological diagnosis.

► **Clinical features.** Clinical features are the same as for seminoma. These germ cell tumors typically produce tumor markers (see ► Table 1.1). Treatment consists of surgical resection followed by radiation and chemotherapy.

► **Differential diagnosis.** Sarcoma, lymphoma, thymoma, and thymic carcinoma should be included in the differential diagnosis. Extragonadal germ cell tumors that are histologically distinct from seminoma also require a histological diagnosis.

► **Key points.** Extragonadal germ cell tumors have a heterogeneous appearance on CT and MRI, with areas of varying density or signal intensity, and show inhomogeneous contrast enhancement. They are diagnosed histologically.

## Liposarcoma

► **Brief definition.** Primary liposarcomas of the mediastinum are very rare malignant masses of adipose tissue with a peak incidence in the fifth decade. Different types are distinguished by their grade of differentiation.

## Sarcomas

► **Brief definition.** Sarcomas are mesenchymal malignancies that may occur in all mediastinal compartments. Primary sarcomas of the mediastinum are very rare. Types other than liposarcoma include fibrosarcoma, chondrosarcoma, osteosarcoma, and

rhabdomyosarcoma. The overall incidence of soft tissue sarcomas (including gastrointestinal stromal tumor) in all body regions in adults is 2 per 100,000 population.

► **Imaging signs.** Well-differentiated liposarcoma is composed mainly of fatty tissue, has negative CT attenuation values, and is isointense to fat on MRI. The presence of septa thicker than 2 mm or of enhancing areas within the tumor are signs of well-differentiated liposarcoma on sectional imaging. Mixed tumors additionally contain other cell types such as fibrocytes. Poorly differentiated liposarcomas contain large areas of denser tissue



Fig. 1.20 Liposarcoma. CT after IV injection of contrast medium. The mass contains areas of variable density and shows inhomogeneous enhancement.

that shows intense enhancement (► Fig. 1.20). The treatment of choice is surgical excision. Sarcomas appear on radiographs as well-circumscribed masses that may have lobulated margins. The tumors are usually inhomogeneous on CT and MRI (► Fig. 1.21). Osteosarcomas may contain calcifications and bone matrix, which are more clearly depicted by CT than MRI.

► **Clinical features.** Symptoms result from the compression of adjacent structures such as the heart, trachea, or esophagus. If compression is absent, B symptoms may be predominant. The treatment of choice is excision followed by radiation.

► **Differential diagnosis.** Lymphomas encase vessels but do not compress them. Seminomas and other extragonadal germ cell tumors cannot be distinguished from sarcomas. Thymomas are located in the thymic compartment and may contain cysts but otherwise show the same characteristics on CT and MRI. Lipomatosis mediastinalis (► Fig. 1.22) usually occurs in obese patients.

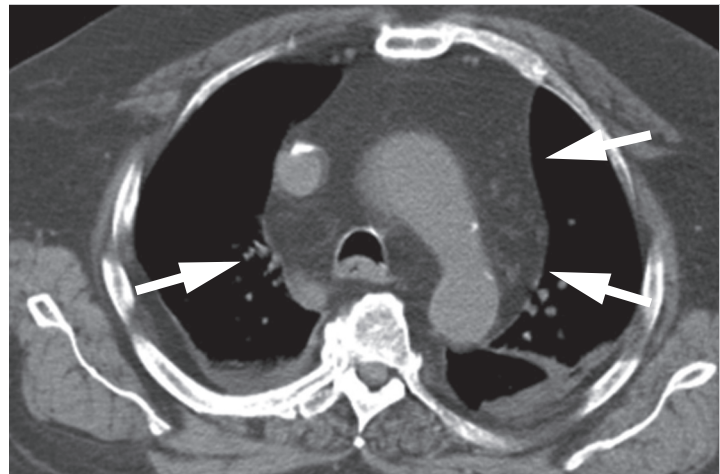


Fig. 1.22 Mediastinal lipomatosis. An increased volume of mediastinal fat is noted in this obese patient. The mediastinal structures are uniformly surrounded by fat (arrows). The thymic compartment is a useful landmark in older patients. The perivascular tissue in the superior mediastinum provides a landmark in patients of all age groups.

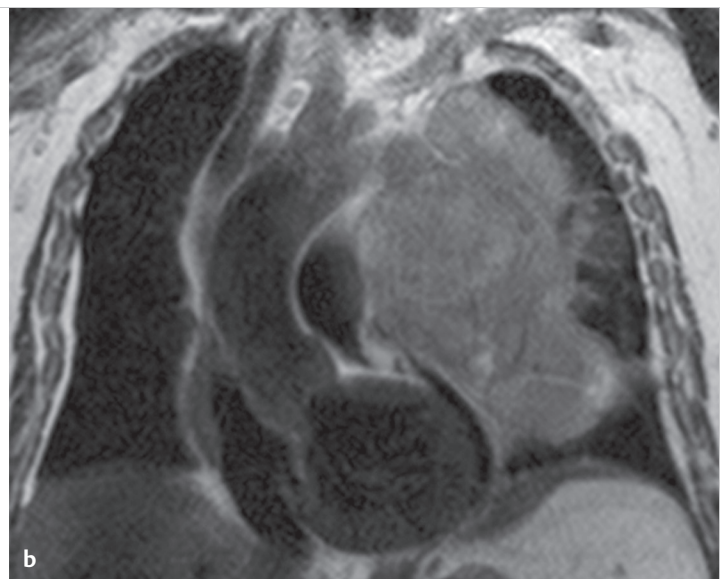
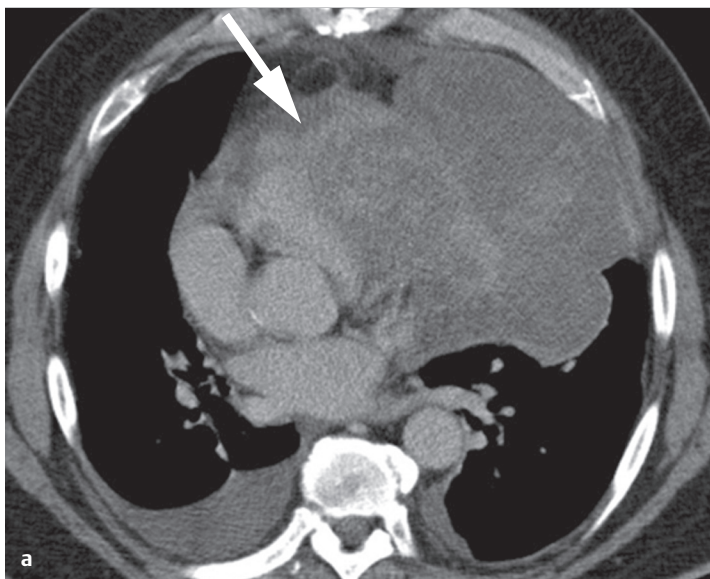


Fig. 1.21 Rhabdomyosarcoma. (a) On CT the tumor shows inhomogeneous density with areas of varying enhancement. Its boundary with the pericardium and heart is indistinct (arrow), suggesting possible invasion. (b) Coronal T2W MRI shows that the tumor has reached the pericardium but has not yet penetrated it.

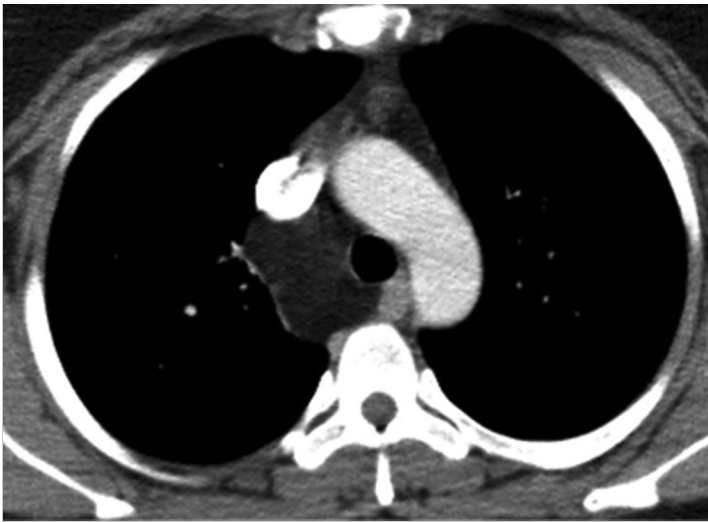


Fig. 1.23 Lipoma. Axial CT demonstrates a circumscribed mass of fat density.

As with lipomas (► Fig. 1.23), density is similar to that of fat in other locations.

► **Key points.** Sarcomas enhance in all modalities. They present a heterogeneous pattern, depending on the parent tissue, and are diagnosed histologically. The role of imaging is to accurately describe the size, location, and surrounding structures. A specific diagnosis requires histology.

## Cystic Masses

Cystic masses of the mediastinum are very rare. Bronchogenic cysts and cysts of the esophagus fall in the category of foregut duplication cysts.

### Bronchogenic Cysts

► **Brief definition.** Bronchogenic cysts are congenital changes that result from abnormal budding of the trachea between the fourth and sixth gestational weeks. They are lined by respiratory epithelium and may contain cartilage. Up to 85% of bronchogenic cysts are located in the mediastinum, usually at the infracarinal level; the rest occur in the lung parenchyma. These cysts develop somewhat later in embryogenesis and are more likely to communicate with the tracheobronchial tree than mediastinal bronchogenic cysts.

► **Imaging signs.** Bronchogenic cysts appear as homogeneous, well-circumscribed densities on chest radiographs. CT and MRI identify them as fluid-filled structures with thin walls (► Fig. 1.24). Only the walls enhance after administration of contrast medium. CT attenuation and MRI signal intensity depend on the protein content of the cyst fluid. Bronchogenic cysts may be air-filled if they communicate with the tracheobronchial tree.

► **Clinical features.** Bronchogenic cysts may cause dyspnea and stridor, depending on their location. If they are located close to the main bronchi, they may lead to areas of compression atelectasis even in infants. Smaller cysts may remain asymptomatic for some time. If the cyst becomes infected, symptoms develop as a result of associated inflammatory signs and rapid enlargement of the cyst with compression of surrounding structures.



Fig. 1.24 Bronchogenic cyst. CT demonstrates a thin-walled cyst with contents of water attenuation. The esophagus is displaced. There is no apparent relationship to the trachea or large bronchi. After resection, the cyst was found to be lined by respiratory epithelium. By its imaging appearance the cyst is indistinguishable from a duplication of the esophageal wall (see ► Fig. 1.27).

► **Differential diagnosis.** Bronchogenic cysts are often indistinguishable from esophageal duplication in terms of their imaging appearance, and a specific diagnosis requires cyst resection and histological identification of respiratory epithelium lining the cyst.

#### Note

As a general rule, morphological imaging studies will not demonstrate the relationship of bronchogenic cysts to the trachea or segmental bronchi.

► **Key points.** Bronchogenic cysts are developmental anomalies of the tracheobronchial tree. They are lined by respiratory epithelium and may become symptomatic due to compression of surrounding structures or superinfection. Often they are indistinguishable from esophageal duplication cysts by their imaging appearance.

### Pericardial Cysts and Diverticula

► **Brief definition.** Pericardial cysts are rare masses that account for approximately 7% of all mediastinal tumors. They are located predominantly in the left (70%) or right (30%) cardiophrenic angle (► Fig. 1.25). They are of mesothelial origin and represent outpouchings of the parietal pericardium (persistence of a pericardial recess during embryogenesis) that do not communicate with the rest of the pericardium. By contrast, pericardial diverticula communicate directly with the pericardial cavity. They may also be acquired and may occur postoperatively. Rapid enlargement over time suggests a pericardial diverticulum rather than a true pericardial cyst (► Fig. 1.26).

► **Imaging signs.** Pericardial cysts and diverticula have smooth, well-defined margins on chest radiographs and abut the cardiac silhouette. CT and MRI show their direct relationship to the heart. Pericardial cysts and diverticula have an extremely thin cyst wall, and internal septa are rarely present. CT attenuation and MRI

signal intensity depend on the protein content of the cyst. Because pericardial cysts usually contain a clear, serous fluid, they have also been termed “spring water cysts.” This results in high T2W signal intensity and low T1W signal intensity. CT attenuation is approximately 10 HU. Asymptomatic patients do not require treatment. The treatment of choice for symptomatic cases is surgical removal; resected cysts do not recur. The cysts can be decompressed by percutaneous aspiration but will refill over time unless obliterated by the injection of alcohol or tissue adhesive.

► **Clinical features.** Most pericardial cysts and diverticula are detected incidentally at imaging. In very rare cases where other structures, such as lung, are compressed by a mass effect, pericardial cysts may lead to dyspnea or even symptoms of heart failure (e.g., by hemodynamically significant compression of the right ventricle). Persistent cough and atypical chest pain have also

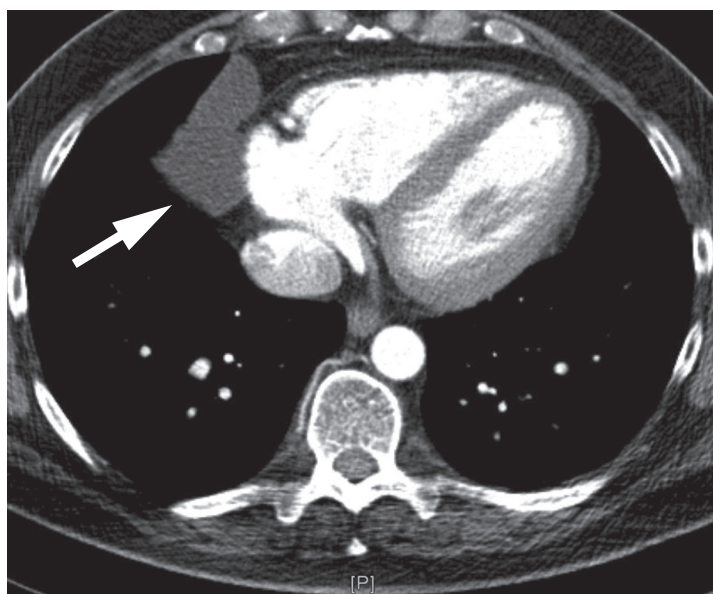
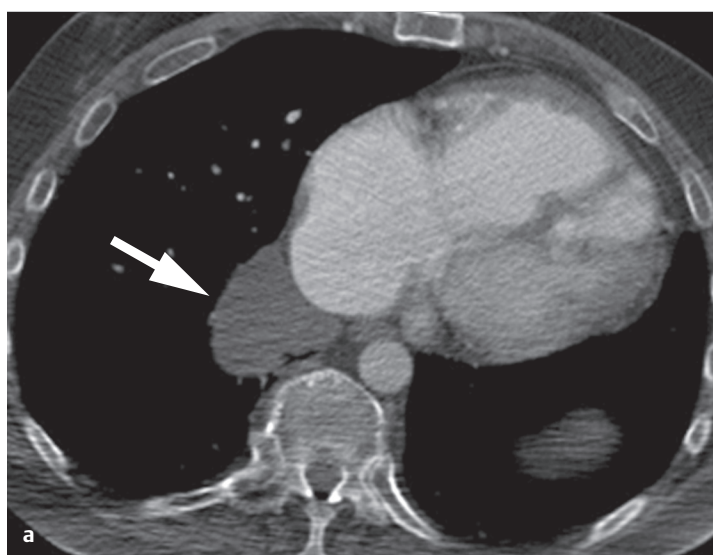


Fig. 1.25 Pericardial cyst. CT demonstrates a thin-walled cyst (arrow) of water attenuation that abuts the pericardium.



been described in a few instances. Intracystic hemorrhage may cause significant cyst enlargement with acute onset of symptoms due to compression of adjacent organs. Cyst infection and rupture are extremely rare.

► **Differential diagnosis.** The differential diagnosis of well-circumscribed masses on the chest radiograph should include large epicardial fat pads as well as mediastinal tumors. CT or MRI is useful for the differentiation of solid tumors and fat.

#### Note

The cardiophrenic angle is the principal landmark for pericardial cysts and diverticula.

► **Pitfalls.** The pericardial reflections at the level of the ascending aorta show small amounts of fluid, even in healthy individuals, and should not be taken to indicate small pericardial cysts.

► **Key points.** Pericardial cysts communicate with the pericardium, while pericardial diverticula communicate with the pericardial cavity. Both entities show the typical characteristics of cysts in sectional imaging studies.

### Esophageal Duplication Cysts

► **Brief definition.** Duplication cysts of the esophagus are rare congenital malformations that result from abnormal budding of the foregut in the third to fourth gestational week. The wall of the cyst may contain smooth or striated muscle. The cysts are lined by esophageal epithelium, which rarely may include areas of ectopic gastric epithelium. Secretions from this tissue may erode through the cyst wall, leading to intracystic hemorrhage or perforation of the cyst.<sup>9</sup>

► **Imaging signs.** Esophageal duplication cysts are often detected incidentally on chest radiographs of asymptomatic patients, appearing as well-circumscribed, oblong densities projected over the posterior inferior mediastinum. The contents are

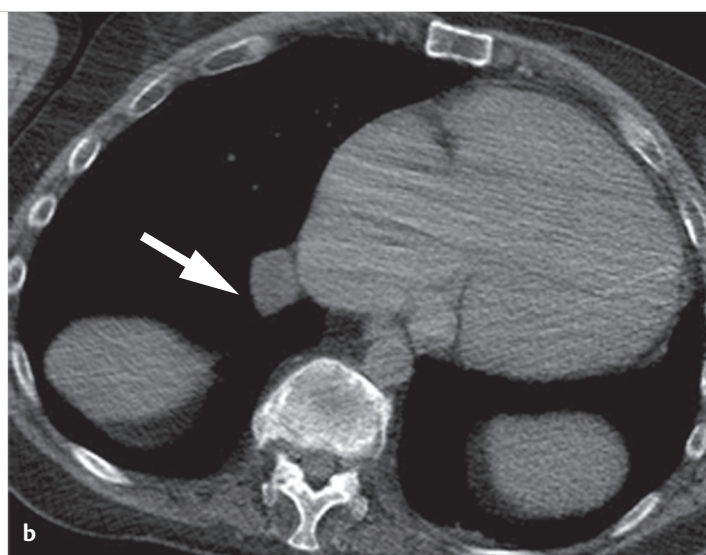


Fig. 1.26 Pericardial diverticulum detected incidentally in a patient with cor pulmonale. (a) CT shows a thin-walled paracardial mass of fluid attenuation (arrow). (b) A later scan documents spontaneous reduction in the size of the mass (arrow). This distinguishes it from a pericardial cyst and confirms the diagnosis of pericardial diverticulum.

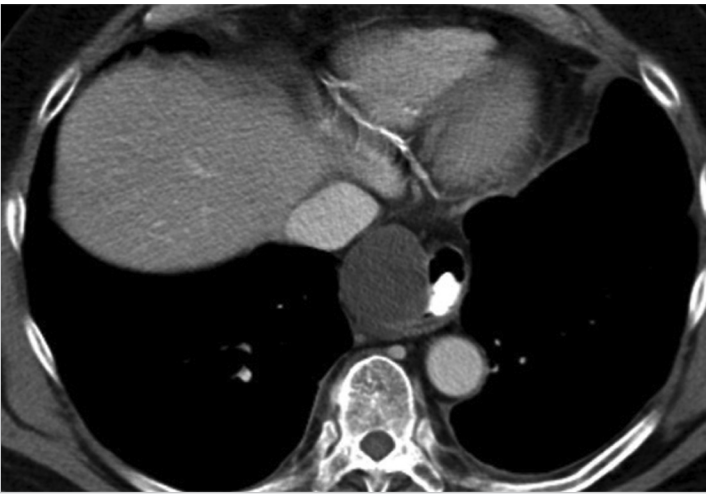


Fig. 1.27 Duplication of the esophagus. CT shows an immediate paraesophageal cyst that does not communicate with the esophageal lumen.

isodense to water on CT and may show soft tissue density due to intracystic hemorrhage. Postcontrast enhancement is limited to the cyst wall. As with other types of cyst, T2 W MRI shows high signal intensity (or low intensity after intracystic hemorrhage), while T1 W images show absent or moderate signal depending on the protein content of the cyst fluid. Esophageal duplication cysts occur in the distal part of the esophagus in the posterior mediastinum. Most are entirely extramural, but some may be located within the esophageal wall (► Fig. 1.27). They often have an elliptical shape with a longitudinal orientation.

► **Clinical features.** Esophageal duplication cysts may lead to esophageal compression and dysphagia, but most are asymptomatic and are detected incidentally on chest imaging.

► **Differential diagnosis.** Differentiation from bronchogenic cysts is not always possible on the basis of imaging appearance alone.

► **Key points.** Esophageal duplication cysts are usually an incidental imaging finding. They are in contact with the esophagus and display the typical characteristics of cysts on sectional images, depending on the protein content of the cyst and possible intracystic hemorrhage.

## Lymphangioma and Cystic Hygroma

► **Brief definition.** Lymphangioma and cystic hygroma are congenital malformations of the lymphatic system formed by heterotopic tissue from one of the five embryonic lymph sacs. This sequestration most commonly arises from the jugular lymph sac, with the result that 75% of these cystic masses are located in the neck. Lymphangiomas may already be present at birth or may present clinically during the second year of life, when the greatest growth of the lymphatic system takes place. A lymphangioma may be of the capillary or the cavernous type, depending on the size of its internal spaces. Cystic hygroma is a special form that consists of multiple large cysts.

► **Imaging signs.** Lymphangioma and cystic hygroma may contain solid components interspersed among the cysts.

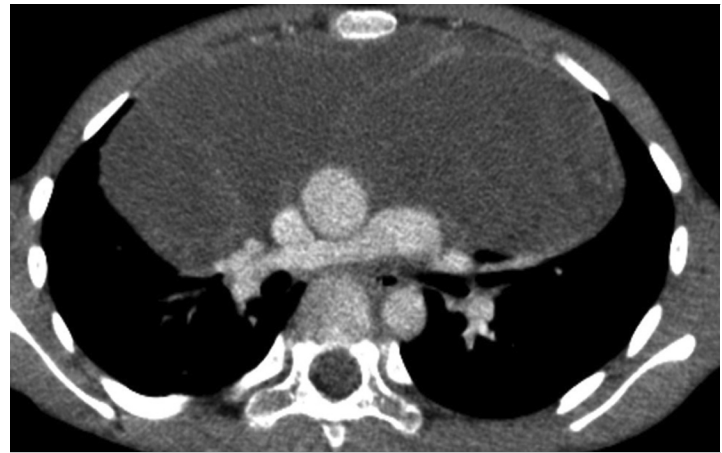


Fig. 1.28 Lymphangioma in the anterior mediastinum. Axial CT demonstrates the septated cystic mass.

Ultrasonography can demonstrate the cystic nature of the mass. Hygromas are hypodense on CT scans, and only their solid portions enhance (► Fig. 1.28). The cysts are hyperintense on T2 W MRI. Their signal intensity on T1 W images depends on their protein content and on possible intracystic hemorrhage, which produces visible fluid levels within the cyst. Only the solid components enhance.

► **Clinical features.** Lymphangioma and cystic hygroma are usually apparent at birth, appearing as a tense swelling in the neck or upper chest. Infection may lead to acute enlargement and compression of the trachea, esophagus, or vessels. Dysphagia and dyspnea may occur acutely or develop over time.

### Note

An accurate description of the tumor's extent and surrounding structures is important if surgical excision of the lymphangioma or cystic hygroma is intended.

► **Differential diagnosis.** Lymphangioma and cystic hygroma may occur in all areas of the mediastinum. They are composed almost entirely of cysts, so generally their diagnosis should present no difficulties. The lack of enhancement of the contents of the cyst serves to distinguish them from vascular malformations and cavernomas.

► **Key points.** Lymphangioma and cystic hygroma are congenital malformations of the lymphatic system. They may contain solid elements in addition to typical cystic components. Intracystic hemorrhage with fluid levels is a typical imaging finding.

## 1.4.2 Middle Mediastinum

Conditions in the middle mediastinum predominantly involve the lymph nodes.

► **Anatomy.** The lymph nodes in the chest are divided into 14 stations described by the American Joint Committee on Cancer (AJCC) and the Union for International Cancer Control (UICC; or

**Table 1.2** Lymph node stations of the mediastinum based on the 1997 classification of the AJCC and UICC<sup>17</sup>

Station	Location
<b>Mediastinal</b>	
1 R/L	Superior mediastinum (cranial to brachiocephalic vein)
2 R/L	Upper paratracheal
3	<ul style="list-style-type: none"> <li>• Retrotracheal (designated as 3P)</li> <li>• Prevascular (designated as 3A)</li> </ul>
4 R/L	Lower paratracheal (R: includes the azygos nodes)
5	Aortic window, pulmonary trunk
6	Para-aortic to the level of the aortic arch
7	Subcarinal
8	Paraesophageal, subcarinal
9	Pulmonary ligament
<b>Pulmonary (within the visceral pleura)</b>	
10 R/L	Hilar
11 R/L	Interlobar
12 R/L	Lobar
13 R/L	Segmental
14 R/L	Subsegmental

Note: R/L designates the right or left side. Lymph node stations without an R/L designation are located in the midline.

Union Internationale Contre le Cancer), as shown in ► Table 1.2. Nine of the lymph node stations are located in the mediastinum (► Fig. 1.29).

## Sarcoidosis

► **Brief definition.** Sarcoidosis is a multisystem disease of unknown etiology in which an abnormal immune response provokes the formation of noncaseating granulomas that contain epithelioid cells, multinucleated giant cells, and lymphocytes. These granulomas may form almost anywhere in the body but occur predominantly in the lung and mediastinal lymph nodes. The peak incidence of the disease is at 40 years of age, with a slight female predilection. The number of new cases per year is approximately 10 to 12 per 100,000 population. Pulmonary and mediastinal sarcoidosis is classified into four radiographic stages (► Table 1.3). Bilateral lymphadenopathy develops in 80% of sarcoidosis patients. The treatment of sarcoidosis is geared toward clinical complaints; acute cases are managed with oral steroids. Up to 95% of acute sarcoidosis cases resolve spontaneously over a period of several months. Chronic sarcoidosis is associated with permanent impairment of lung function in 20 to 30% of patients, with progression to pulmonary fibrosis occurring in 10%.

► **Imaging signs.** The chest radiograph shows symmetrical enlargement of the hilar lymph nodes. Enlargement of the mediastinal lymph nodes causes widening of the mediastinum. The mediastinal lymphadenopathy in sarcoidosis has a markedly

symmetrical appearance on axial CT (► Fig. 1.30). Symmetrical involvement of the hila is also seen in most cases. Over time, approximately 40% of patients develop an eggshell pattern of lymph node calcification. Stage 2 disease is marked by the appearance of reticulonodular changes with nodules up to 5 mm in diameter; they are usually bilateral. The granulomas show a typical subpleural distribution along lymphatic vessels, along interlobar fissures, accompanying the bronchovascular bundles, and along interlobular septa. This pattern of involvement on CT is diagnostic of sarcoidosis.

► **Clinical features.** The clinical presentation includes B symptoms that may be associated with dry cough, dyspnea, arthritis, erythema nodosum, and facial nerve palsy depending on the pattern of involvement. Clinical and radiological suspicion is confirmed by bronchoalveolar lavage, which indicates a greater than 2:1 ratio of CD4<sup>+</sup> to CD8<sup>+</sup> T cells (T-helper cells and T-suppressor cells).

► **Key points.** Symmetrical enlargement of the hilar lymph nodes (station 10) and mediastinal nodes is characteristic of sarcoidosis. The nodules in stage 2 disease show a typical distribution on CT: peribronchial along the lymphatics, subpleural, and along the interlobar fissures.

## Lymphoma

► **Brief definition.** Lymphomas are neoplasms of the lymphatic system. They are divided into two main groups: Hodgkin's lymphoma (lymphogranulomatosis) and non-Hodgkin's lymphoma. The incidence of all lymphomas is approximately 12 new cases per 100,000 population per year.

- *Hodgkin's lymphoma* has a bimodal age distribution with peaks in young adults (15 to 35 years) and after age 50 years. Generally the disease starts in a localized nodal region and then spreads to adjacent lymph node stations. Affected lymph nodes are enlarged and painless. The lymph nodes of the anterior mediastinum are affected in 60% of patients (► Fig. 1.31, ► Fig. 1.32). Over time the disease spreads from the initial site to adjacent nodal stations and then to extranodal tissues. Untreated, it leads to death. Treatment depends on histological subtype in the Rye classification (lymphocyte-predominant, nodular sclerosis, mixed cellularity, lymphocyte depletion). One histological characteristic of Hodgkin lymphoma is the presence of (multinucleated) Sternberg–Reed giant cells and large blasts (Hodgkin cells).
- *Non-Hodgkin's lymphomas* are a heterogeneous group of lymphomas composed of various cell types, include T-cell and B-cell lymphomas, and have a peak incidence in older adults. The incidence is greatly increased in immunosuppressed patients (organ recipients, AIDS sufferers). Besides the dysregulation of immune homeostasis, chromosomal translocations play an important role in the pathogenesis of non-Hodgkin's lymphoma. The majority of cases present with painless lymph node swelling, similar to lymphogranulomatosis. The abdominal lymph nodes are more commonly affected than the mediastinal nodes. Non-Hodgkin's lymphoma tends to affect lymph node stations not typically involved by Hodgkin's lymphoma (► Fig. 1.33) such as the posterior mediastinal nodes. Low- and high-grade non-Hodgkin's lymphomas are distinguishable by their clinical course and histology. The Kiel classification identifies subtypes based on the predominance of “cytes” or “blasts.” As with Hodgkin's lymphoma, treatment is based on tumor histology.

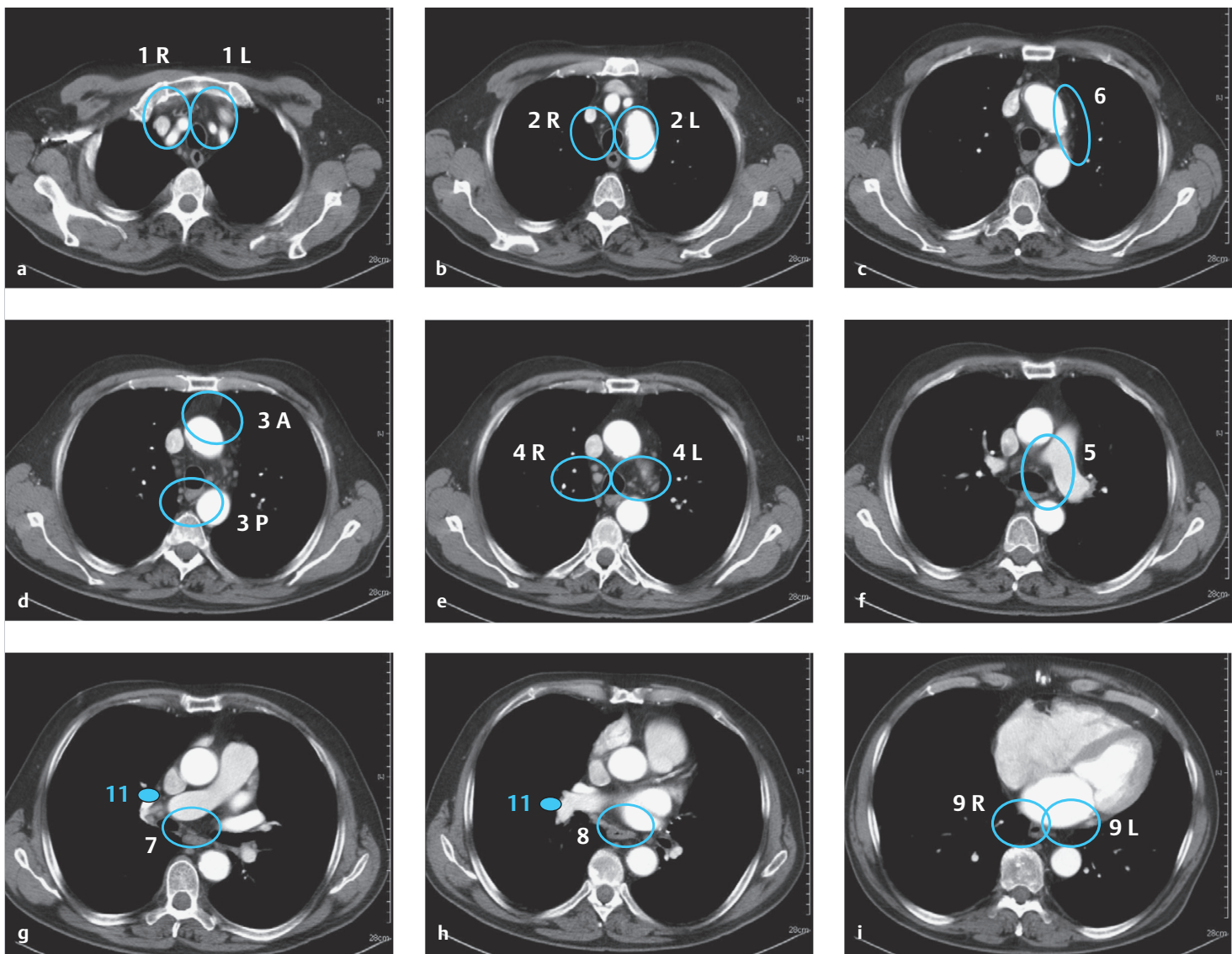


**Fig. 1.29** Lymph node stations (light blue outlines) in the mediastinum based on the 1997 classification of the AJCC and UICC.<sup>17</sup> R/L designates the side (right/left). Lymph node stations without a R/L designation (5 to 8) refer to unpaired sites. Other, unmarked lymph node stations are station 12 (lobar), station 13 (segmental), and station 14 (segmental). Stations 11 to 14 are parabronchial. (a) Station 1 (high mediastinal). (b) Station 2 (high paratracheal). (c) Station 6 (para-aortic). (d) Station 3 (prevascular, retrotracheal). (e) Station 4 (low paratracheal, tracheobronchial). (f) Station 5 (subaortic [aortopulmonary window]). (g) Station 7 (subcarinal) and station 10 (hilar). (h) Station 8 (paraesophageal) and station 11 (interlobar). (i) Station 9 (pulmonary ligament).

**Table 1.3** Staging of sarcoidosis

Stage	Description
0	Normal chest radiograph
1	Thoracic lymphadenopathy
2	Thoracic lymphadenopathy and lung changes
3	Nodular lung changes without thoracic lymphadenopathy
4	Pulmonary fibrosis

► **Imaging signs.** The chest radiograph shows enlargement of the hilar lymph nodes and opacity of the aortopulmonary window due to lymphadenopathy, or a large well-circumscribed mass usually located in the anterior mediastinum or at other sites in the case of non-Hodgkin's lymphoma. Large lymphomas generally encase vessels without occluding them (see ► Fig. 1.32). Vascular compression occurs only with very large tumors and then is limited chiefly to veins.

► **Clinical features.** Lymphomas typically present with B symptoms, consisting of fever, night sweats, and weight loss. Affected lymph nodes are enlarged and painless.

#### Caution

In the work-up of lymphoma, do not use a fine needle for the percutaneous biopsy of lymph nodes. Use an 18G or 16G core needle to ensure that the pathologist will have enough tissue with which to determine the histological type.

► **Differential diagnosis.** The differential diagnosis of large lymphomas should include sarcoma. The enhancement characteristics of the two entities may be identical. Sarcomas are distinguished by their tendency to compress and occlude blood vessels.

► **Key points.** Lymphomas are divided into *Hodgkin's lymphoma*, characterized histologically by Sternberg–Reed giant cells with

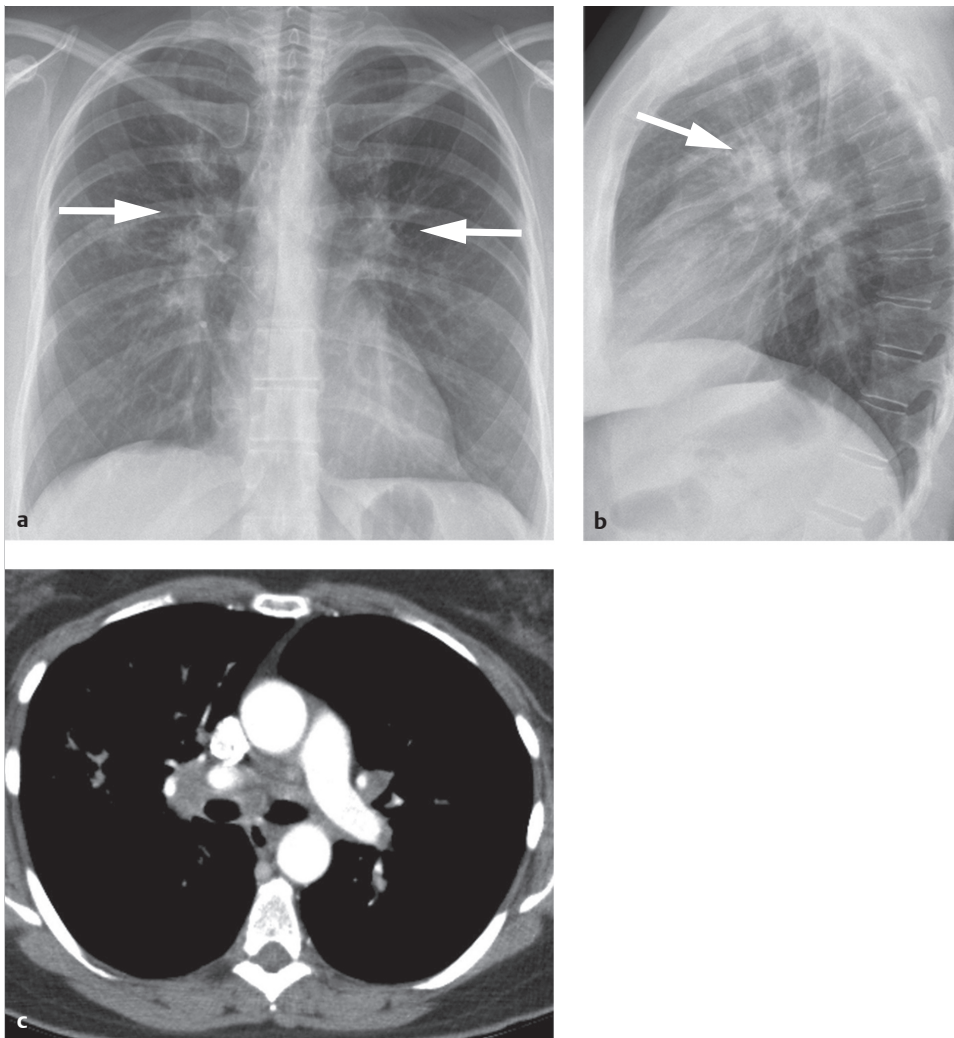


**Fig. 1.30 Sarcoidosis.** (a) Stage 1 and 2 disease is marked by symmetrical, bilateral lymphadenopathy (arrows). (b) Opacity of the aortopulmonary window due to lymphadenopathy (arrow; for landmarks see ► Fig. 1.2). (c) Axial CT shows symmetrical enlargement of the lymph nodes at stations 7, 8, and 10R and L.

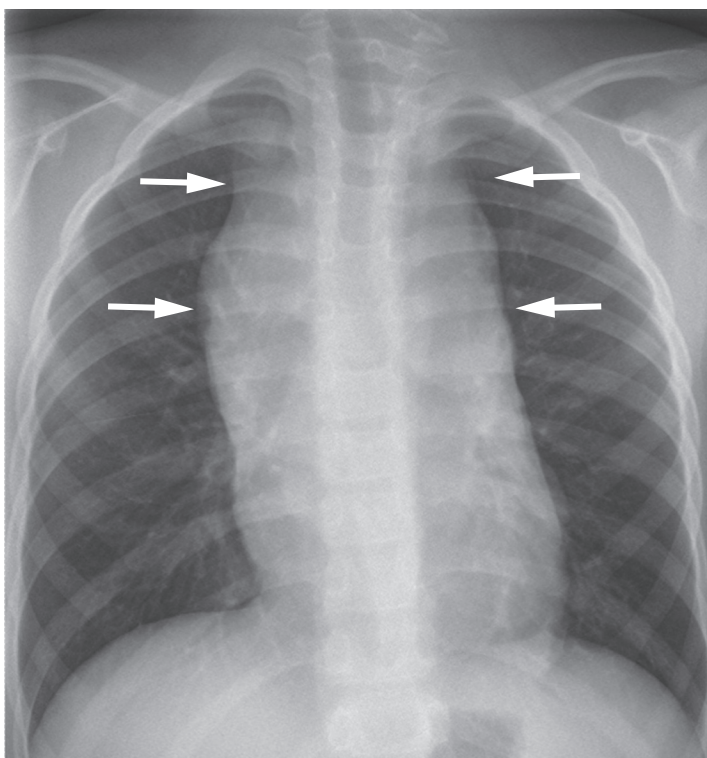


**Fig. 1.31 Hodgkin's lymphoma.** The lymphoma has caused a typical "chimney" appearance of mediastinal widening (arrows). The lateral radiograph showed opacity of the retrosternal space and superior mediastinum.

multiple cell nuclei and Hodgkin cells (large blasts), and *non-Hodgkin's lymphomas*, a histologically diverse group of B-cell and T-cell tumors. Lymph node enlargement is a characteristic feature. Lymphomas are diagnosed histologically. Percutaneous CT-guided biopsy requires a core needle, as fine-needle aspiration is inadequate for classification. The role of CT is to provide an accurate description of all affected lymph node stations and sites of extranodal involvement.

### Castleman's Disease (Angiofollicular Hyperplasia)

► **Brief definition.** The pathologist Benjamin Castleman's first described this rare disease in the 1950s.<sup>10</sup> Its prevalence is estimated at 1 per 1 million population. Today the disease is attributed to infection with human herpesvirus 8, which is also responsible for Kaposi sarcomas in AIDS. The cytokine interleukin-6 leads to immune dysregulation with the proliferation of lymphocytes. In the more common hyaline vascular type of Castleman's disease, the lymph node follicles are characterized by regressive changes in the germinal centers and thickening of the mantle zone, which contains many very small lymphocytes. In the plasma cell type of Castleman's disease, the germinal centers are hypertrophic due to the accumulation of polyclonal plasma cells. In addition, a localized form of Castleman's disease is distinguished from a multicentric form with multiple sites of occurrence. The localized form

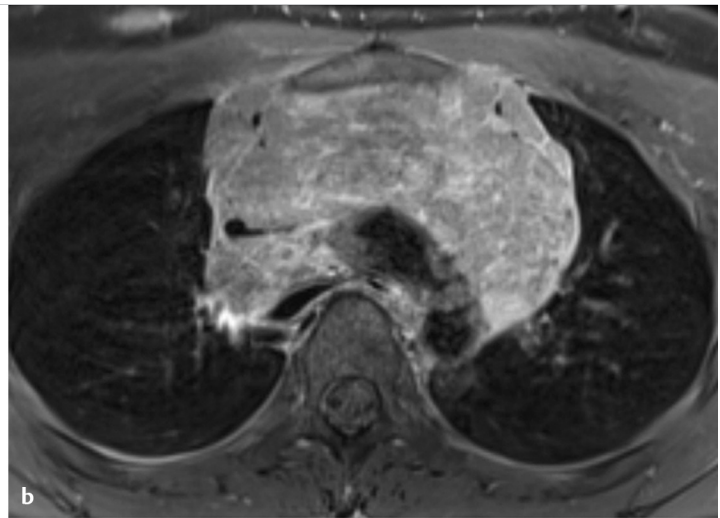
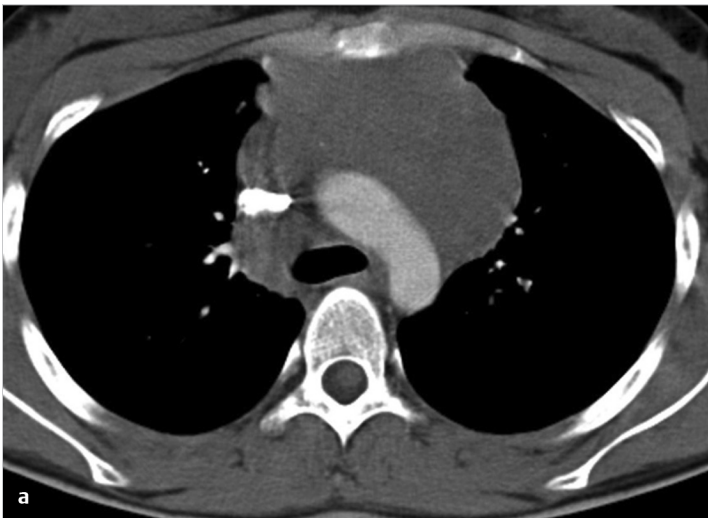


**Fig. 1.32 Hodgkin's lymphoma.** (a) The mass shows slight contrast enhancement on CT. There is no evidence of vascular compression. (b) T1 W MRI with fat suppression after IV injection of contrast medium.

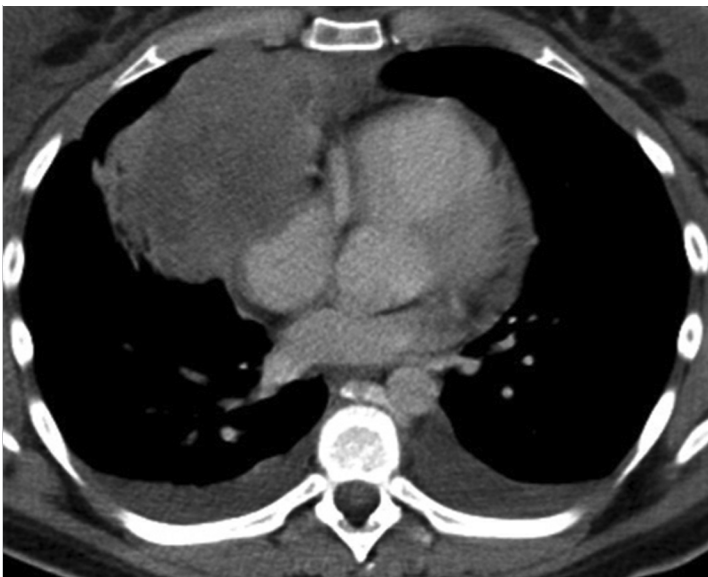


**Fig. 1.33 B-cell lymphoma.** The tumor shows slight, inhomogeneous enhancement on CT. The differential diagnosis would include sarcoma.

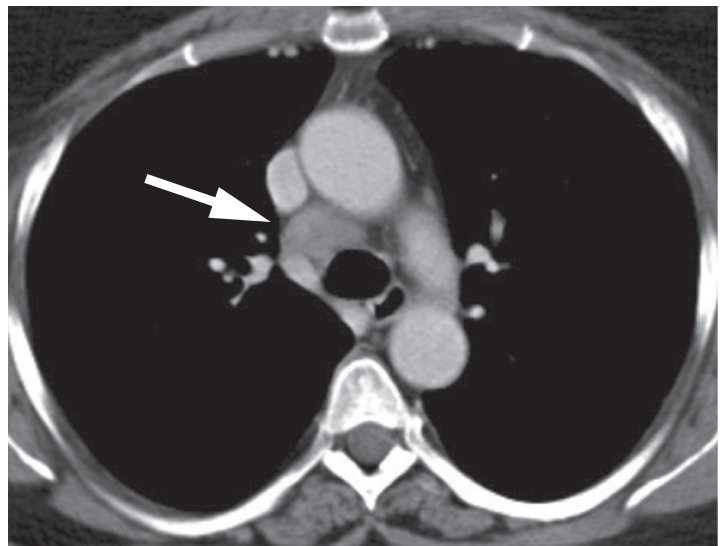


**Fig. 1.34 Castleman's disease.** CT demonstrates markedly enlarged station 4R lymph nodes (arrow) that show intense, homogeneous enhancement.

has an excellent prognosis, and excision of the isolated focus is generally curative. The multicentric form is associated with a much poorer prognosis.

► **Imaging signs.** The chest radiograph shows a mediastinal mass or lymphadenopathy that is indistinguishable from the changes characteristic of lymphoma. Both types of Castleman's disease are associated with the proliferation of blood vessels among the affected enlarged and confluent lymph nodes, resulting in intense enhancement on CT and MRI (► Fig. 1.34). Three distinct CT patterns have been described<sup>11</sup>:

- Approximately 50% of all patients have a solitary, noninvasive mass.
- In 40% of patients the mass is invasive and accompanied by lymphadenopathy.
- The remaining 10% of patients show lymph node enlargement at a single nodal station in the mediastinum.

Calcifications are found within the masses in up to 10% of cases.

► **Clinical features.** The more common hyaline vascular type of Castleman's disease is usually asymptomatic. The less common plasma cell type is associated with B symptoms, most notably fever and anemia. The unifocal form has a very good prognosis, and surgical resection of the tissue is curative in most cases. The multifocal form is associated with a poorer prognosis. It is treatable with chemotherapy and radiation, but often the disease will still progress to lymphoma. One study in patients with the plasma cell type reported a 20% incidence of non-Hodgkin's lymphoma over an approximately 2-year period.<sup>12</sup>

► **Differential diagnosis.** The main differentiation required is that from lymphoma and this is aided by the intense, homogeneous lesion enhancement that occurs in Castleman's disease.

► **Key points.** The localized form limited to a single site is distinguished from the multifocal form and is curable by local excision. The hyaline vascular type of Castleman's disease is

distinguished from the plasma cell type. Both are characterized by enlarged lymph nodes that show intense, homogeneous enhancement.

### 1.4.3 Posterior Mediastinum

The most common masses in the posterior mediastinum are neurogenic tumors. Extramedullary hematopoiesis and hernias may also manifest in that region.

## Neurogenic Tumors

### Schwannoma (Neurinoma)

► **Brief definition.** Schwannomas (synonym: neurinomas) are common benign tumors that arise from the Schwann sheath cells of peripheral nerves and have a true fibrous capsule. Schwannomas may occur at any age but are most prevalent in young adults (the fourth to sixth decades). Histologically, areas with compact cells in a “shoal-of-fish” arrangement, palisading nuclei, and high vascular density (Antoni type A) are distinguished from hypocellular areas with a myxoid stroma (Antoni type B).

► **Imaging signs.** Schwannomas appear on chest radiographs as well-circumscribed tumors in the posterior mediastinum. Schwannomas show intense contrast enhancement on CT and MR images. On MRI, schwannomas are hypointense on unenhanced T1 W images and hyperintense on T2 W images. Regressive changes (cystic areas, calcifications, fat deposits) are common and are independent of tumor size. Generally speaking, the nerve from which the tumor arises can be visualized (► Fig. 1.35).

#### Note

It is typical for schwannomas to protrude from neural foramina, forming a dumbbell-shaped mass that enlarges the foramen. It is also common for schwannomas to grow along a nerve in the posterior mediastinum below the ribs.

► **Clinical features.** Most benign neurogenic tumors (schwannoma/neurinoma, neurofibroma) are asymptomatic and are detected incidentally at chest radiography, CT, or MRI. Some lesions may cause dysesthesia if sensory nerve branches are involved. The treatment of choice is complete surgical excision.

► **Key points.** Schwannomas are benign tumors of Schwann cells that develop on peripheral nerves. Spinal schwannomas tend to widen the neural exit foramina. They appear on sectional imaging as well-circumscribed, intensely enhancing lesions.

### Neurofibroma

► **Brief definition.** Neurofibromas are benign tumors that arise from peripheral nerve sheaths. They are distinguished histologically from schwannomas by the involvement of mesenchymal cells of the peri- and epineurium (endo- and perineural fibroblasts) and the absence of a capsule. Neurofibromas may show a localized or diffuse growth pattern, and the lesions may be solitary (negative family history) or multiple in neurofibromatosis type 1 (von Recklinghausen’s disease). Neurofibromatosis type 1 is a phacomatosis with neurocutaneous manifestations and the involvement of multiple organ systems. The disease has an autosomal dominant mode of inheritance and an incidence of 1 in 3,000 births. Approximately 50% of all new cases are spontaneous mutations. A defect on the long arm of chromosome 17 is responsible for neurofibroma formation. Neurofibromatosis type 1 is characterized by the development of multiple neurofibromas on peripheral nerves, café au lait spots on the skin, sphenoid dysplasia, pigmented iris nodules, and optic nerve glioma. Plexiform neurofibromas are pathognomonic for neurofibromatosis type 1. They occur in very early childhood, preceding the appearance of cutaneous neurofibromas, and involve a long nerve segment including its branches. The neurofibromas in neurofibromatosis type 1 have a 4% likelihood of malignant transformation. One clinical feature of neurofibromas is their rapidly progressive growth. Only about 10% of patients with a solitary neurofibroma are diagnosed with neurofibromatosis.

► **Imaging signs.** Neurofibroma appears on CT as a well-circumscribed mass that is isodense or hypodense to muscle on unenhanced images and usually shows predominantly central enhancement. On MRI, neurofibromas are hyperintense in T2 W images due to their myxoid stroma (► Fig. 1.36) and enhance intensely on T1 W images after IV administration of contrast medium.

► **Clinical features.** Neurofibromas may be asymptomatic or may cause symptoms due to the compression of surrounding structures. Rapid growth of a neurofibroma suggests malignant transformation.

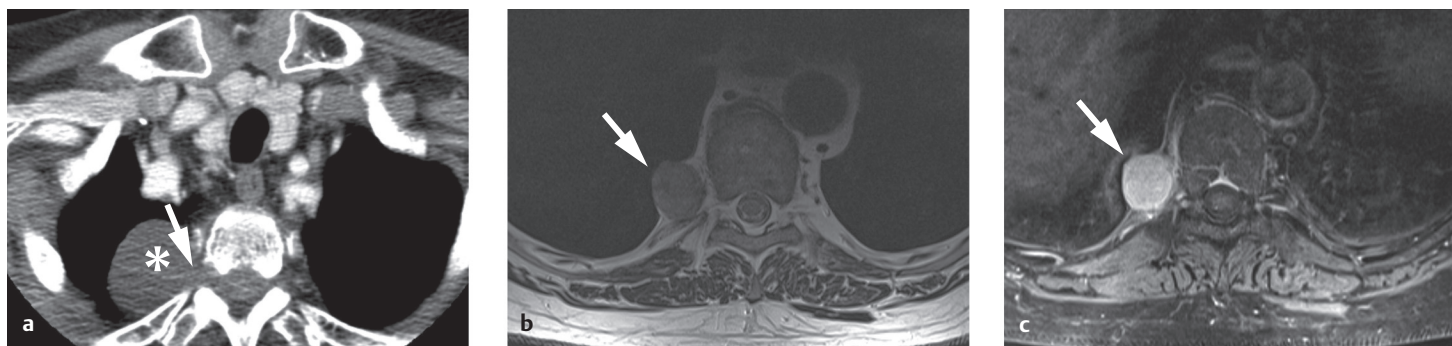
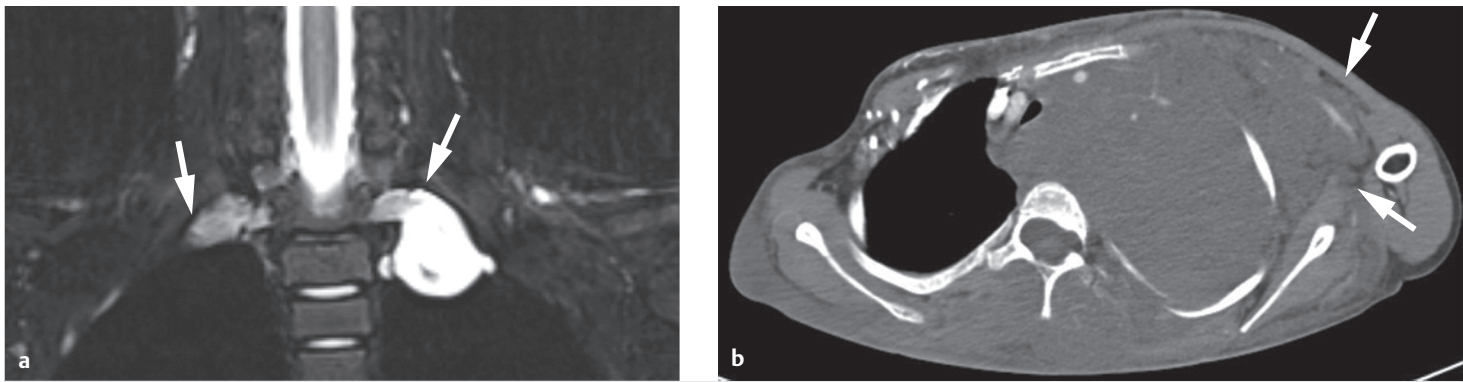


Fig. 1.35 Neurinoma. (a) CT displays the tumor (asterisk) as a dumbbell-shaped mass growing through the neural foramen and enlarging it (arrow). (b) T2 W MRI in a different patient demonstrates the location of the tumor (arrow) in relation to surrounding structures. (c) T1 W image in the same patient after IV administration of contrast medium shows marked enhancement of the neurinoma (arrow).



**Fig. 1.36 Neurofibroma.** (a) The tumors (arrows) show high signal intensity on T2W MRI. (b) CT scan in a different patient with a large neurofibroma involving peripheral nerves (arrows). The tumor shows only slight enhancement.

► **Differential diagnosis.** Neurofibromas and malignant nerve sheath tumors cannot always be positively differentiated from one another at imaging. Nevertheless, a well-circumscribed tumor with predominantly central enhancement and a target pattern on T2W MRI is typical of neurofibroma, whereas irregular, predominantly peripheral enhancement of a tumor with indistinct margins is suggestive of malignant transformation.

► **Key points.** Neurofibromas are benign tumors that arise from peripheral nerve sheaths. They are distinguished histologically from schwannoma by the involvement of mesenchymal cells of the perineurium and epineurium. Neurofibromatosis type 1 is characterized by the formation of multiple tumors along peripheral nerves. At imaging, neurofibromas have smooth margins and show intense, predominantly central enhancement after IV administration of contrast medium. Neurofibromas are hyperintense on T2W MRI due to their myxoid stroma.

## Neuroblastoma

► **Brief definition.** Neuroblastoma is an embryonic cell tumor derived from neural-crest progenitor cells of the autonomic nervous system. The peak incidence of this tumor occurs in infancy; the average age at diagnosis is 17 months. The incidence is 1 in 5,000 births. After Wilms's tumor, neuroblastoma is the second most common malignancy in children under 3 years of age.<sup>13</sup> Only 15% of all neuroblastomas occur in the mediastinum. Mediastinal neuroblastomas arise from the sympathetic trunk.

► **Imaging signs.** Chest radiographs show a posterior mass that disrupts the paraspinal line on the affected side (see ► Fig. 1.37). On CT, calcifications are found in the tumor matrix of thoracic neuroblastomas in up to 80% of cases. The masses are inhomogeneous and contain areas of relatively low density. Only moderate enhancement is seen on CT and MRI. The T1 and T2 times are prolonged on MRI, resulting in low signal intensity on unenhanced T1W images and high signal intensity on T2W images. A characteristic feature is tumor ingrowth into the spinal canal through the neural foramina. In some cases this is defined more clearly by MRI than by CT (► Fig. 1.37).

► **Clinical features.** Symptoms in most children result from catecholamine production by the primary tumor or from metastasis. Elevated urinary vanillylmandelic acid, a catecholamine breakdown product, is found in 78% of patients. Elevated

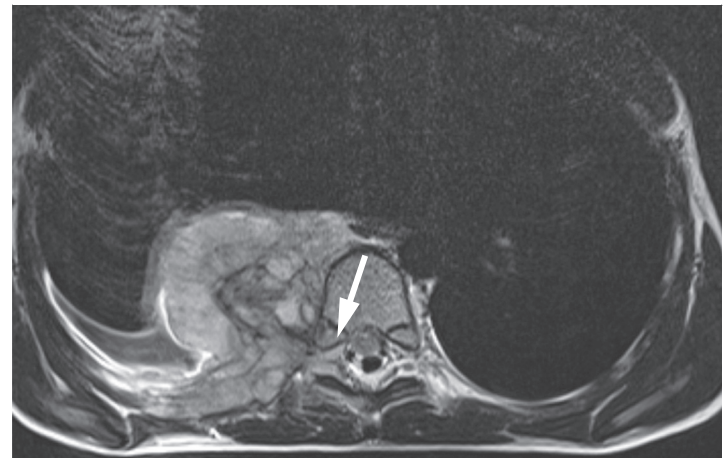


**Fig. 1.37 Neuroblastoma.** Same patient as in ► Fig. 1.3. Tumor ingrowth into the neural foramina (arrow) is clearly depicted in this T2W MR image (but not on CT).

catecholamine levels in the blood may induce episodes of flushing and hypertension. Neuroblastomas of the sympathetic trunk may extend into the spinal canal and cause symptoms due to cord compression (paraparesis, pain, dysesthesia).

### Note

Neuroblastomas occur at immediate paravertebral sites along the sympathetic trunk.

► **Differential diagnosis.** Neuroblastoma is virtually the only differential diagnosis for posterior mediastinal masses in very small children.

► **Key points.** Neuroblastoma is the first differential diagnosis for posterior mediastinal masses in small children. Laboratory findings and sectional imaging narrow the diagnosis. Ingrowth into the spinal canal through the neural foramina is typical and is clearly visualized by MRI.

## Paraganglioma

► **Brief definition.** Paragangliomas are derived from the chromaffin cells of the paraganglia. Paragangliomas in the mediastinum arise from the vagus nerve and para-aortic ganglia. They may occur sporadically or may be inherited as an autosomal dominant trait. Although the tumor shows no histological signs of

malignancy, it still metastasizes in 5% of cases. It has a reported growth rate of approximately 5 mm per year, with a peak age of incidence in the fourth and fifth decades. The incidence of paraganglioma is 1 per 1 million population per year. Paragangliomas are composed of chief cells and surrounded by a fibrous pseudocapsule. The tumor matrix is richly vascularized. Paragangliomas may show locally invasive growth.

► **Imaging signs.** Paragangliomas may occur in the course of the vagus nerve in the anterior mediastinum, at para-aortic sites, and at cardiac sites in the roof of the right atrium, in the posterior wall of the left ventricle, and in the atrial septum. Due to their rich blood supply, paragangliomas show prominent enhancement in all modalities. Paragangliomas appear as well-circumscribed tumors on CT (► Fig. 1.38). They are hyperintense in T2W MR images and isointense to muscle in unenhanced T1W images. A specific diagnosis requires clinical correlation with attention to potentially elevated catecholamine breakdown products in the urine. Hormonally inactive tumors require a histological diagnosis.

► **Clinical features.** Hormonally inactive tumors (50% of paragangliomas) mainly cause symptoms by compressing adjacent organs. Hormonally active (catecholamine-secreting) tumors lead to hypertension, hyperhidrosis, and flushing. The treatment of choice is complete surgical removal. Irradiation can be used for paragangliomas located at unfavorable sites or in inoperable patients, but radiotherapy is palliative.

► **Differential diagnosis.** The differential diagnosis should include neurinomas and metastases from hypervascular tumors such as renal cell carcinoma or neuroendocrine tumors.

► **Key points.** Paragangliomas may be locally invasive and metastasize in 5% of cases. They are richly vascularized and show correspondingly intense enhancement. Laboratory values (vanillylmandelic acid, a catecholamine breakdown product) should be considered in making the diagnosis.

### Extramedullary Hematopoiesis

► **Brief definition.** Extramedullary hematopoiesis is a compensatory mechanism for severe anemia, usually occurring in

the organs of the reticuloendothelial system (spleen, liver, and lymph nodes) and very rarely in other organs such as the kidneys, adrenal glands, or even the brain. It is attributed to the presence of ectopic pluripotent stem cells in parenchymal organs and lymph nodes. Intrathoracic extramedullary hematopoiesis may occur at paravertebral sites in the posterior inferior mediastinum. Based on current information, this results from the contiguous spread of hematopoietic marrow from the medullary cavities of the vertebral bodies and ribs. The recent literature consists mainly of individual case reports. In a small series of 29 patients with thalassemia, 65% of the patients were found to have paravertebral sites of extramedullary hematopoiesis in the chest.<sup>14</sup>

► **Imaging signs.** Imaging reveals lobulated paravertebral masses with smooth margins (► Fig. 1.39). CT shows masses of soft tissue density that are isoattenuating to spleen and have the same enhancement characteristics as the spleen. The hematopoietic tissue is isointense to spleen on MRI.

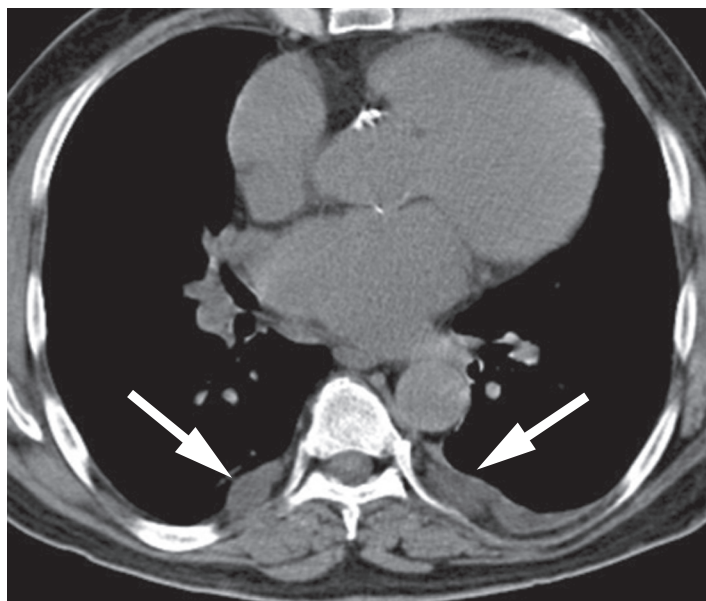


Fig. 1.39 Extramedullary hematopoiesis. Unenhanced CT shows multiple bilateral, paravertebral masses of soft tissue density (arrows).

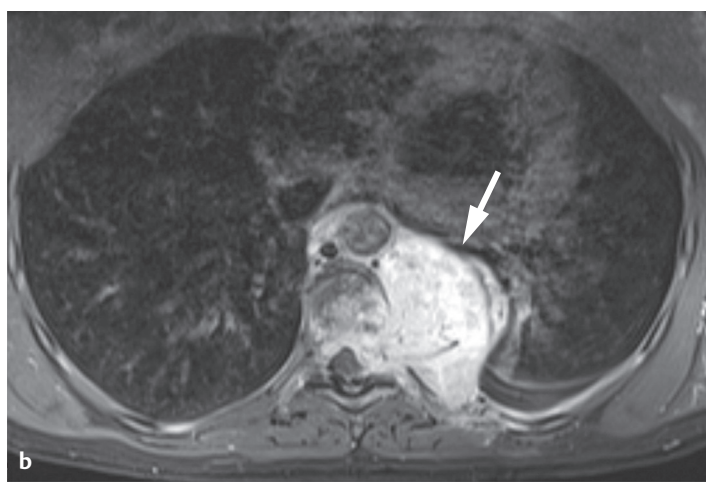
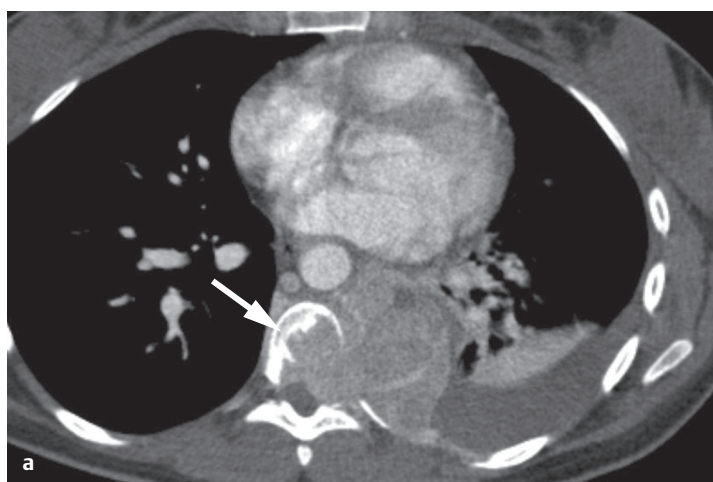
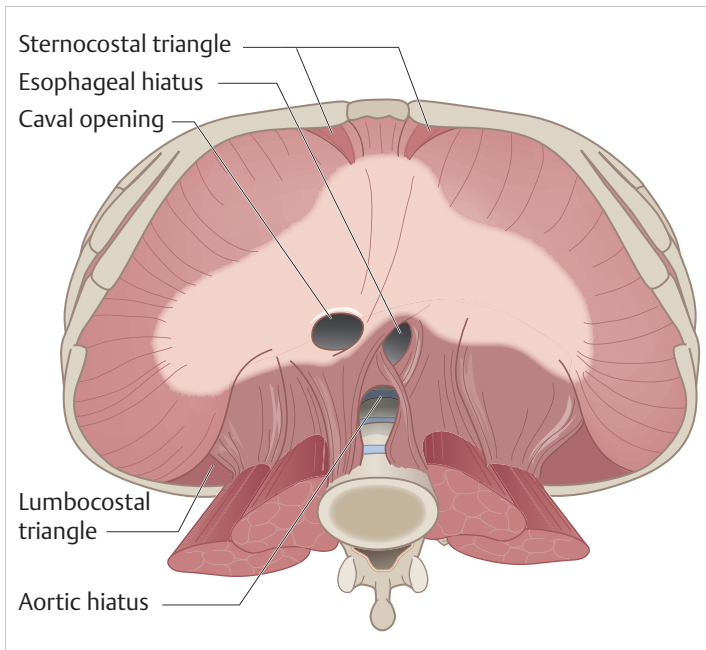


Fig. 1.38 Paraganglioma arising from a para-aortic ganglion. (a) CT demonstrates a paravertebral mass that is infiltrating the vertebral body (arrow) and shows homogeneous enhancement. (b) On T1W MRI after IV administration of contrast medium, the tumor shows intense homogeneous enhancement (arrow).



**Fig. 1.40** Schematic representation of the diaphragm and its weak spots. Anterior: sternocostal triangle; posterolateral: Bochdalek triangle (lumbocostal triangle).

► **Clinical features.** The dominant clinical features are those of the known disease underlying extramedullary hematopoiesis (myelofibrosis and hereditary anemias: thalassemia, sickle cell anemia, hereditary spherocytosis), while the extramedullary hematopoiesis itself is generally asymptomatic. Intraspinal extension with neurologic symptoms relating to cord compression has been described in a few cases.

#### Note

In equivocal cases where an underlying disease has not yet been identified, the diagnosis of extramedullary hematopoiesis can be established by fine needle aspiration biopsy.

► **Key points.** Sites of extramedullary hematopoiesis in the mediastinum appear as prevertebral and paravertebral masses that have the same characteristics as splenic tissue on sectional imaging.

### Bochdalek, Morgagni, and Larrey Hernias

► **Brief definition.** The diaphragm has two anterior and two posterior regions that are devoid of muscle, are covered only by connective tissue, and form sites of predilection for diaphragmatic hernias (► Fig. 1.40):

- The *Bochdalek triangle* is a posterior region on each side of the diaphragm, located between the costal and lumbar muscle bundles, where a Bochdalek hernia may occur (► Fig. 1.41).
- The *sternocostal triangle* is an anterior parasternal region located at the sternocostal junction on each side. Abdominal contents, usually consisting of fat, greater omentum, or loops of small or large bowel, may herniate into the anterior inferior mediastinum through the right sternocostal triangle to form a Morgagni hernia (► Fig. 1.42) or through the left sternocostal triangle to form a Larrey hernia. Hiatal hernias are described in the chapter on the gastrointestinal tract.

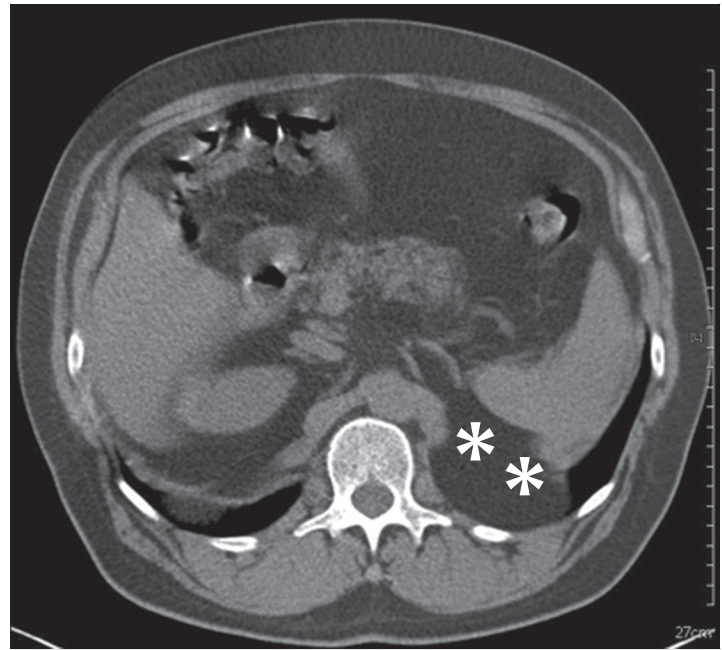


**Fig. 1.41** Bochdalek hernia on the left side. CT demonstrates the hernia opening (asterisks), which is located posterolaterally at approximately the level of the renal upper pole.

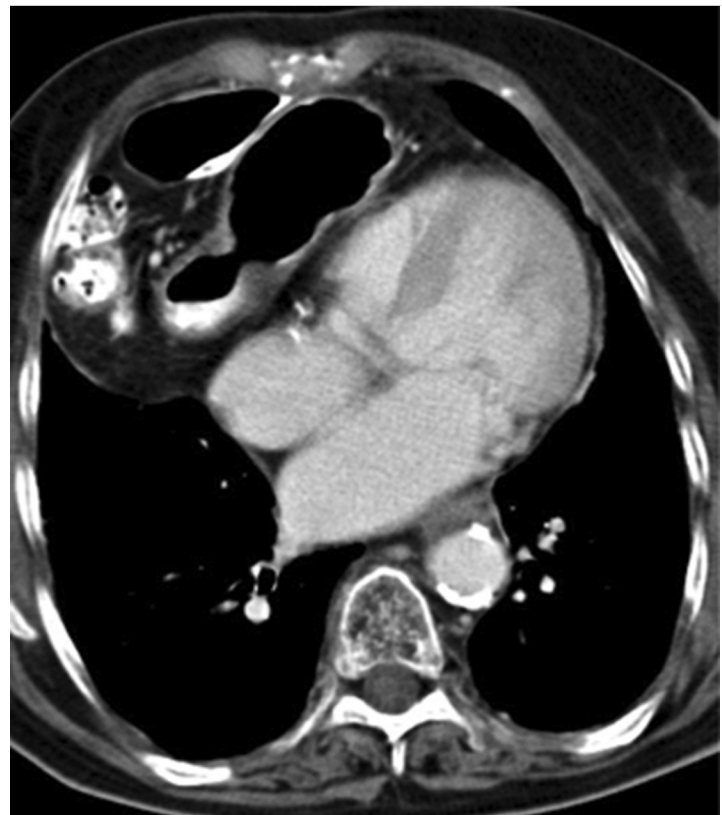


**Fig. 1.42** Morgagni hernia with intrathoracic herniation of mesenteric fat and bowel loops.

#### ► Imaging signs

- A *Bochdalek hernia* is usually detected incidentally on the lateral chest radiograph, appearing as a well-circumscribed opacity in the posterior inferior mediastinum. It is differentiated from a solid tumor (e.g., neurinoma) by CT, which demonstrates the herniation of fat or the upper renal pole through the lumbosacral triangle on the left side. A Bochdalek hernia on the right side is very rare because the liver covers the lumbosacral triangle on that side.

- A *Morgagni hernia* or a *Larrey hernia* appears on the PA chest radiograph as a well-circumscribed paracardiac mass. The lateral radiograph localizes it to the anterior mediastinum. The Morgagni hernia (right-sided) is more common than the Larrey hernia (left-sided).<sup>15</sup> The defect in the diaphragm can be directly visualized by sectional imaging and the herniated fat, omentum, or bowel can be visually traced from the chest into the abdomen.

► **Clinical features**

- *Bochdalek hernias* are usually asymptomatic. With a small hernia, there may be pain due to incarceration of the herniated tissue. With a large hernia, displacement of the mediastinum and lung may lead to dyspnea and, less commonly, tachycardia. The defect should be surgically repaired in symptomatic patients.
- The majority of *Morgagni* and *Larrey hernias* are also asymptomatic and detected incidentally on the chest radiograph, CT, or MRI. Symptomatic patients may complain of retrosternal pressure, upper abdominal pain, or sudden and severe retrosternal pain in extremely rare cases of incarceration. As a general rule, Morgagni and Larrey hernias do not require treatment. Symptomatic patients can be treated by laparoscopic repair of the defect in the sternocostal triangle.

► **Pitfalls.** The lumbosacral triangle is located far laterally and posteriorly, well away from the esophageal hiatus. Axial and para-axial hernias should not be confused with a Bochdalek hernia. The upper pole of the kidney is located below the lumbosacral triangle and can provide a differentiating landmark.

► **Differential diagnosis.** If only the chest radiograph is available, the main differentiation required is from solid masses, depending on the nature of the herniated tissue.

► **Key points.** The sternocostal triangle, an anterior region located at the sternocostal junction on each side, is the site where a Morgagni hernia may occur on the right side or a Larrey hernia on the left side. The Bochdalek triangle is located posterolaterally between the costal and lumbar muscle bundles on each side and is the site where the eponymous hernia may form. These hernias appear on chest radiographs as masses of soft tissue density unless they include air-filled bowel loops. They are easily diagnosed on sectional images, which can define the hernial opening and herniated tissue.

## 1.5 Trauma with Mediastinal Injury: Pneumomediastinum

► **Brief definition.** Pneumomediastinum (mediastinal emphysema) refers to air in the mediastinum. It occurs in approximately 10% of patients who have sustained blunt trauma to the chest. It may also occur spontaneously due to a rise of intra-alveolar pressure in response to weight lifting, a Valsalva maneuver, vigorous coughing or vomiting, or barotrauma in divers or stunt pilots, for example. The pathogenic mechanism has been well understood since animal studies conducted in the 1930s: small tears in the alveoli permit air to escape into the interstitium. Because the pressure in the mediastinum is lower than in the peripheral lung,

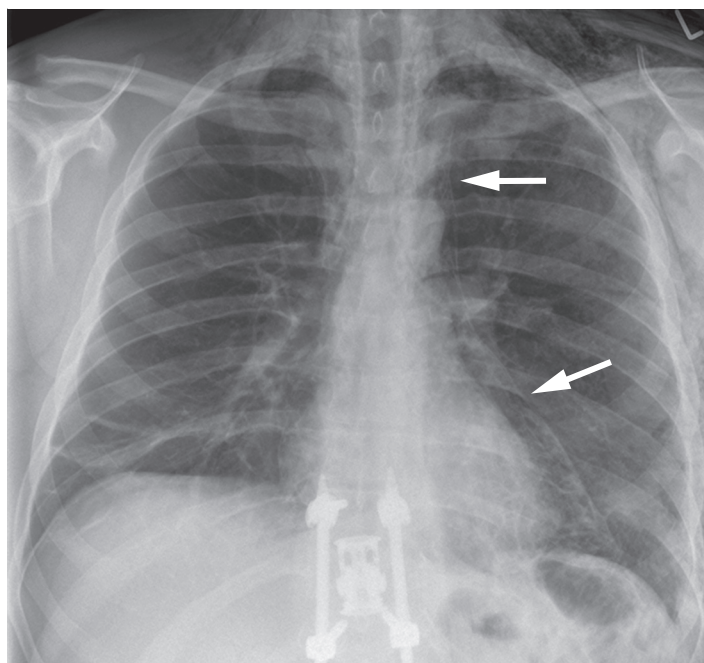


**Fig. 1.43 Pneumomediastinum.** Air has elevated a long segment of pleura away from the mediastinum (arrows).

the air migrates centrally along the bronchovascular bundles. From there the air spreads along the anatomical structures of the mediastinum in the interstitium and may continue to spread into the neck and into the subcutaneous tissues of the limbs.<sup>16</sup> This mechanism also underlies the pneumothorax that occurs with blunt thoracic trauma. Generally these cases will resolve spontaneously, although this process will take several days due to the high nitrogen content of approximately 78% in room air (nitrogen has low solubility in blood). CT cannot demonstrate the small tears in the alveoli and therefore is not indicated in patients with a small pneumomediastinum whose cause cannot be determined from the history. CT is appropriate only in patients with a suspected severe tracheal injury following difficult intubation, for example. In contrast to pneumopericardium, in which the air collection is confined to the pericardium, the air crescent associated with a pneumomediastinum may extend far into the superior mediastinum (► Fig. 1.43).

► **Imaging signs.** Pneumomediastinum can usually be diagnosed on standard chest radiographs and a number of typical signs have been identified:

- The *continuous diaphragm sign* occurs when air is trapped between the pericardium and the diaphragm, and the diaphragm can be traced continuously across the midline from both sides of the chest in the AP or PA radiograph. The continuous diaphragm sign should not be mistaken for free air in the abdominal cavity.
- The *V sign* describes a V-shaped air collection in the left hemithorax between the diaphragm and paravertebral line.
- Air might be detectable as areas of hypertransparency around large vessels such as the aortic arch, superior vena cava, or azygos vein.
- Air in the interstitium around the bronchial wall creates high contrast between the bronchial wall and surrounding structures, causing the bronchus to form a visible ring when viewed in an end-on projection (the *bronchial ring sign*).

- Air around the thymus in young adults, adolescents, and children accentuates its typical bilobar structure. The *thymus sign* results from the silhouette phenomenon, in which structures of equal density are delineated by intervening material of a different density, in this case air.

► **Clinical features.** Pneumomediastinum leads to crepitus as a result of soft tissue emphysema in the neck. Patients with mild to moderate pneumomediastinum are usually asymptomatic. Some patients complain of pain radiating to the back of the neck. A large pneumomediastinum may cause dyspnea in rare cases.

► **Key points.** Pneumomediastinum (mediastinal emphysema) denotes the presence of air in the mediastinum, which occurs in approximately 10% of patients who have sustained blunt thoracic trauma but may also occur spontaneously due to a rise of intra-alveolar pressure (from weight lifting, vigorous coughing or vomiting, or barotrauma in divers or stunt pilots). It is caused by minute tears in the alveoli. CT is indicated only in patients with a suspected severe tracheal injury (usually iatrogenic after difficult intubation or bronchoscopy).

## Bibliography

- [1] Sandner A, Börgermann J. Update on necrotizing mediastinitis: causes, approaches to management, and outcomes. *Curr Infect Dis Rep.* 2011; 13(3):278–286
- [2] Ridder GJ, Maier W, Kinzer S, Teszler CB, Boedeker CC, Pfeiffer J. Descending necrotizing mediastinitis: contemporary trends in etiology, diagnosis, management, and outcome. *Ann Surg.* 2010; 251(3):528–534
- [3] Jain D, Fishman EK, Argani P, Shah AS, Halushka MK. Unexpected sclerosing mediastinitis involving the ascending aorta in the setting of a multifocal fibrosclerotic disorder. *Pathol Res Pract.* 2011; 207(1):60–62
- [4] Romagnoli M, Poletti V. Multifocal fibrosclerosis with lung, mediastinal, pancreatic and retroperitoneal involvement in a 58-year-old man. *Sarcoidosis Vasc Diffuse Lung Dis.* 2009; 26(1):73–75
- [5] Nasserri F, Eftekhari F. Clinical and radiologic review of the normal and abnormal thymus: pearls and pitfalls. *Radiographics.* 2010; 30(2):413–428
- [6] Ströbel P, Marx A, Zettl A, Müller-Hermelink HK. Thymoma and thymic carcinoma: an update of the WHO Classification 2004. *Surg Today.* 2005; 35(10):805–811
- [7] Otsuka H. The utility of FDG-PET in the diagnosis of thymic epithelial tumors. *J Med Invest.* 2012; 59(3–4):225–234
- [8] Sperger JM, Chen X, Draper JS, et al. Gene expression patterns in human embryonic stem cells and human pluripotent germ cell tumors. *Proc Natl Acad Sci U S A.* 2003; 100(23):13350–13355
- [9] Mourra N, Lewin M, Parc Y. Clinical challenges and images in GI. Esophageal tubular duplication. *Gastroenterology.* 2008; 134(3):669–899
- [10] Castleman B, Iverson L, Menendez VP. Localized mediastinal lymphnode hyperplasia resembling thymoma. *Cancer.* 1956; 9(4):822–830
- [11] McAdams HP, Rosado-de-Christenson M, Fishback NF, Templeton PA. Castleman disease of the thorax: radiologic features with clinical and histopathologic correlation. *Radiology.* 1998; 209(1):221–228
- [12] Oksenhendler E, Boulanger E, Galicier L, et al. High incidence of Kaposi sarcoma-associated herpesvirus-related non-Hodgkin lymphoma in patients with HIV infection and multicentric Castleman disease. *Blood.* 2002; 99(7):2331–2336
- [13] Papaioannou G, McHugh K. Neuroblastoma in childhood: review and radiological findings. *Cancer Imaging.* 2005; 5:116–127
- [14] Dore F, Cianciulli P, Rovasio S, et al. Incidence and clinical study of ectopic erythropoiesis in adult patients with thalassemia intermedia. *Ann Ital Med Int.* 1992; 7(3):137–140
- [15] Schubert H, Haage P. Images in clinical medicine. Morgagni's hernia. *N Engl J Med.* 2004; 351(13):e12
- [16] Macklin CC. Histological indications of the sites of air leakage from the lung alveoli into the vascular sheaths during local overinflation of the living cat's lung. *Can Med Assoc J.* 1938; 38(4):401–402
- [17] Mountain CF, Dresler CM. Regional lymph node classification for lung cancer staging. *Chest.* 1997; 111(6):1718–1723

## 2 Heart and Pericardium

Gabriele A. Krombach

2

### 2.1 Heart

#### 2.1.1 Anatomy

##### Cardiac Borders

During embryogenesis, the heart initially forms as a symmetrical midline organ in the chest and subsequently undergoes a rotation in which the cardiac apex is slightly raised and rotated to the left. This process moves the right ventricle to a position directly behind the sternum. Approximately two-thirds of the heart is to the left of the midline and one-third is to the right. The left atrium rotates posteriorly; a blind pouch in its wall, the left atrial appendage, contains stretch receptors and forms atrial natriuretic peptide (ANP) in response to atrial wall distension.

► **Selection of modalities.** Chest radiography is the imaging modality of first choice for examining patients with unexplained cardiac disease. It is also useful in the follow-up of patients with known heart disease. CT is used for risk stratification and for imaging the coronary arteries in patients with an intermediate pretest probability. In evaluation of transcatheter aortic valve implantation (TAVI), CT is used to measure the dimensions of the aortic annulus and the distance between the origins of the coronary arteries. MRI is the gold standard for the quantification of regional and global cardiac function. For this the ventricles are covered with contiguous slices and their volumes are measured. This differs from echocardiography, in which the chamber volumes are not measured directly but derived from geometric assumptions based on short-axis and long-axis scans. As a result, the determination of functional parameters by echocardiography is imprecise, especially in diseased hearts with changes in ventricular shape. When it comes to perfusion imaging, MRI is superior to single-photon emission computed tomography (SPECT) in its sensitivity and specificity, and its use for detecting perfusion defects is already recommended in professional guidelines.<sup>1</sup> MRI is used for the assessment of myocardial viability after heart attacks. Additionally, MRI has become well established for the characterization of cardiomyopathies, the examination of patients with cardiac tumors, and the examination of patients with congenital heart disease based on its ability to measure flow and also to quantify cardiac function.

##### ► Radiographic landmarks

- **PA radiograph** (standard projection for radiographs in the standing position):
  - The right atrium forms the right border of the cardiac silhouette. It forms a convex bulge toward the lung and is continuous superiorly with the superior vena cava (► Fig. 2.1).
  - The left ventricle forms the left border of the cardiac silhouette. Just above it is a small portion of the left atrial appendage and the left pulmonary trunk, followed by the aorta (see ► Fig. 2.1).

- **Lateral radiograph:**

- The right ventricle forms the retrosternal border of the cardiac silhouette. It is continuous superiorly with its outflow tract, the pulmonary trunk.
- The left atrium forms the posterior border (see ► Fig. 2.1). The inferior vena cava is visible inferiorly as a small triangle.

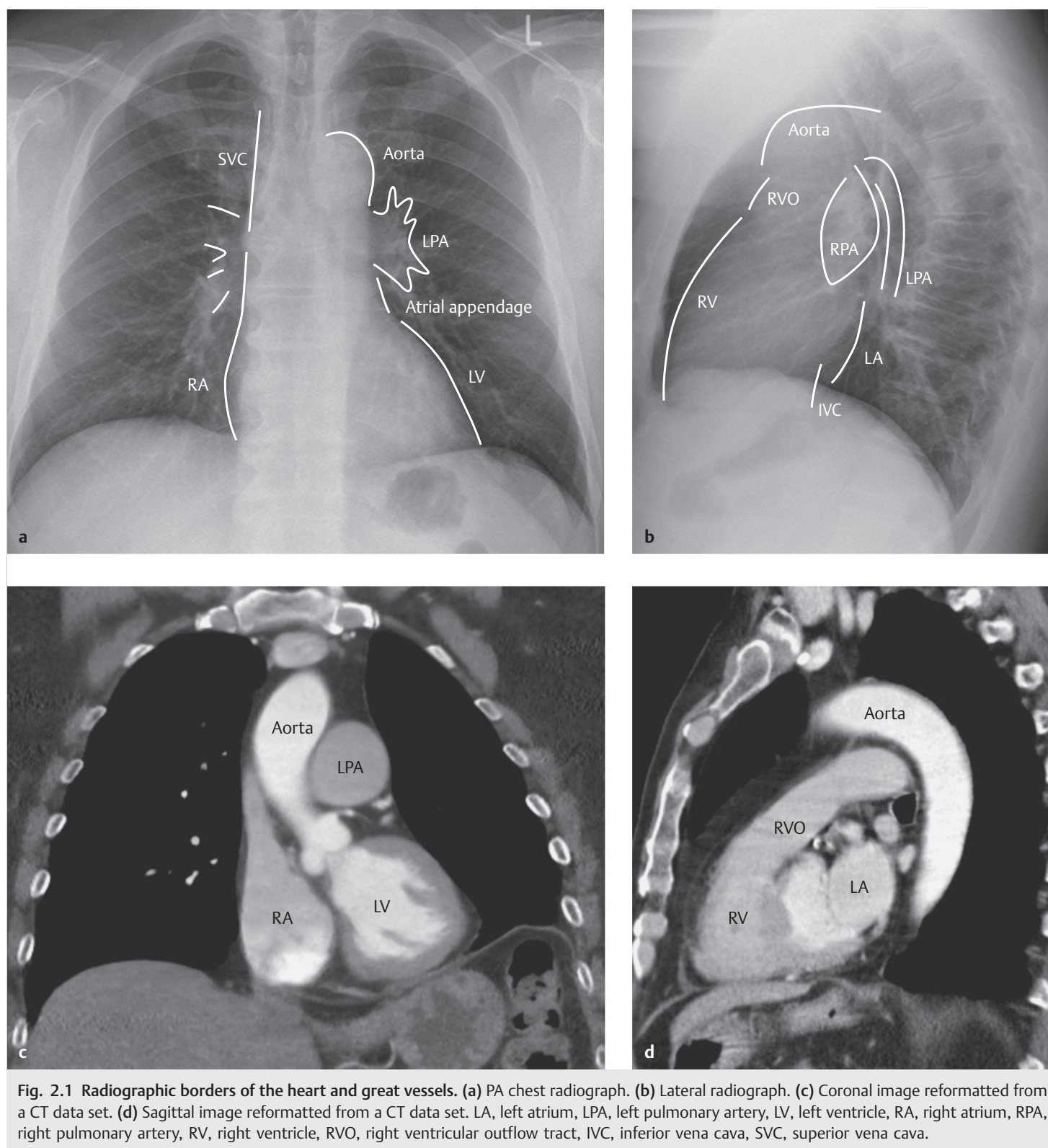
##### Cardiac Chambers (► Fig. 2.2)

The left ventricle is conical in shape. In a healthy heart, imaging of the left ventricle in slices directed at 90° to its long axis yields a series of circular cross sections of the chamber (► Fig. 2.3). Called “short-axis views” of the left ventricle, they represent the standard slice orientation for cardiac imaging by MRI, echocardiography, and CT. Volume measurements are easily performed in this slice orientation by scanning the left ventricle from the apex to the base (valvular plane) in contiguous slices and then summing the areas of the slices. The maximum wall thickness measured in the septum during diastole should not exceed 12 mm (► Fig. 2.4). The left ventricle contains the two papillary muscles (anterior and posterior papillary muscles). The muscles are connected to the mitral valve by fine tendons called the chordae tendineae. The left ventricle is less trabeculated than the right ventricle. This difference is grounded in embryogenesis: The myocardium of both ventricles initially has a spongy structure and is composed of very heavily trabeculated muscle tissue. The outer portions of each ventricle subsequently fuse to form a compact wall. This process is more pronounced on the left side than on the right, with the result that the left ventricle is less trabeculated but has a thicker wall.

##### Note

The maximum wall thickness of the left ventricle should not exceed 12 mm (measured in the septum during diastole). The maximum wall thickness of the right ventricle in a healthy individual is generally less than 6 mm, measured in the free wall of the right ventricle (see ► Fig. 2.4). Measurements that exceed those values indicate hypertrophy of the chamber in question. This hypertrophy may result from a chronic pressure increase due, for example, to pulmonary or aortic valve stenosis, arterial hypertension, or pulmonary hypertension. It may also result from a chronic (obstructive) hypertrophic cardiomyopathy due to a genetic cause.

► **Imaging landmarks.** A uniform slice orientation must be used in comparing different imaging modalities such as echocardiography or SPECT with MRI. The slice orientations in MRI are referred to the axes of the left ventricle, as in echocardiography, so as to obtain reproducible imaging planes (see ► Fig. 2.3). The position of the diaphragm, which is influenced by the volume of intra-abdominal fat, contributes to positional variants such as a heart that is broadly apposed to the diaphragm or one that is narrower and more upright. The orientation of the slices must accordingly



be individually adapted. To aid location description for the pathologist, the left ventricle is divided into a basal portion (valvular third), a midventricular portion (middle third), and an apical portion (apical third; ▶ Fig. 2.5). It is also customary to further subdivide the left ventricle into 17 segments based on a system first adopted for echocardiography in the late 1980s and later applied to MRI. Each third is systematically divided into segments that are designated with the appropriate descriptors. The anterior wall has one segment at each of at the basal, midventricular, and apical levels, and each segment is designated by its level and the

word “anterior”—thus, basal anterior, midventricular anterior, and apical anterior. The same is done with the posterior wall, using the designation “inferior” (basal inferior, and so on). The septum and lateral wall are each divided into a basal and midventricular segment (inferoseptal and inferolateral, anteroseptal and anterolateral). This segmentation scheme is illustrated in ▶ Fig. 2.6. The anterior and inferior attachments of the right ventricle serve as landmarks for determining the position of the septal segments. The segments in the lateral wall are designated accordingly (basal inferolateral, and so on).

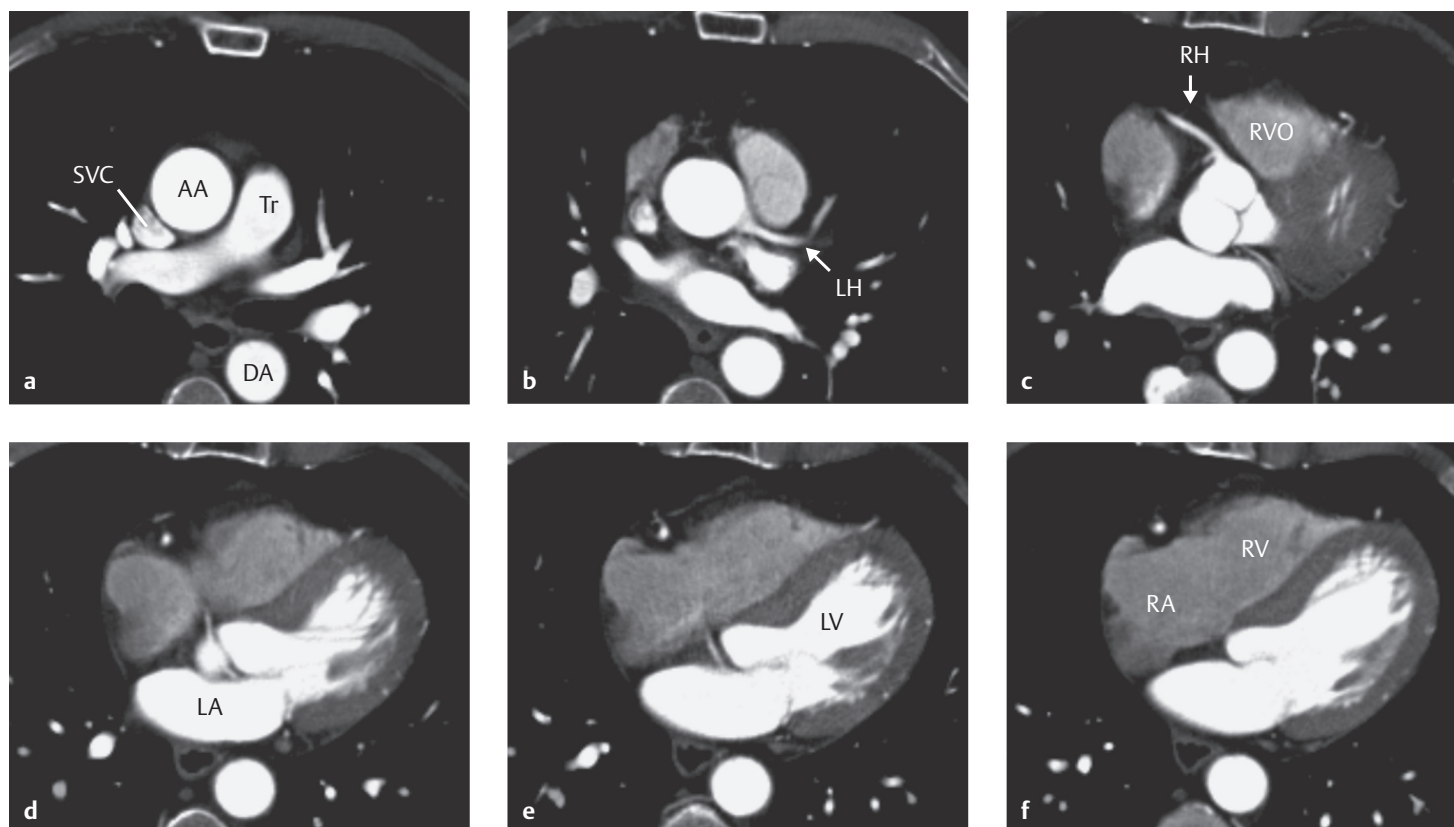


Fig. 2.2 Cardiac chambers and great vessels on axial CT scans. (a) Pulmonary trunk (Tr), ascending aorta (AA), descending aorta (DA), and superior vena cava (SVC). (b) Left coronary artery (LH). (c) Right coronary artery (RH) and right ventricular outflow tract (RVO). (d) Left atrium (LA). (e) Left ventricle (LV). (f) Right ventricle (RV) and right atrium (RA).

### Note

In patients with ischemic heart disease, the location of the ischemic region helps to identify the affected coronary vessel. If the coronary circulation is “balanced,” the anterior and anterolateral segments are supplied by the anterior interventricular branch of the left coronary artery, the inferolateral and anterolateral segments by the circumflex branch of the left coronary artery, and the inferoseptal and inferior segments by the right coronary artery. The segmental distribution pattern is different in hearts with a right-dominant or left-dominant coronary circulation.

The PA chest radiograph is taken with the patient standing upright and the X-ray source placed 2 meters from the detector (► Fig. 2.7a). Because the heart occupies a retrosternal position and is close to the detector, it is projected in approximately its true size. For the same reason, the lateral radiograph is taken with the patient lying on his or her left side. The situation is different with an AP radiograph taken in a supine position. In this case the X-ray tube is positioned closer to the cassette, while the heart is farther away. This causes the heart to be projected larger than its actual size (► Fig. 2.7b).

### Note

In an upright chest radiograph taken at full inspiration, the transverse cardiac diameter should not exceed 50% of the transverse thoracic diameter (► Fig. 2.8). In a supine radiograph, it should not exceed 60% of the transverse thoracic diameter.

When the heart decompensates in response to a chronic pressure load or volume load, the result is cardiac enlargement.

## 2.1.2 Diseases

### Heart Failure

► **Brief definition.** Heart failure develops as a result of myocardial damage, which can have many potential causes. With heart failure due to coronary disease, an acute infarction and, in certain cases of myocarditis, pulmonary congestion develop as a result of backward failure. This congestion can be recognized from typical radiographic signs. In patients with right ventricular failure, on the other hand, the principal effect is a damming back of blood in the systemic circulation, with associated lower leg edema and nocturia. Frequently both chambers are affected, resulting in mixed symptoms. In these cases, however, minimal changes may be noted in the chest radiograph if the inability of the left ventricle to deliver adequate blood to the systemic circulation is balanced by an absence of congestion in the pulmonary circulation due to right ventricular failure.

### Caution

An acute pressure load on the heart, due for example to acute fulminant pulmonary embolism, leads to cardiac dilatation in the acute stage. In contrast, a chronic pressure load on the heart due to aortic or pulmonary valve stenosis, arterial hypertension, or pulmonary arterial hypertension leads to cardiac hypertrophy. This hypertrophy leads to wall thickening with no increase in outer diameter (concentric hypertrophy) and is not detectable on chest radiographs (► Fig. 2.9).